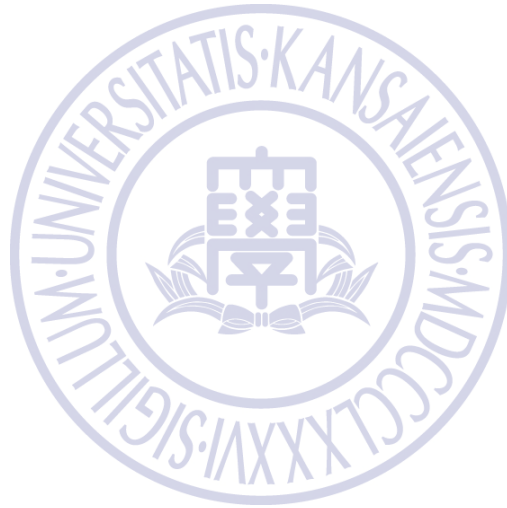


**FACTORS AFFECTING THE INITIATION OF
TSUNAMI EVACUATION**



by

KARINA APRILIA SUJATMIKO

A THESIS

Submitted to Kansai University
in Partial Fulfillment of Requirements
for the Degree

DOCTOR of PHILOSOPHY

2022 JUNE

THESIS SUMMARY

Title Factors affecting the initiation of tsunami evacuation
Author Karina Aprilia Sujatmiko

This study aims to understand better the natural phenomenon of landslide-induced tsunamis and the social phenomenon of a tsunami evacuation. The outcomes provide data to compare and contrast of the evacuation process during a typical seismic tsunami and a non-typical seismic tsunami. This research also compares the evacuation behavior in Indonesia and Japan. With this information, researchers could identify issues and make evacuation advice for future non-typical seismic and non-seismic tsunami events.

Chapter 1 explained the background and the context of this study by detailing the aims and objectives of this thesis. This chapter introduces the 2018 Palu earthquake and tsunami events and provides information on the location, disaster timeline, and casualties. The development of tsunami risk reduction in Indonesia also present to give the illustration of the current situation

Chapter 2 present our finding from the analysis of landslide-induced tsunami that submarine landslide is enough to generate a destructive tsunami. The scientific communities and Government of Indonesia focused the research and countermeasure for tsunami earthquake disaster. Development of tsunami warning technology also addressed for earthquake tsunami. This tendency is understandable since more than 75% tsunami generated by earthquake and survey for landslide-induced tsunami is hard to conduct. This study proposed a new approach to address the difficulty of determining the parameter of submarine landslide by using the soil investigation inland to be used as input for the landslide-induced tsunami simulation. Hopefully, in the future tsunami hazard analysis, the landslide-induced tsunami is not neglected. It is possible that only a landslide, without a strong earthquake, is enough to generate a destructive tsunami. It means ground motion will not be available as a critical evacuation trigger. Therefore, the evacuation plan will consider the risk of landslide-induced tsunami disaster.

Chapter 3 explains the definitions and concepts about tsunami evacuation used in this research. The framework of this study is the intuitive tsunami evacuation, specifically the

behavior changes from the response stage into the evacuation initiation stage. Two crucial aspects affecting their decision are reality-of-evacuation-start (RES) and awareness-level-of-danger (ALD). The environmental, social, and warning information cues caused the “must-escape” situation, or in this research called as RES sources are the interest of this study. The method was developed to analyze RES sources quantitatively and qualitatively from the post-disaster survey, video analysis and numerical simulation.

Chapter 4 shows the standard ranking of evacuation trigger and revealed six triggers worked for Indonesian people. Which is receiving a message from the authorities, seeing evacuees, feeling ground motion, seeing unusual sea surface or tsunami, hearing loud sounds from the sea, and hearing evacuees calling for evacuation. The observation of 53 individuals from 6 static cameras installed in the hotel located at the east coast of Palu Bay provides information about the impact and exposure that the field survey does not capture. Feeling ground motion is the first RES source exposed to people. People did not evacuate immediately after feeling ground motion. Early evacuees are 38 individuals (68%) who start evacuating before tsunami coming. Late evacuee are 17 individuals (32%), who started to evacuate after seeing the tsunami come into their location. The observation of 200 individuals captures on the 4 phone cameras in the commercial area (Palu Grand Mall), located on the west coast of Palu bay found that hearing other people calling for an evacuation is likely more impactful than revealed in the post-tsunami interview surveys. At least in this case study, RES sources generated by social cues, both seeing and/or hearing other people, are not constantly influential and gradually increase as the distance between the source and people decreases.

Chapter 5 shows the implementation of tsunami evacuation simulation in the residential area located on the east coast of Palu bay. This model analyzes the reality-of-evacuation-start in a spatiotemporal manner. The influenced weight of RES sources generated by social cues, both seeing and/or hearing other people, are not constant. Instead, the impact should gradually increase as the distance between the source and people decreases. Based on the scenario, it is found that to achieve 75% of residents decide to do early evacuation before tsunami came, then at least 47% of resident should evacuate immediately after feeling ground motion. This group of people should not be waiting for other cues, such as receiving message to evacuate from the authorities, observing other people behavior or waiting until they see or hear the tsunami arrival. The comparison between tsunami evacuation in 2018 Palu Tsunami, Indonesia and 2011 Tohoku Tsunami in Ishonomaki, Japan revealed that in Indonesia, seeing other people had a significantly higher influence on people to initiate evacuation. In Japan, hearing had a greater impact than seeing. The low percentage of hearing was probably because of small exposure

area of RES source and due to unclear instruction from shouting people. Case study comparison has the advantage to show the difference in detail, but a general comparison is needed to provide a broader picture. General comparison of evacuation standard ranking in Indonesia and Japan shows that receiving messages from authorities is the number one rank of evacuation trigger in both countries. The feeling of ground motion become the number two rank in Japan and number three in Indonesia. Interestingly, there is a wide gap between the rankings of "seeing other evacuees", it is on rank two for Indonesian people, but it is the lowest rank for Japanese people. In the video and the questionnaire, Indonesian people tend to quit the building after feeling ground motion and staying outside the building. In Japan, after the earthquake, people stayed inside the building and sought disaster information through media. Therefore, they could not see what other people were doing outside the building.

Further research on the difference in tsunami evacuation initiation is important because this indicates that the disaster risk reduction strategy should not be generic among countries. Educational material for tsunami training and drills must consider the local characteristics. Further research should examine RES sources in order to determine appropriate evacuation strategies for non-seismic tsunamis. To mitigate future similar disasters in the region, the high-frequency ocean surface radars is a potential tsunami observing systems. This warning system could be very impactful for Indonesian people, especially if we consider that receiving message from authorities rank as the number one RES sources.

Table of Contents

THESIS SUMMARY	I
TABLE OF CONTENTS	IV
LIST OF TABLES	VI
LIST OF FIGURES	VII
CHAPTER 1 INTRODUCTION	1
1.1 BACKGROUND AND RESEARCH OBJECTIVE	1
1.2 OVERVIEW OF THE 2018 PALU CASCADING DISASTER	4
1.3 THE IDENTIFIED PROBLEMS DURING THE 2018 PALU TSUNAMI	6
1.4 DEVELOPMENT OF DISASTER RISK REDUCTION IN INDONESIA	6
1.5 THESIS OUTLINE	8
REFERENCES	8
CHAPTER 2 ANALYSIS OF LANDSLIDE INDUCED TSUNAMI HAZARD.....	11
2.1 ESTIMATION OF LANDSLIDE VELOCITY IN JONO-OGE USING VIDEO ANALYSIS	12
2.1.1 <i>Identification of landslide movement direction.....</i>	<i>16</i>
2.1.2 <i>Identification of the video starting point.....</i>	<i>16</i>
2.1.3 <i>Image angle analysis using length ratio of the red-roofed house</i>	<i>17</i>
2.2 NUMERICAL SIMULATION OF LIQUEFACTION IN JONO-OGE, PALU	18
2.2.1 <i>Model Element</i>	<i>18</i>
2.2.2 <i>Governing Equation.....</i>	<i>19</i>
2.2.3 <i>Model Geometry, Mesh and Boundary Conditions</i>	<i>19</i>
2.2.4 <i>Input Ground Motion</i>	<i>19</i>
2.2.5 <i>Soil Parameters</i>	<i>19</i>
2.3 RESULT OF LANDSLIDE SIMULATION	21
2.3.1 <i>Evidence to The Validation Analysis.....</i>	<i>21</i>
2.3.2 <i>The Pore Water Pressure Response.....</i>	<i>21</i>
2.3.3 <i>Surface Displacement Response.....</i>	<i>21</i>
2.3.4 <i>Shear Stress-Shear Strain Relationship of Soil Element.....</i>	<i>21</i>
2.4 NUMERICAL SIMULATION OF LANDSLIDE INDUCED TSUNAMI INSIDE PALU BAY	23
2.4.1 <i>General Framework of Tsunami Simulation</i>	<i>23</i>
2.4.2 <i>Estimation of the retarding stress between landslide mass and ground.</i>	<i>24</i>
2.4.3 <i>Setting of Landslide Geometry as Tsunami Source</i>	<i>25</i>
2.4.4 <i>Tsunami Simulation Result</i>	<i>26</i>
REFERENCES	28
CHAPTER 3 DEFINITION AND CONCEPT OF INTUITIVE TSUNAMI EVACUATION	31
3.1 DEFINITION AND EXAMPLE OF INTUITIVE TSUNAMI EVACUATION	31
3.1.1 <i>Tsunami evacuation and evacuation phase</i>	<i>31</i>
3.1.2 <i>Logical and Intuitive evacuation behavior</i>	<i>32</i>
3.2 EVACUATION TRIGGERS.....	34
3.3 EVACUATION MODELING.....	34
3.4 REALITY-OF-EVACUATION-START AND FACTORS AFFECTING IT.....	35
3.5 DEFINITION OF REALITY-OF-EVACUATION-START SOURCE	36
3.5.1 <i>Impact of RES source.....</i>	<i>36</i>

3.5.2	<i>Exposure of RES source</i>	37
3.5.3	<i>Estimation of RES source weight</i>	38
3.6	DEFINITION OF AWARENESS LEVEL OF DANGER (ALD) AND ALD THRESHOLD	38
	REFERENCES	39
CHAPTER 4	GENERAL CHARACTERISTICS OF EVACUATION INITIATION IN INDONESIA	41
4.1	TSUNAMI EVACUATION TRIGGERS IN INDONESIA	41
4.2	STANDARD MODEL AND RANKING OF EVACUATION TRIGGERS IN INDONESIA	42
4.3	VIDEO ANALYSIS OF EVACUATION INITIATION	45
4.3.1	<i>The Static Video Analysis</i>	45
4.3.2	<i>The Dynamic Video Analysis</i>	48
	REFERENCE	50
CHAPTER 5	ANALYSIS OF THE REALITY-OF-EVACUATION-START SOURCES	52
5.1	MODEL SETTING	52
5.2	ENVIRONMENTAL SOURCE - EARTHQUAKE	55
5.3	SOCIAL SOURCE	58
5.3.1	<i>Seeing other's evacuee</i>	58
5.3.2	<i>Hearing other's evacuee calling for evacuation</i>	60
5.3.3	<i>Comparison of RES sources and Evacuation Triggers between Indonesia and Japan</i>	61
	REFERENCES	66
CHAPTER 6	CONCLUSION	68
	REFERENCES	72
	ACKNOWLEDGEMENTS	73

List of Tables

Table 1.1. Chronological of earthquake, tsunami, and early warning during the 2018 Palu event	5
Table 1.2. Development of technology, science and law of disaster risk reduction in Indonesia	7
Table 2.1. Parameters and distance calculation based on ratio method using red-roofed house image sequence.	17
Table 2.2. Input of soil physical parameters.....	20
Table 2.3. Input of dilatancy parameters	20
Table 2.4. Input of permeability and shear resistance at steady state.....	20
Table 3.1. Classification of RES sources by the area exposure	37
Table 4.1. Survey result on tsunami evacuation triggers in Indonesia from 2006 – 2018	42
Table 4.2. Ratio of evacuee who initiate to move when the second tsunami arrive at land....	48
Table 5.1. Parameters and setting condition to the tsunami evacuation initiation model.	53
Table 5.2. Questionnaire survey asking what is the reason that makes them start to evacuate.	53
Table 5.3. Weight of RES source for input parameter in the evacuation simulation.	54
Table 5.4. Scenarios based on ratio of evacuee start evacuating only after feeling ground motion (EQ), total number of people (n) is 53 people.	57
Table 5.5. Weight of RES source for input parameter in the evacuation simulation.	59
Table 5.6. Survey result on tsunami evacuation triggers in Japan from 1946 – 2019.....	64

List of Figures

Figure 1.1. Map of tsunami history in Indonesia since 1990 - 2021. The color shows the number of casualties for each tsunami event. Data from Global Historical Database.	1
Figure 1.2. The bar chart of number of deaths caused by tsunami, only tsunamis caused more than 10 casualties are shown in the chart. Data from Global Historical Database. 1	1
Figure 1.3. Numbers of tsunami research in Indonesia from 2004 – 2022. Data from caribencana.id	2
Figure 1.4 Map of Indonesia and red box shows Palu where the disaster occurred (insert). Location of epicenter (red star), shaking intensity, and landslide locations (black box).....	4
Figure 2.1. Map of epicenter (red star), shaking intensity, Palu bay coastal area (red box), and in-land area (black box) (USGS, 2020). A) bathymetry around palu bay, L1-L3 (orange circle) are the possible submarine landslide location (Nakata et al., 2020). B) Four liquefaction area around Palu valley, Sibalaya not shown in the figure, it is located 20 km south of Jono-Oge.	12
Figure 2.2. A) Jono-Oge elevation countour map, point A to B were the location where the possible landslide velocity known, point J1 is the boring site location. B) Elevation and slope of Jono-Oge along I-II.	13
Figure 2.3. Image sequence in the video recorded Jono-Oge landslide (photographs captured from video).	14
Figure 2.4. Flowchart of landslide velocity estimation using video content analysis method.15	15
Figure 2.5. Calculation method using ratio of object in the image sequence to calculate camera angle.....	15
Figure 2.6. Landscape and situation captured at the beginning of the video until the first 17 seconds.....	16
Figure 2.7. Identified building from the video plotted in the satellite image before and after the landslide occurred. Possible landslide pathway connected by the church (GPID Patmos Jono Oge) before (white color of church symbol) and after the landslide occurred (black color of church symbol).....	17
Figure 2.8. Images taken from the video for angle analysis of red-roofed house.	17
Figure 2.9. Camera position on possible landslide pathway, based on Table 2.1.	18
Figure 2.10. Soil profile at Jono-Oge, data taken from survey conducted by JICA, 2019. Model geometry for this simulation determined by the slope information and soil properties data.....	20
Figure 2.11. Time history of ground motion N-S component used as acceleration input. (digitized from (Kiyota et al., 2020)).	20
Figure 2.12. (a) Excess pore water pressure during 70 s, when the ground shaking started at 18 second the water pressure getting high. (b) Longer time histories pore water pressure show the dissipation.	22
Figure 2.13. Computed depth and displacement in the horizontal direction.....	22
Figure 2.14. Shear stress and shear strain of the soil element near the bottom between node 12 and 13 in Fig. 2.16.....	22

Figure 2.15. The schematic figure shows the difference between of the tsunami height calculated from the simulation and the run-up height gained from the field survey. (Takagi et al., 2019).....	25
Figure 2.16. Locations of the identified landslides and run-up observation points from post tsunami survey. The inset figure (red box) shows the tsunami height in that area. The blue dot, represent the tsunami height from the survey, in this figure the tsunami height is 5m. The nearest grid of computed tsunami height to the blue dot, shows that the tsunami height is 6m.	26
Figure 2.17. Simulation result using different shear strength, (A) 20kPa and (B) 1.5 kPa. The points are in the order of west to east and following along the coastline.	26
Figure 3.1. Phase during tsunami evacuation process (Makinoshima et al., 2020)	32
Figure 3.2. Time required for evacuation (Yung, 2008)	32
Figure 3.3. A) Initiation of evacuation based on logical judgment. B) Initiation of evacuation based on intuitive judgment (Dohi et al., 2016)	33
Figure 3.4. The intuitive decision-making for evacuation initiation.	35
Figure 3.5. Evacuation initiation process as result from the effect of reality-of-evacuation (RES) sources to the awareness level of danger (ALD) in people.	37
Figure 4.1. Flowchart of method to determine evacuation trigger ranking.	43
Figure 4.2. Evacuation trigger ranking based on the data collected from previous field surveys. The larger circles indicate this source chosen by majority of people as the reasons why they initiate evacuation.	44
Figure 4.3. Schematic graph of standard model of RES sources rankings based on its influence to initiate evacuation and the point at which such sources work during the beginning of an earthquake to tsunami in Indonesia.	44
Figure 4.4. Environmental setting of the 2018 Palu tsunami (open street map, 2020) recorded in the KN Hotel (-0.86404 E, 119.879 S) CCTV. Video from (Carvajal et al., 2019)	46
Figure 4.5. Analysis of the responses of 53 people exposed to the RES source observed from CCTV recording	47
Figure 4.6. Comparison between people response to evacuation triggers from questionnaire survey to the dynamic of evacuation start process from footage analysis.....	47
Figure 4.7. Analysis of the responses of 278 people exposed to the RES source observed from video recorded by mobile phone.	49
Figure 5.1. Palu map, A) The residential area as a target area for tsunami evacuation simulation and B) location of CCTV, installed at Hotel Nelayan. (map from google earth, accessed in 2020).....	52
Figure 5.2. Numerical simulation of the evacuation during the 2018 Palu tsunami using a set of parameters obtained from the analysis of a previous Indonesian disaster case.	55
Figure 5.3. Footage shows a group of early evacuees. First, they were captured in camera 2 (P2) and in camera 4 (P3); the map shows the direction of their movement. (video from Carvajal et al., 2019).....	56
Figure 5.4. Simulation result based on ratio of evacuee start evacuating after feeling ground shaking.....	57

Figure 5.5. Distribution ratio of early evacuees (G1 and G2) based on, A) assuming only EQ work as RES source and B) EQ and SPe work as RES sources.	57
Figure 5.6. Distance between people capture by camera 2 (Figure 4.4) to the evacuee running in front of them (68m) and the radii of group of people waiting in this area (11m).	59
Figure 5.7. Simulation result using the scenario of different influence between seeing early evacuee and seeing late evacuee.....	59
Figure 5.8. Simulation result using the scenario of different influence between seeing and hearing early evacuee and seeing and hearing late evacuee.	60
Figure 5.9. Building setting of the commercial area. A point of view from the left side of the 2 nd floor, B aerial view of the building, and C floor setting of the building. (picture from, (“Google Maps,” 2022)(“foursquare palu grand mall,”2022) , (CNN Indonesia,2022)).....	61
Figure 5.10. (top) Illustration of the circumstances at the building shown in Figure 5.9 during the 2018 Palu tsunami. (bottom) The detail of evacuation trigger exposure to the people capture in the video at commercial area.	62
Figure 5.11. Evacuation trigger based on the data collected from previous field surveys in Japan (Table 5.5). The larger circles indicate this source chosen by majority of people as the reasons why they initiate evacuation.	63

CHAPTER 1 INTRODUCTION

1.1 Background and Research Objective

In 2018, two tsunamis occurred within four months in Indonesia—September 28 at Palu, Sulawesi and December 22 at Sunda Strait. These tsunamis were unusual because they were not generated by standard earthquakes, such as thrust or reverse faults. The source of the Krakatau tsunami at the strait was a flank collapse caused by the eruption of the Anak-Krakatau volcano (Mulia et al., 2020) (Grilli et al., 2019). On the other hand, the Palu tsunami remains a mystery. Some scientists say it was a seismic tsunami (Higuera et al., 2021); some believe it was a landslide-induced tsunami (Liu et al., 2020; Nakata et al., 2020; Sassa and Takagawa, 2019); and others say it was generated by a combination of both, earthquakes and tsunamis (Gusman et al., 2019). The warning did not work properly because the Indonesian tsunami-

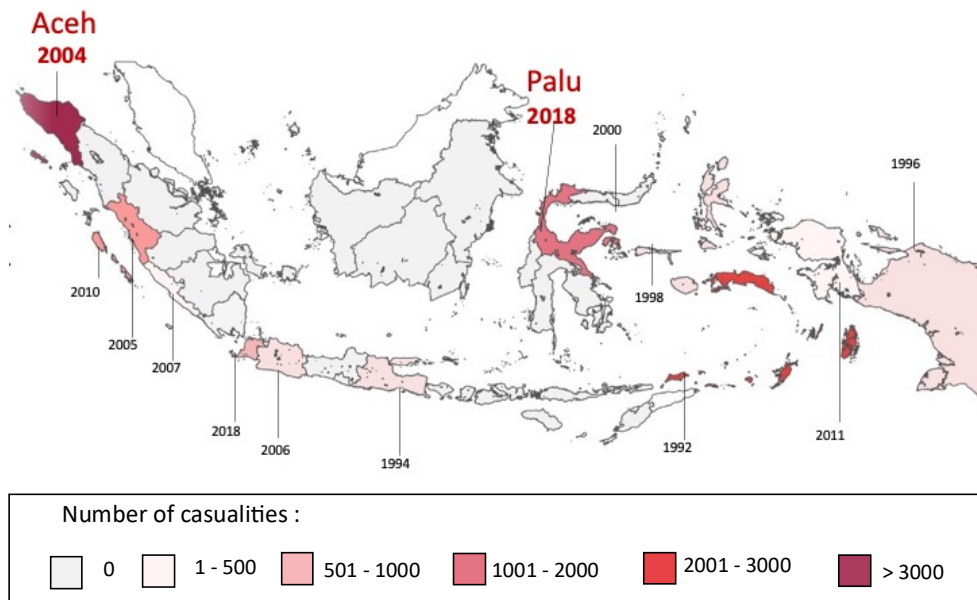


Figure 1.1. Map of tsunami history in Indonesia since 1990 - 2021. The color shows the number of casualties for each tsunami event. Data from Global Historical Database.

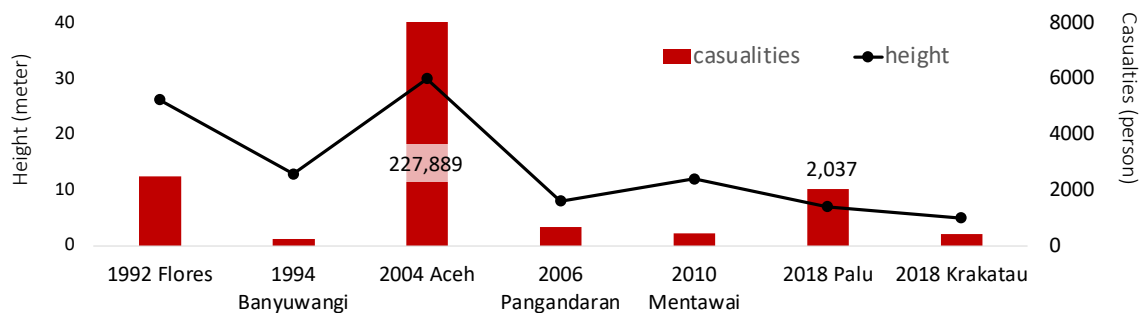


Figure 1.2. The bar chart of number of deaths caused by tsunami, only tsunamis caused more than 10 casualties are shown in the chart. Data from Global Historical Database.

warning system was designed for a typical subduction-zone earthquake source. Neither the government, the scientific community, nor the residents expected the tsunami to strike the coast. The short duration between the tsunami’s occurrence and the coast’s engulfment forced the local community to struggle in response.

Tsunamis have not been unusual in Indonesia—approximately 130 tsunamis have been documented between 1900 and 2022 (National Geophysical Data Center n.d.). A map of the tsunami history of Indonesia from 1990 to 2021 is shown in **Figure 1.1**. Of all the tsunami sources, 78% were seismic, 15% were non-seismic, and 7% were unknown. The total number of resulting deaths exceeded 12,371 (**Figure 1.2**), excluding the 227,899 deaths that occurred during the 2004 Indian Ocean tsunami (9.1 Mw).

People in the area have been familiar with tsunami phenomenon, and each region has had its local name for a tsunami. However, immediately after the 2004 Indian Ocean tsunami, which caused numerous casualties (227,899 deaths), the Indonesian government undertook disaster management to reduce losses. The last two tsunamis in Indonesia, the 2018 Palu and Sunda Strait tsunamis, killed approximately 5000 people. The Palu tsunami was a cascading disaster. The earthquake caused significant liquefaction, coastal subsidence, and landslide-induced tsunami. At that time, the scientific community, especially in Indonesia, lacked knowledge of this unprecedented disaster.

Three years have passed since the 2018 Palu Tsunami. Recovery and reconstruction have been performed continuously until now. To minimize the loss if the disaster occurs again, future development should include better mitigation. The Sendai Framework (Sendai framework for disaster risk reduction 2015–2030) provides a method to “achieve the substantial reduction of disaster risk and losses in lives, livelihoods and health and in the economic, physical, social, cultural and environmental assets of persons, businesses, communities and countries over the next 15 years”. The Sendai Framework outlines seven targets and four priorities for action to prevent new and existing disaster risks. This dissertation seeks to contribute to Sendai’s priorities: understanding disaster risk and enhancing disaster preparedness. These lessons learned from past disasters are the key to mitigation and risk reduction if the disaster occurs again.

Evacuation is the primary risk-reduction strategy for preventing casualties during tsunami events. There is limited real-event evacuation data to enhance the understanding of responses to warnings, evacuation decision-making, movements, and activities after evacuation (Tilley,

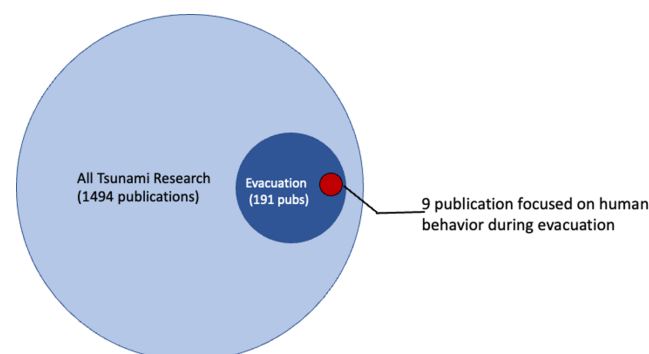


Figure 1.3. Numbers of tsunami research in Indonesia from 2004 – 2022. Data from caribencana.id

2020). Since the 2004 Indian Ocean Tsunami, 1494 papers related to tsunami research in Indonesia have been published, of which only 191 (10%) focused on evacuation research (“cari bencana,” n.d.) Most of those studies focused on aspects of the physical environment, whereas only 9 discussed human behavior during evacuations (**Figure 1.3**). Considering that Indonesia has historically suffered tremendously from tsunamis, we believe that more evacuation research is necessary.

This research is divided into two parts. The first part focuses on understanding landslide-induced tsunamis as a natural phenomenon. Many aspects of the 2018 Palu tsunami are relatively well-known. However, some uncertainties remain unresolved. Till date, at least 11 studies have been conducted on the Palu tsunami mechanism. They have used numerical simulations with different interpretations regarding the primary source of tsunami generation. Owing to the difficulty in sampling and measuring submarine landslides, rough assumptions of landslide parameters were often made, leading to significant uncertainties. In the 2018 Palu event, the earthquake was followed by immediate cascading disasters of coastal subsidence, landslides on land and submarines, and tsunamis. This situation provides opportunities to analyze landslide phenomena on land to characterize the submarine landslide causing the tsunami.

Part two of this research analyzes evacuation behavior as a social phenomenon. When a disaster occurs, the intensive decision-making process is considerably affected by a sense of urgency. A public (non-expert) decision to start evacuating does not always follow logical judgment. When people obtained warning information from authorities, they would nevertheless choose whether to evacuate or not based on their own knowledge and experience. The logical decision-making framework cannot explain many tsunami-evacuation scenarios. Before the 2004 Indian Ocean tsunami, residents of the affected area had no prior knowledge of tsunamis. A survivor from Banda Aceh testified that he did not believe that seawater could rise far inland. However, when he heard an elderly neighbor shouting, “Go, the seawater has risen,” he followed the instructions and moved away (Suwignyo, 2019). In the 2006 South Java tsunami, the post-tsunami interviews revealed that residents were warned by people screaming while running away and observing unusually receding seawater (Muhari et al., 2012). In the 2010 Mentawai tsunami, a survivor reported that there was no tsunami warning, the ground shaking was weak, and he escaped after hearing a loud sound approximately five minutes after shaking (Satake et al., 2013). The lives of all residents on the coastal side of the village were saved because one person heard a tsunami approaching and ran to the hill to transmit information to other residents (Tomita et al., 2011). In the 2018 Palu tsunami, the government gave incorrect warnings and failed to disseminate them. A resident of Palu city said that she thought the tsunami was not real because the siren had not sounded and the water did not recede (UNDRR and UNESCO-IOC, 2019). In this event, observing others’ evacuation played a significant role in prompting evacuation (Harnantyarini et al., 2020). There was no warning during the 2018 Sunda Strait tsunami because it was generated by the flank collapse of Anak Krakatau with no preceding earthquake. More than half of the survivors decided to evacuate after hearing or seeing an approaching tsunami (Takabatake et al., 2019).

These examples demonstrate that residents initiated the evacuation intuitively because of “must escape” vibe. We refer to this situation as the reality of evacuation start (RES). Its intensity level depends on environmental, social, and warning cues. They are referred to as

RES sources. The urgency to immediately save lives is elevated by numerous sources impacting people, long exposure to RES sources, and high RES intensity. The sense of urgency affects people differently. It depends on their familiarity with the disaster, owing to training, experience, or emergency drills. We refer to this as awareness level of danger (ALD).

Based on the explanation above, there are three important aspects for understanding tsunami evacuation. First, finding the types of RES sources that worked, triggering Indonesians to start evacuating. Second, estimating the impact and exposure of RES sources. Third, analyzing evacuation behavior during a tsunami event, considering the tsunami characteristics. Observing the evacuation process in the 2018 Palu event, it is important to address the gap in understanding tsunami-evacuation behaviors, especially the initiation process. We found similarities and differences between seismic and non-seismic tsunami evacuations. Moreover, we conducted a case study comparing the evacuation process in Indonesia and Japan. Finally, this study provided valuable information for better tsunami mitigation.

1.2 Overview of the 2018 Palu Cascading Disaster

The September 28, 2018 earthquake in Palu-Sulawesi was a strike-slip earthquake with a magnitude of 7.5, which occurred at 18:02 hours local time. The earthquake caused significant liquefaction, coastal subsidence, and landslide-induced tsunamis. The epicenter (red star) and shaking intensity (estimated by The United States Geological Survey (USGS)) show strong shaking (MMI 7.0–8.0) around Palu Valley (black box) as shown in **Figure 1.4**. The tsunami occurred along the coast of Palu Bay and was recorded in the Pantoloan Port tide gauge, located in the central-eastern part of the bay. The timeline of this earthquake and tsunami, as presented by the Indonesia Meteorology and Geophysical Agency (Badan Meteorologi, Klimatologi, dan Geofisika Indonesia (BMKG), n.d.) is shown in **Table 1.1**. From the record, it is known that



Figure 1.4 Map of Indonesia and red box shows Palu where the disaster occurred (insert). Location of epicenter (red star), shaking intensity, and landslide locations (black box).

Table 1.1. Chronological of earthquake, tsunami, and early warning during the 2018 Palu event

Time	Condition
18:02	The earthquake happened.
18:07	High alert-level tsunami early warning (0.5–3 m high) in Palu (evacuation).
17:10-17:13	Tsunami arrival time. Viral video of the tsunami in Palu at dusk (but still daylight) with duration ± 3 min; confirmed with a statement that the tsunami struck shortly after the big earthquake.
17:27	Tsunami observed in Mamuju. The monitored tide-gauge results show the tsunami height is 6 cm. The tsunami is not significant.
17:36	The tsunami warning officially ended by BMKG.

the tsunami arrived only 6 min after the earthquake, with a wave height of approximately 2 m. The short time window made it impossible for the public to receive a tsunami alert and react before the tsunami arrived.

Besides the tsunami, the earthquake caused massive landslides along the Palu Valley (black box in **Figure 1.4**, Balaroa (in the southwest of the map), Petobo (around 8 km to the southeast), and Jono Oge (12 km to the southeast). The Palu Valley is located in the Palu–Koro system, which is a major active fault in Sulawesi. Based on the USGS Catalog, significant earthquakes occurred close to the Palu–Koro Fault in 1968 (Mw 6.7), 1998 (Mw 6.7 and 6), 2005 (Mw 6.3), 2012 (Mw 6.3), and 2018 (Mw 7.5 and 6.1). However, there was no historical record of a moderate-to-large earthquake in the Palu Valley prior to 2018.

In the Palu Valley area, there was no observation station dedicated to monitoring the ground movement with an instrument or sensor. Thus, the exact time of the tsunami was unknown. The BMKG also lacked an early-warning system for landslides. Hence, there was no warning before the liquefaction. The information available from videos captured by local residents showed that liquefaction inland occurred after ground shaking.

Shortly after the earthquake occurred, electricity failure created a blackout situation, constraining communication and blocking the reception of warnings for earthquakes and tsunamis (Yulianto et al., 2020). Power shortages also occurred at the tide-gauge station in Pantoloan. Thus, the central government was not aware of the tsunami occurrence inside Palu Bay. The TEWS failed to disseminate warning messages to the residents.

After the Palu earthquake, the alert from the BMKG indicated that Palu's strike-slip fault could have produced only a small tsunami height. However, the actual tsunami was higher than the warning. The BMKG stated that the InaTEWS successfully delivered early warnings to communities. No instrument or transmission errors were observed. Warning information was sent to the National Disaster Management Authority (BNPB), local government, media, and at-risk communities. Despite government claims, the 4340 casualties caused by earthquakes, liquefaction, and tsunamis, show that disaster management in Indonesia was inadequate to mitigate the calamity, especially for cascading disasters. Despite the massive destruction, several post-event surveys found that the number of tsunami victims was very low, or even nil, in some coastal locations (UNDRR and UNESCO-IOC, 2019).

1.3 The Identified Problems During The 2018 Palu Tsunami.

The summary from the literature review found several problems regarding the 2018 Palu tsunami.

1. Unidentified risks in the Palu area: The 2016-20 Palu disaster risk-analysis document (Amri, 2016) states that out of eight sub-districts, seven are in the category of high tsunami risk; and only one is in the low tsunami-risk category. The total number of tsunami-prone areas is 1,785 ha. The 2016-20 Donggala Disaster Risk Analysis document states that 14 sub-districts are in the category of high tsunami risk, with a total tsunami-prone area of 5,846 ha. However, although several scientific analyses and historical data detailing repeated tsunami occurrences in these areas, both documents state that there had never been a tsunami disaster in Palu or Donggala. Both documents reflected a lack of historical disaster information that could have been used as a reference for disaster risk-reduction policy.
2. Lack of knowledge of unprecedented disasters: Landslide-induced tsunamis are rare compared to tsunamis generated by earthquakes. Despite the low frequency, the 2018 Palu tsunami demonstrated that the impact of the landslide-induced tsunami could be severe. This event surprised not only the public but the scientific community too, owing to the relatively unknown risk of submarine landslides.
3. Unreliable communication during the disaster phase (Yulianto et al., 2020): It was found that when a disaster occurred, people at risk did not receive warning information, as it is disseminated using SMS on cellular phones, television, and radio. The electricity failure rendered people incapable of accessing the information from electronic media.
4. Limitations of early warning technology (Titov, 2021) (UNDRR and UNESCO-IOC, 2019): The philosophy of early warning is to enable sufficient time for communities at risk so that individuals can save themselves before a natural-hazard impact. The InaTEWS system has limitations with respect to near-source tsunamis. It is more effective for tsunamis triggered by earthquakes from subduction zones, in which the wave arrival time is typically 20 min or more. With tsunami arrival times of less than 10 min, there is not enough time for people to successfully evacuate.
5. Uncertain levels of disaster awareness and preparedness in local communities: Considering numerous casualties, it can be concluded that the level of people's awareness and preparedness was very low, as stated in some academic papers (Titov, 2021). However, based on post-event reports (Harnantyari et al., 2020; Omira et al., 2019; UNDRR and UNESCO-IOC, 2019), we believe that the levels varied between regions. Some local possessed high-level knowledge and awareness of tsunamis, while others did not.

1.4 Development of Disaster Risk Reduction in Indonesia

The devastating event of the 2004 Indian Ocean tsunami, which caused numerous casualties and extensive damage, awakened the Indonesian government to realize the high threat and vulnerability of tsunamis. The government undertook disaster management to reduce the losses. The development of technology science and the law of disaster-risk reduction in Indonesia are shown in **Table 1.2**. With the help of Germany, the first early-warning system in Indonesia began to develop in 2005 and was named the German-Indonesia Tsunami Early Warning System (GITEWS). In 2008, this system was fully operated only by the Indonesian government

and changed its name to the Indonesia Tsunami Early Warning System (Ina-TEWS). Despite the advanced numerical performance, TEWS still relies on precomputed databases based on seismic sources. The Ina-TEWS has not been used for tsunamis caused by landslides and volcanic eruptions. When an expected tsunami is a near field tsunami, landslide-induced tsunami or volcanic-induced tsunami this system does not function properly. This was proven by the Mentawai 2010, Sulawesi 2018, and Sunda Strait 2018 tsunamis. Enormous casualties occurred due to failed warnings and poorly prepared communities.

Because the available timespan between a warning and the impact of a tsunami wave in Indonesia is generally very short, all the necessary preparations should have been made in advance. Besides TEWS development, proper evacuation plans are essential for providing communities with the necessary references, guidance, and information. Each country has different cultural and social backgrounds and geographical features. They affect society's actions and perceptions about tsunami risk and people's threshold to the sense of danger.

Table 1.2. Development of technology, science and law of disaster risk reduction in Indonesia

Year	Month	Event	Location
2004	December	Indian Ocean Tsunami	Aceh
2005		Establishment of Indonesia Tsunami Early Warning System	
	December	Tsunami Drill 1	Padang
2006	July	Pangandaran Tsunami	West Java
	September	Ministerial Decree of The Coordinating Minister for People Welfare no. 21/2006	
	December	Tsunami Drill 2	Bali
2007	April	Indonesia Law 24/2007 - Disaster Management Law	
	December	Tsunami Drill 3	Banten
2008	November	Indonesia Tsunami Early Warning System (InaTEWS) launched	
2009		Improvement of tsunami warning dissemination from 10 to 5 minutes	
2010	October	Mentawai Tsunami	
2018	September	Palu Tsunami	Central Sulawesi
	December	Krakatau Tsunami	Sunda Strait, Banten
2019	January	Formulated Presidential regulation on the strengthening of the national multi-hazard early warning system (SISMAS PERDIMANA)	

Considering Indonesia to be one of the world's most disaster-prone countries, there is very little evacuation research and no standardized survey method. This situation causes some important factors in the evacuation process to not be covered. This research contributes to understanding the Indonesian people's responses after they are subjected to numerous sources containing information about tsunami danger.

1.5 Thesis Outline

This thesis comprises six chapters.

Chapter 1 establishes the context of this study by detailing the aims and objectives of this thesis. This chapter introduces the 2018 Palu earthquake and tsunami events and provides information on the location, disaster timeline, and casualties.

Chapter 2 provides an analysis of the natural phenomena that occurred during the 2018 Palu earthquake and tsunami. This section provides insight into the uncertainty and problems in completely understanding hazard mechanisms. It explains the proposed new approach for using parameters obtained from liquefaction analyses (inland) for a landslide-induced tsunami simulation.

Chapter 3 explains the definitions and concepts of tsunami evacuation used in this study. First, the chapter summarizes the definitions of evacuation and evacuation phases. Then it explains the internal and external factors affecting human behavior during evacuation. Specifically it covers the influence of natural and social conditions urging people to initiate tsunami evacuations.

Chapter 4 presents the findings of tsunami-evacuation triggers used as the standard for general evacuation cases in Indonesia. That is followed by an in-depth analysis of the evacuation behavior of people indoors and outdoors, using post-survey reports and videos recorded during the 2018 Palu tsunami.

Chapter 5 presents tsunami-evacuation simulation using the observations to obtain realistic evacuation-modeling outputs. The results were used for quantitative and spatiotemporal analyses of each reality-of-evacuation-start source. Correlations between the uniqueness of the natural phenomena at Palu in 2018 and its influence on evacuation behavior are discussed.

Chapter 6 presents a summary and conclusions of this research. The chapter point out the finding from understanding the hazard mechanism and evacuation-initiation process response to the 2018 Palu earthquake and tsunami and recommends what needs to be carried out in future work.

REFERENCES

- Amri, Mohd.R., 2016. RBI : risiko bencana Indonesia / penulis, Mohd. Robi Amri [and seven others] ; editor, Raditya Jati, Mohd. Robi Amri. Badan Nasional Penanggulangan Bencana, [Jakarta].
- Badan Meteorologi, Klimatologi, dan Geofisika Indonesia (BMKG) [WWW Document], n.d. URL <https://www.bmkg.go.id/press-release/?lang=ID&p=gempabumi-tektunik-m7-7-kabupaten-donggala-sulawesi-tengah-pada-hari-jumat-28-september-2018-berpotensi-tsunami&tag=press-release> (accessed 2020-02-03).
- Auto crawling machine to find out recent & locally-relevant research papers and journal on in Indonesia : cari bencana, <https://caribencana.id/> (accessed 2022-02-21)
- Grilli, S.T., Tappin, D.R., Carey, S., Watt, S.F.L., Ward, S.N., Grilli, A.R., Engwell, S.L., Zhang, C., Kirby, J.T., Schambach, L., Muin, M., 2019. Modelling of the tsunami from the December 22, 2018 lateral collapse of Anak Krakatau volcano in the Sunda Straits, Indonesia. *Sci Rep* 9, 11946. <https://doi.org/10.1038/s41598-019-48327-6>
- Gusman, A.R., Supendi, P., Nugraha, A.D., Power, W., Latief, H., Sunendar, H., Widiyantoro, S., Daryono, Wiyono, S.H., Hakim, A., Muhari, A., Wang, X., Burbidge, D., Palgunadi, K., Hamling, I., Daryono, M.R., 2019. Source Model for the Tsunami Inside Palu Bay Following the 2018 Palu Earthquake, Indonesia. *Geophys. Res. Lett.* 46, 8721–8730. <https://doi.org/10.1029/2019GL082717>

- Hamzah, L., Puspito, N.T., Imamura, F., 2000. Tsunami Catalog and Zones in Indonesia. *Journal of Natural Disaster Science* 22, 25–43. <https://doi.org/10.2328/jnds.22.25>
- Harnantaryi, A.S., Takabatake, T., Esteban, M., Valenzuela, P., Nishida, Y., Shibayama, T., Achiari, H., Rusli, Marzuki, A.G., Marzuki, M.F.H., Aránguiz, R., Kyaw, T.O., 2020. Tsunami awareness and evacuation behaviour during the 2018 Sulawesi Earthquake tsunami. *International Journal of Disaster Risk Reduction* 43, 101389. <https://doi.org/10.1016/j.ijdr.2019.101389>
- Higuera, P., Sepulveda, I., Liu, P.L.-F., 2021. Filling in the gaps of the tsunamigenic sources in 2018 Palu Bay tsunami. *arXiv:2105.07718*.
- Kelfoun, K., Giachetti, T., Labazuy, P., 2010. Landslide-generated tsunamis at Réunion Island. *J. Geophys. Res.* 115, F04012. <https://doi.org/10.1029/2009JF001381>
- Liu, P.L.-F., Higuera, P., Husrin, S., Prasetya, G.S., Prihantono, J., Diastomo, H., Pryambodo, D.G., Susmoro, H., 2020. Coastal landslides in Palu Bay during 2018 Sulawesi earthquake and tsunami. *Landslides* 17, 2085–2098. <https://doi.org/10.1007/s10346-020-01417-3>
- Muhari, A., Muck, M., Diposaptono, S., Spahn, H., 2012. Tsunami mitigation planning in Pacitan, Indonesia: A review of existing efforts and ways ahead. *Science of Tsunami Hazards* 31, 244–267.
- Mulia, I.E., Watada, S., Ho, T., Satake, K., Wang, Y., Aditya, A., 2020. Simulation of the 2018 Tsunami Due to the Flank Failure of Anak Krakatau Volcano and Implication for Future Observing Systems. *Geophys. Res. Lett.* 47. <https://doi.org/10.1029/2020GL087334>
- Nakata, K., Katsumata, A., Muhari, A., 2020. Submarine landslide source models consistent with multiple tsunami records of the 2018 Palu tsunami, Sulawesi, Indonesia. *Earth Planets Space* 72, 44. <https://doi.org/10.1186/s40623-020-01169-3>
- National Geophysical Data Center, n.d. Global Historical Tsunami Database. <https://doi.org/10.7289/V5PN93H7>
- Omira, R., Dogan, G.G., Hidayat, R., Husrin, S., Prasetya, G., Annunziato, A., Proietti, C., Probst, P., Papparo, M.A., Wronna, M., Zaytsev, A., Pronin, P., Giniyatullin, A., Putra, P.S., Hartanto, D., Ginanjar, G., Kongko, W., Pelinovsky, E., Yalciner, A.C., 2019. The September 28th, 2018, Tsunami In Palu-Sulawesi, Indonesia: A Post-Event Field Survey. *Pure Appl. Geophys.* 176, 1379–1395. <https://doi.org/10.1007/s00024-019-02145-z>
- Sassa, S., Takagawa, T., 2019. Liquefied gravity flow-induced tsunami: first evidence and comparison from the 2018 Indonesia Sulawesi earthquake and tsunami disasters. *Landslides* 16, 195–200. <https://doi.org/10.1007/s10346-018-1114-x>
- Satake, K., Nishimura, Y., Putra, P.S., Gusman, A.R., Sunendar, H., Fujii, Y., Tanioka, Y., Latief, H., Yulianto, E., 2013. Tsunami Source of the 2010 Mentawai, Indonesia Earthquake Inferred from Tsunami Field Survey and Waveform Modeling. *Pure Appl. Geophys.* 170, 1567–1582. <https://doi.org/10.1007/s00024-012-0536-y>
- Sendai framework for disaster risk reduction 2015–2030. In: UN world conference on disaster risk reduction, 2015 March 14–18, Sendai, Japan. Geneva: United Nations Office for Disaster Risk Reduction; 2015. http://www.wcdrr.org/uploads/Sendai_Framework_for_Disaster_Risk_Reduction_2015-2030.pdf
- Suwignyo, A., 2019. A Tsunami-Related Life History of Survivors in Banda Aceh, Indonesia and Sendai, Japan. *JSP* 23, 120. <https://doi.org/10.22146/jsp.49876>
- Takabatake, T., Shibayama, T., Esteban, M., Achiari, H., Nurisman, N., Gelfi, M., Tarigan, T.A., Kencana, E.R., Fauzi, M.A.R., Panalaran, S., Harnantaryi, A.S., Kyaw, T.O., 2019. Field survey and evacuation behaviour during the 2018 Sunda Strait tsunami. *Coastal Engineering Journal* 61, 423–443. <https://doi.org/10.1080/21664250.2019.1647963>
- The United States Geological Survey (USGS) catalog, <https://earthquake.usgs.gov/earthquakes/search/> (accessed 2020-11-20).
- The United States Geological Survey (USGS), <https://www.usgs.gov/news/magnitude-75-earthquake-near-palu-indonesia>. (accessed 2020-11-20).

- Tilley, L.R., 2020. Assessing tsunami evacuation behaviour and dynamics of a near-source threat – the case study of Kaikōura township following the 2016 Kaikōura earthquake. <https://doi.org/10.26021/10367>
- Titov, V.V., 2021. Hard Lessons of the 2018 Indonesian Tsunamis. *Pure Appl. Geophys.* <https://doi.org/10.1007/s00024-021-02731-0>
- Tomita T., Arikawa T., Kumagai K., Matsutomi H., Harada K., Diposaptono S., 2011. Field Survey of 2010 Mentawai Earthquake Tsunami. *Journal of Japan Society of Civil Engineers, Ser. B2 (Coastal Engineering)* 67, I_1281-I_1285. https://doi.org/10.2208/kaigan.67.I_1281
- UNDRR, UNESCO-IOC, 2019. Limitations and Challenges of Early Warning Systems: A Case Study of the 2018 Palu-Donggala Tsunami, IOC Technical Series. United Nations Office for Disaster Risk Reduction (UNDRR), Regional Office for Asia and the Pacific, and the Intergovernmental Oceanographic Commission of United Nations Educational, Scientific and Cultural Organization.
- Yulianto, E., Utari, P., Satyawan, I.A., 2020. Communication technology support in disaster-prone areas: Case study of earthquake, tsunami and liquefaction in Palu, Indonesia. *International Journal of Disaster Risk Reduction* 45, 101457. <https://doi.org/10.1016/j.ijdrr.2019.101457>

CHAPTER 2 ANALYSIS OF LANDSLIDE INDUCED TSUNAMI HAZARD

Indonesia is surrounded by large tectonic plate, the collision of the Indo-Australian tectonic plates in the south, the Eurasian Plate in the North and the Pacific Plate in the Northeast to the southwest and considered as one of the most tectonic active areas in the world. From 1600 to 2007, Indonesia has experienced several tsunamis, with approximately 172 tsunamis occurring. From the statistical tsunami in Indonesia it is known that 90% have been caused by earthquakes, 8 % by volcanic eruption and 1% by landslides (Hamzah et al., 2000). During 1990 – 2020, there were 13 tsunamis happened in Indonesia. Tsunami cause by earthquake 11 events, by landslides 1 event, and by volcanic eruption 1 event.

As mentioned on **Chapter 1**, unidentified risk and lack of knowledge of unprecedented disaster are problems for disaster preparedness. Learn a lesson from the past disaster would be a key for the mitigation and risk reduction if disaster happened again in the future. The 2018 Palu tsunami is quite unique because it was not generated by ‘typical’ subduction-zone earthquake sources. Hence, the tsunami generated by strike-slip earthquake and submarine landslide. Since the tsunami mechanism is not a general one then the established tsunami preparedness is not sufficient. Improvement of disaster preparedness, such as warning system and evacuation plan, needs to be done based on new understanding of the nature of tsunami hazard. This chapter will address problems related to understanding the tsunami hazard.

Tsunami simulation is a tool to analyze and give the appropriate interpretations. Landslide-induced tsunami simulation using a two-layer method, where the model simulates the tsunami genesis by the interaction of two fluids (landslide and water) were commonly used. The landslide-induced tsunami simulation in this study employed a numerical package develop by Kelfoun (Kelfoun et al., 2010) called Volcflow, an open-source program and can be accessed online (<https://lmv.uca.fr/volcflow/>). The code has been used and tested against various landslide-induce tsunami cases, such as tsunami triggered by the Güimar debris avalanche (Kelfoun and Druitt, 2005), flank failure of Fogos volcano (Kelfoun, 2008) and the latest flank failure of Anak Krakatau volcano (Mulia et al., 2020).

Data and parameter needed for the landslide-induced tsunami simulation are the location of potential source area, the landslide geometry, water density and viscosity, solid mass density and shear stress. The potential source and landslide geometry refer to the previous landslide-induced tsunami research (Nakata et al., 2020), and parameter value for water density and viscosity, and solid mass density refer to (Kelfoun et al., 2010). The simulation needs landslide parameters to accurately simulate the tsunami genesis. However, such parameters are often roughly estimated due to the difficulty in sampling and measuring of submarine landslides. In the 2018 Palu event, almost immediately after the earthquake, coastal subsidence, landslides both on land and submarine occurred, which then followed by the tsunami. This situation gives us opportunities to analyze the landslide phenomena on land and used the result as the input for the landslide-induced tsunami simulation. So, we can compare simulation used the shear stress proposed for general cases and shear stress calculated from the inland liquefaction.

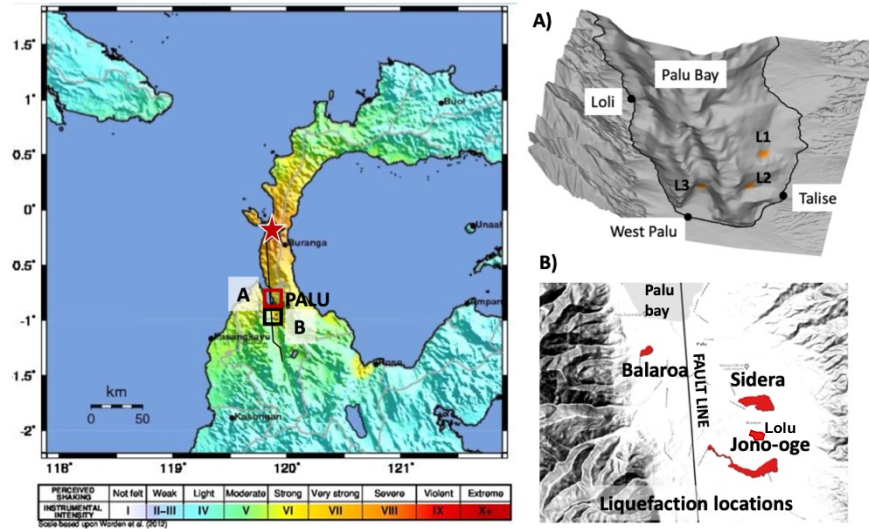


Figure 2.1. Map of epicenter (red star), shaking intensity, Palu bay coastal area (red box), and in-land area (black box) (USGS, 2020). A) bathymetry around palu bay, L1-L3 (orange circle) are the possible submarine landslide location (Nakata et al., 2020). B) Four liquefaction area around Palu valley, Sibalaya not shown in the figure, it is located 20 km south of Jono-Oge.

Unfortunately, there was no instrument recorded the shaking and movement of the landslide at the site. However, we found the video recorded the landslide in Jono-Oge, one of the area in Palu valley where the liquefaction occurred (Likui-faksi jono oge(palu,sigi,donggala). Si perekam video terbawa likuifaksi., n.d.). Therefore, first we did video analysis using optical and mathematical approach to obtain landslide characteristics which cannot be regained from a field survey. To find the shear stress that can be used as one of input parameters in the tsunami model, the pore water pressure and displacement should agree with the result from the analytical approach.

In this study, we focus on the southern part of the Palu bay. The bay profile and potential submarine landslide locations considered in this study can be seen in **Fig.2.1A**. There were five major liquefaction areas as shown in **Fig. 2.1B**, except Sibalaya because it is 40 km from Palu Bay. The landslide in Jono-oge was the area that we analyzed to get input parameters for the landslide in the tsunami simulation. We choose Jon-oge area because in this location there was a footage capturing the landslide movement which could be used to verify our model.

2.1 Estimation of landslide velocity in Jono-Oge using video analysis

The landslide velocity is an important factor in disaster mitigation, and can be calculated using the slope geometry (Souisa et al., 2018), remote sensing (Zhao and Lu, 2018), and real-time video recording (Jiang et al., 2016). A real-time video of a landslide may include significant information on the slide, such as pre-failure behaviors, failure format, sliding characteristics and velocity, runout region, post-failure characteristics, and destructiveness (Jiang et al., 2016). To date, there have been no studies using video recordings focused on the liquefaction-induced landslide velocity. This study aims to use the available video to obtain one of the landslide characteristics, specifically the landslide velocity, which cannot be

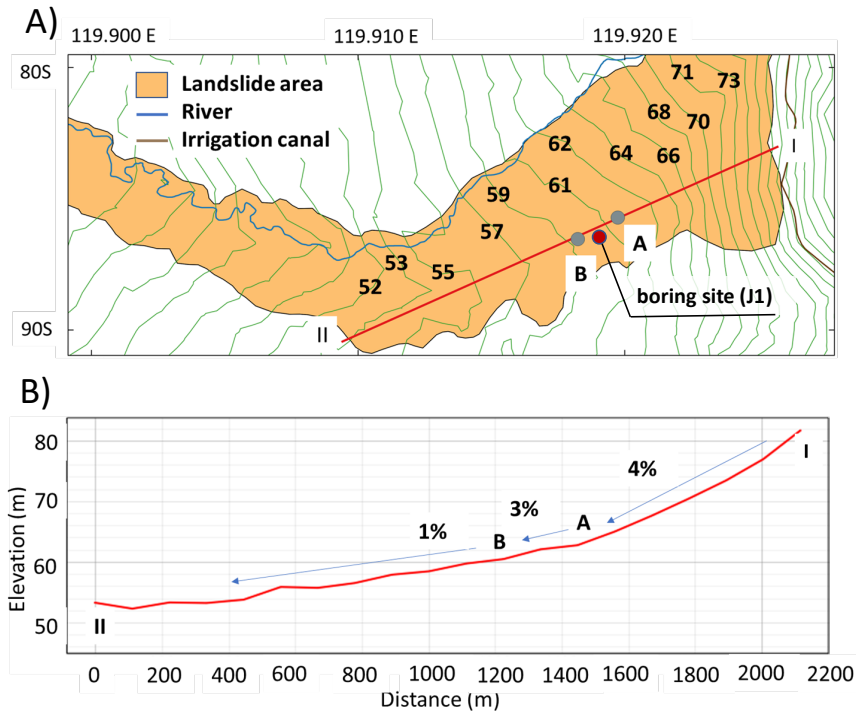


Figure 2.2. A) Jono-Oge elevation countour map, point A to B were the location where the possible landslide velocity known, point J1 is the boring site location. B) Elevation and slope of Jono-Oge along I-II.

regained from a field survey. because it is important to clarify the sliding mechanisms and develop a model with a precise prediction function. Furthermore, this velocity information can be used as information for a landslide-induced tsunami simulation model

Based on the Jono-Oge land-use map, the majority of this area was used for paddy fields and gained water from the irrigation canal. Field surveys (Montgomery et al., 2021; Robertson et al., 2019) revealed that the starting point of all landslides on the east side, including Jono-Oge, were bounded by an irrigation canal. The landslide appeared to have initiated when the elevation transitioned from 80 to 70 m, as the slope decreased from approximately 4% to 1%, as shown in **Figure 2.2** The average slope in the Jono-oge area was only 1%, which is an extremely gentle alluvial slope. Therefore, researcher suggested that irrigation in this paddy field has raised the water table and could create a liquefied layer (Bradley et al., 2019; Watkinson and Hall, 2019).

The video was recorded by the survivor climbed to the rooftop of his house after feeling a strong ground motion (Kisah Nyata Korban Selamat Likuifaksi Palu Eps 72 Part 1,). The ground then started to move, and he recorded the situation using his smartphone. This video is unique in that it was taken from a house that was brought along by a debris flow. The video shows that the land movement was like a flow of water carried along with buildings and trees, with some structures remaining on the ground. The video can be accessed online (Likuifaksi jono oge, <https://www.youtube.com/watch?v=tXT8MSKehuM>), and frames of the video used as the material for this research are shown in **Figure 2.3**. In this study, a video content analysis (VCA) is applied to determine the velocity of the recorded landslide, using the ffmpeg program (www.ffmpeg.org). The VCA was conducted using an image sequence converted into a single



Figure 2.3. Image sequence in the video recorded Jono-Oge landslide (photographs captured from video).

image per second, with a video duration of 2 min and 5 s, 125 images were produced. We chose the following sequences: the beginning of the video to identify the recording location (**Figure 2.3A**) and scenes of unmoved structures to analyze the camera angle and position (**Figure 2.3B - Figure 2.3E**).

The video was recorded using a mobile phone which created particular quality problems, such as low-quality resolution due to video compression and blurry effect caused by camera vibration. Unlike fixed cameras, moving cameras operate with various degrees of movement and autonomy. In the simple case of a fixed camera, changes between consecutive frames are only caused by moving objects; therefore, it is easier to use an auto-tracking motion program. Previous studies found that difficulties in using a moving camera arise when detecting moving objects owing to changes in the depth and complex movements (Yazdi and Bouwmans, 2018). Therefore, in this study, we decided to obtain the landslide velocity by eliminating using an auto-tracking motion program. Instead, we use information from past survey reports, satellite imagery (“Digital Globe Maxar,” 2020), and Digital Elevation Models (DEM) data, and apply basic rules of geometrical optics and perspective vision with Google Earth and QGIS (QGIS Development Team, 2020) to determine the location, pathway, and velocity of the recorded landslide.

The velocity was calculated using a simple formula, as described in **Eq. 2.1** To use the formula, two essential components are required, namely, where the start and end locations (l_0 and l_1) are and how long (t_0 and t_1) it takes to record between those locations. This information can be obtained through a video content analysis. The stages of analysis are divided into three parts: initial location identification, camera movement path estimation, and camera angle analysis..

$$v = \frac{L}{T} = \frac{l_1 - l_0}{t_1 - t_0} \quad (2.1)$$

The first step is to identify the initial location at which the recording started. In practice, we conducted the initial location identification after estimating the camera movement direction, as described later. The second step is to estimate the path and direction of the camera movement. This step was necessary because this video was recorded from the top of the house, which was carried away by the landslide. Based on surveys and satellite imagery, it is known that the recorded landslide occurred in the Jono-Oge area moved from east to west.

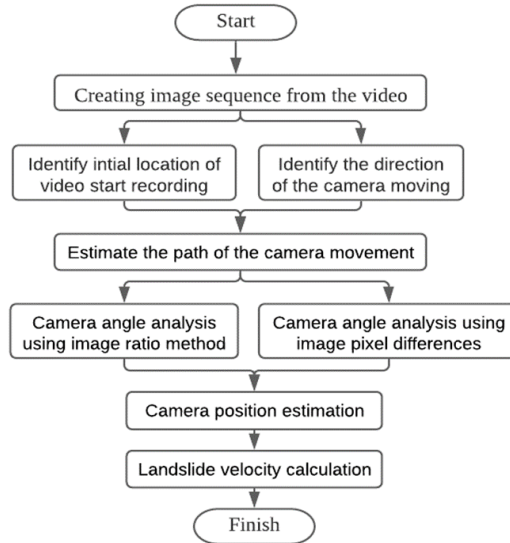


Figure 2.4. Flowchart of landslide velocity estimation using video content analysis method.

The change in the object in the image was measured by determining a point on the object in the images. Here, the camera path was estimated based on the initial position of the camera and the direction of the camera movement. In addition, we applied two types of camera angle analyses, namely, the image ratio method and pixel differences method. Thus, the flow of the landslide velocity analysis is summarized in the flowchart shown in **Figure 2.4**.

The third step is applying a camera angle analysis to determine the exact location of the camera when capturing an object. During this step, the reference object is required to determine the location of the camera. For this purpose, the red-roofed house recorded in the video shown in **Figure 2.3C and D**, was used. Using digital imagery (“Digital Globe Maxar,” 2020) taken after the disaster on September 28, 2018, it was found that there is one red-roofed house in the middle of the Jono-Oge Landslide with coordinates of -0.98579 E, 119.91965 S. When comparing with the satellite image taken before the disaster, it was confirmed that the red-roofed house had the same coordinates, which indicated that it was not moving during the Jono-Oge landslide. This result is also validated through a survey (Montgomery et al., 2021)(Robertson et al., 2019) by which it was found that the red-roofed house in Jono-Oge remained in the original position, despite the mudflowing through the building.

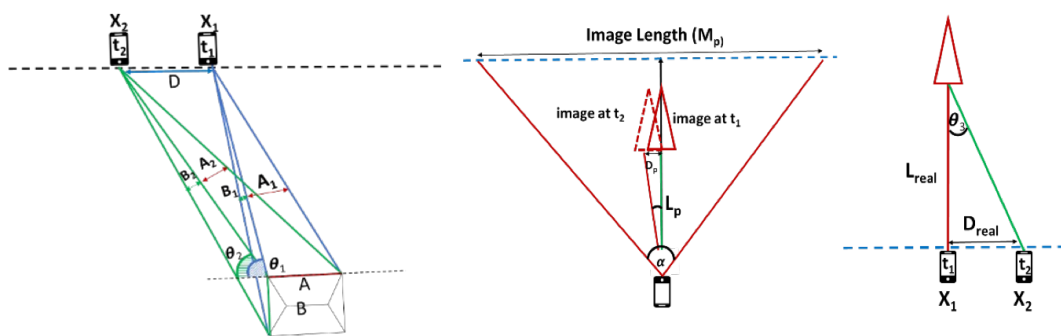


Figure 2.5. Calculation method using ratio of object in the image sequence to calculate camera angle.

The camera angle analysis for the red-roofed house was conducted using the ratio of some lengths in the images of a reference object. When the camera does not directly face an object, the angle becomes smaller (θ) and the object will appear smaller. Thus, as shown in **Figure 2.5**, the angle of recording can be calculated from the ratio of the sizes of the two walls in different directions as shown in **Eq. 2.2**.

$$\theta_i = \arctan\left(\frac{A_i/A}{B_i/B}\right) \quad (2.2)$$

2.1.1 Identification of landslide movement direction

From the video sequence (**Figure 2.3**), there are two structures that can be identified: a house with a red roof (**Figure 2.3 C-D**) and a steel tower (**Figure 2.3 E-F**). From 103 s until the end of the video recording, only a tree was recorded, and no other buildings could be identified. From the post-disaster survey (Montgomery et al., 2021), they found the church ruins at coordinates -0.98942 S, 119.91007 E. The church position after the disaster, represented by the black color of the church symbol, can be seen in **Figure 2.6**. The original position of the church before the disaster, represented by white color of the church symbol in **Figure 2.6**, and the coordinates is -0.98508 S, 119.919244 E. The landslide pathway estimated by connecting the church position before the disaster to the after disaster. We assumed that all houses near here moved parallel to the estimated pathway.

2.1.2 Identification of the video starting point

The initial location of the recording video is unknown; however, there is some information indicating that; 1) the house had already moved before the video started recording, 2) there were no other houses on the right or left, and 3) during the initial recording, the camera video capturing the area surrounded by trees and paddy fields (**Figure 2.6**). Based on the VCA and satellite image, the house is located close to the possible landslide pathway obtained from the church location (dotted line) as shown in **Figure 2.7**. The state around the house was also similar to the landscape captured in the video. Thus, we identified the house as the possible location of the initial point of the video recording with coordinates of -0.98450 S, 119.92089 E, and we assume that the position of the video recording moved parallel to the church landslide pathway.



Figure 2.6. Landscape and situation captured at the beginning of the video until the first 17 seconds.



Figure 2.7. Identified building from the video plotted in the satellite image before and after the landslide occurred. Possible landslide pathway connected by the church (GPID Patmos Jono Oge) before (white color of church symbol) and after the landslide occurred (black color of church symbol).

2.1.3 Image angle analysis using length ratio of the red-roofed house

The reference object in the analysis is the rooftop of a red-roofed house. The images used in the analysis were at $t = 27$ and 30 second, as shown in **Figure 2.8** and the angle in degrees was calculated by applying the ratio method using The camera angle analysis for the red-roofed house was conducted using the ratio of some lengths in the images of a reference object. When the camera does not directly face an object, the angle becomes smaller (θ) and the object will appear smaller. Thus, as shown in **Figure 2.5**, the angle of recording can be calculated from the ratio of the sizes of the two walls in different directions as shown in **Eq. 2.2**. The estimated angles of the images are listed in **Table 2.1**. The possible camera locations were identified in line with the possible landslide pathway, as shown in **Figure 2.9**. From this plot, we obtained the



Figure 2.8. Images taken from the video for angle analysis of red-roofed house.

Table 2.1. Parameters and distance calculation based on ratio method using red-roofed house image sequence.

Time (s)	27	30
A (pixel)	83	57
B (pixel)	22	28.7
Ratio A	0.8	0.7
Ratio B	0.2	0.3
Angle (degree)	75.15	63.27
Distance (m)	80.9	86.5

length between points X_1 and X_2 as 15.3 m. Then, using The velocity was calculated using a simple formula, as described in **Eq. 2.1**, $L \approx 15.3$ m, $t_1 - t_0 = 3$ s, and velocity (v) ≈ 5.1 m/s.

From the elevation map (**Figure 2.2**) it is known that the red roofed house is located 1600 m from the top of the irrigation. The elevation changes from 80 to 66 m, and thus the slope is approximately 3%. However, after 1600 to 1000 m, the elevation changes from 66 m to 58 m, making the slope only approximately 1%. The landslide acceleration is related to the slope, one reason for which might be the gentler slope slowing the velocity. A previous study by (Ichii et al., 2015) reported that the velocity at the toe of a steep hill during a landslide (debris flow) that occurred in 2014 in Hiroshima, Japan was 8.68 m/s. Thus, in reality, an estimated velocity of 5.1 m/s can possibly occur.

2.2 Numerical simulation of liquefaction in Jono-Oge, Palu

For the landslide analysis we used the Finite element analysis program of Liquefaction Process/Response of Soil structure systems during Earthquakes (FLIP ROSE) (https://www.flip.or.jp/en/e_flip7series.html). To model the behavior of sand we used the FLIP ROSE (ver.7.3, 2020) with the cocktail glass model as the constitutive model to express the stress-strain relationship of the soil. The cocktail glass model was incorporated in a two-dimensional dynamic effective stress analysis of the FLIP ROSE. The program can analyze earthquake responses accompanied by liquefaction by considering the permeability of the ground. The program provides a multistage analysis function that enables the analysis to reproduce the initial stress state accurately by considering the construction process.

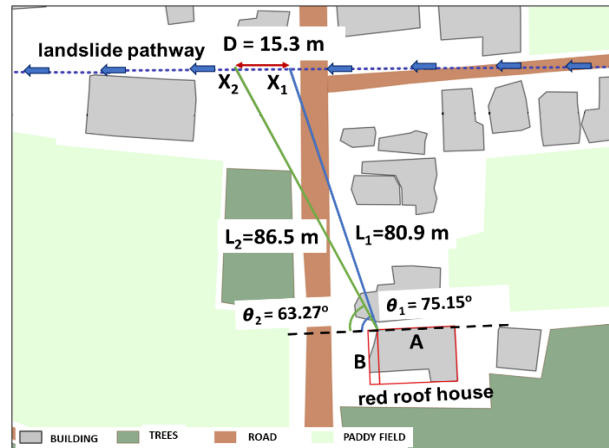


Figure 2.9. Camera position on possible landslide pathway, based on **Table 2.1**.

2.2.1 Model Element

The program is based on a Finite Element Method (FEM). We used the pore water elements (partially drained) for modeling the behavior of the pore water and the cocktail glass model elements for modeling the behavior of the sand soil skeleton. The pore water element is based on u-p formulation by (Zienkiewicz and Bettles, 1982).

The cocktail glass model element is based on the model proposed by (Iai et al., 2011). For simulation of soil behavior below the ground water table, the pore water element (partially drained) is superposed with the cocktail glass model element by sharing the same nodes. This cocktail glass model is commonly used, and it showed good performance in the analysis of the structures during the 1995 Kobe earthquake (Ichii et al., 2020). This model also had been used for liquefaction analysis in gently sloping ground from earthquakes (Iai, 2020).

2.2.2 Governing Equation

The governing equations for porous media saturated with pore waters are given as a combination of the equilibrium equation and the mass balance equation of pore water (u-p formulation). The difficulty of liquefaction analysis is the nonlinear stress-strain relationship of soil element, which was modeled as constitutive model of geotechnical material. For the modeling of soil behavior, the cocktail glass model was used. In the cocktail glass model, dilatancy is given as the sum of contractive part and dilative part. The increment of contractive part of dilatancy is given by the strain increment in a multiple shear mechanism and dilative part of dilatancy is given by the current shear strain in an arbitrary direction. The value of dilative part of dilatancy was determined to make no work under shear. As a result, the void ratio decreases from the initial value to a possible limiting value, but the current void ratio of the soil element depends on the current strain level.

2.2.3 Model Geometry, Mesh and Boundary Conditions

From the soil profile by Japan International Cooperation Agency ((JICA, 2019)) (), we estimated the possible depth of liquefaction was 10 meters. Then for the simulation we divided the 10 m depth into 12 layers. The model geometry of the FEM can be seen on **Figure 2.10**. Both length and width of the mesh are 1 m. The boundary condition at the side were free both in horizontal and vertical direction. However, the displacement at the left and right side of the meshes nodes were set to be identical for each direction. This approach was taken to simulate the horizontally layered movement.

2.2.4 Input Ground Motion

There was no seismograph installed in Jono-oge area but there was one seismic station around Palu which operated by JICA and BMKG. The station is located approximately 80 km from the epicenter and close to Balaroa (**Figure 2.1**). It is located 12 km on the north side of landslide area at Jono Oge. The ground motion input for this model was digitized from ground motion data (Kiyota et al., 2020) that was recorded in this station. The time history of acceleration in N-S direction which we used in the analysis is shown in **Figure 2.11**.

2.2.5 Soil Parameters

The physical parameter used in this case is tabulated in **Table 2.2** as a result from boring survey conducted at the top end of a landslide in the Balaroa (Yamamoto and Tobita, 2020). The model layer setting was based on Jono-oge boring while the physical parameter given from the result at Balaroa. However, since there was no available data, we decided to use data from Balaroa area which is located 12 km to the north of Jono-Oge (**Figure 2.1**). The dilatancy parameters (**Table 2.3**) are based on the results of laboratory tests of silt sand collected locally in the Sibalaya, which is located 20 km to the south from Jono-Oge. Dilatancy parameters were determined by fitting the liquefaction strength curve (shear strain peak amplitude = 7.5%) of silty sand ($D_r = 12.1$ to 13.1%) (Yamamoto and Tobita, 2020). Ideally, the physical and dilatancy parameters should be from Jono-Oge boring survey. However, Jono-oge, Balaroa and Sibalaya located in the Palu valley, therefore even-though the input parameters were from different sites they may have the same geological feature. Therefore, we could assume that those three sites have quite similarity.

We assumed both sand and silt layer have the same permeability value due to the occurrence of cracks at silt layer which make the permeability larger (**Table 2.4**). The shear resistance value at steady state (q_{us}) were determined through numerous simulations. We used the landslide displacement and velocity obtained from analytical analysis of liquefaction video in Jono Oge to validate our result. We used the $q_{us} = 0.025$ kN/m² which produces landslide velocity closest with the velocity (5.1 m/s) obtained from video analysis.

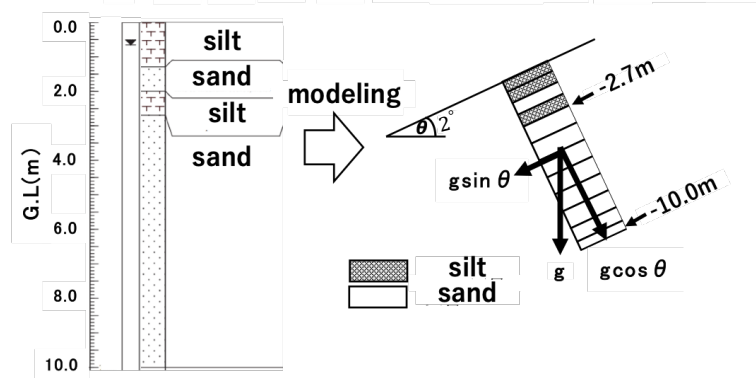


Figure 2.10. Soil profile at Jono-Oge, data taken from survey conducted by JICA, 2019. Model geometry for this simulation determined by the slope information and soil properties data.

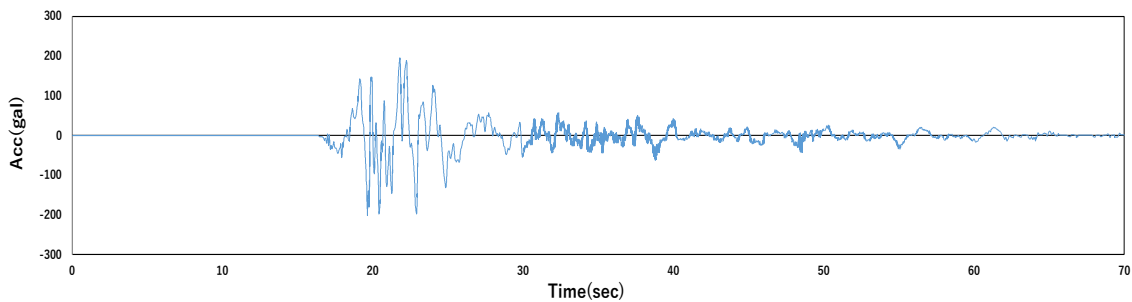


Figure 2.11. Time history of ground motion N-S component used as acceleration input. (digitized from (Kiyota et al., 2020)).

Table 2.2. Input of soil physical parameters

Parameters	
Shear modulus	49,334 kPa
Bulk modulus	128,655 kPa
Mean effective constraint	98 kPa
Density	2.064g / cm ²
Cohesion (C)	0
Internal friction angle (ϕ)	35.16 °
Maximum value of damping factor	0.24 (general value)

Table 2.3. Input of dilatancy parameters

ϵ_{dcm}	: 0.15	q_1	: 3.8	r_k	: 0.49
$r \epsilon_{cd}$: 2	q_2	: 1	c_1	: 1
$r \epsilon_d$: 1.6	l_k	: 2	s_1	: 0.005

Table 2.4. Input of permeability and shear resistance at steady state

Parameters	
Permeability	Sand layer: 1.0×10^{-4} m / s Silt layer: 1.0×10^{-4} m / s
Shear resistance at steady state (qus)	0.025 kN / m ²

2.3 Result of Landslide Simulation

2.3.1 Evidence to The Validation Analysis

To find the shear stress that can be used as one of input parameters in the tsunami model, the pore water pressure and displacement should agree with the result from the optical and geometry calculation. From the previous study, it was known that the liquefaction in Jono-Oge happened after the ground shaking and the landslide velocity was 5.1 m/s.

2.3.2 The Pore Water Pressure Response

Fig. 2.15 shows when the ground start shaking at 18 second the pore water pressure increases and slowly dissipates afterward. Surface layer (no.1) have the lowest water pressure while bottom layer (no.13) has the highest water pressure. On the figure, it is shown that in 150 seconds there was some fluctuation of pore water pressure due to the model instability. However, from 150 s to 3000 s in the plot shown in **Figure 2.12** the pore water pressure was stabilized and slowly dissipate into 0. The excess pore water pressure ratio has increased about 18 seconds after the start of the earthquake at both the depth 10 m and 2,7m. The excess pore water pressure ratio was close to 1 at both of this depth, which means the soil was being liquefied at this moment and would easily slide.

2.3.3 Surface Displacement Response

Figure 2.13 shows the horizontal displacement on the ground surface. It can be seen from this figure that about 250 m horizontal displacement occurred within 70 seconds after the earthquake. Then, from the result of the horizontal displacement of the ground surface, the velocity from the start of the earthquake was obtained from 40 seconds to 50 seconds. As a result, the velocity of the landslide for 40 to 50 seconds from the start of the earthquake was about 4.3 m/s. From this, it can be said that the velocity of 5.1 m/s from video analysis was almost reproduced

2.3.4 Shear Stress-Shear Strain Relationship of Soil Element

The shear stress and shear strain relationship during the first 150 second is shown in **Figure 2.14**. From the 20 seconds - 23.2 seconds the shear stress significantly changes but then start to stabilize at 70 second. This analysis shows that the shear stress was constant in the long run. Therefore, this shear stress can be used as the input value in the landslide-induced tsunami simulation at the Palu bay. **Figure 2.13** shows that large displacements occur in the top and bottom layers. Therefore, **Figure 2.14** shows the relationship between shear stress and shear strain in the bottom layer. The shear strain has not increased rapidly due to the influence of seismic motion until about 20 seconds at the start of the earthquake. However, the shear strain increases rapidly at a constant value with shear stress from about 23 seconds at the start of the earthquake.

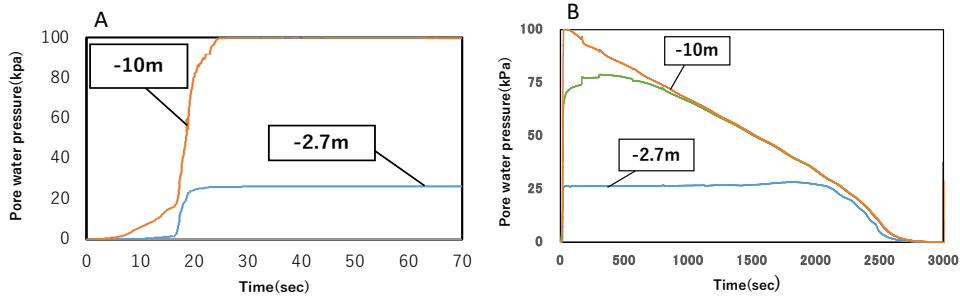


Figure 2.12. (a) Excess pore water pressure during 70 s, when the ground shaking started at 18 second the water pressure getting high. (b) Longer time histories pore water pressure show the dissipation.

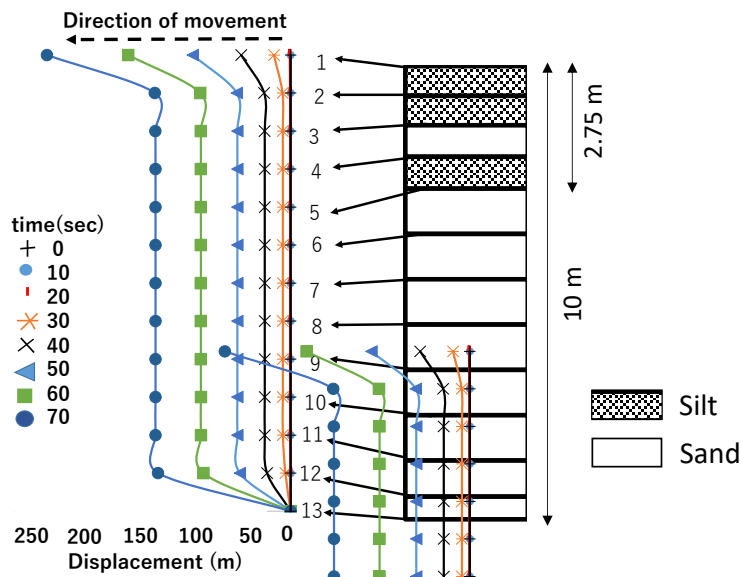


Figure 2.13. Computed depth and displacement in the horizontal direction

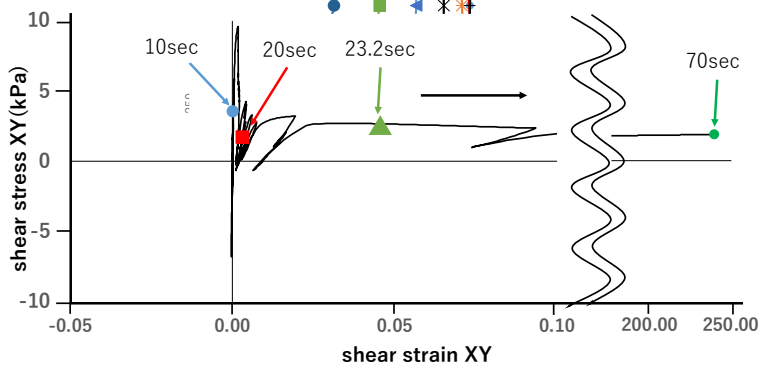


Figure 2.14. Shear stress and shear strain of the soil element near the bottom between node 12 and 13 in Fig. 2.16

2.4 Numerical Simulation Of Landslide Induced Tsunami Inside Palu Bay

2.4.1 General Framework of Tsunami Simulation

Based on the way that a particular model treats the tsunami generation phase, the landslide numerical models can be classify into three groups (Heidarzadeh et al., 2014):

- (1) models that treat the submarine mass motion like the flow of a fluid with a particular density,
- (2) models that estimate the initial water surface using semi-empirical equations, and
- (3) models that are fed by the transient seafloor deformation at different times.

In this study, the model we used is categorized as the first group. More specifically, we employed a numerical package called Volcflow, an open-source program and can be accessed online (<https://lmv.uca.fr/volcflow/>). The code has been used and tested against various landslide- induce tsunami cases, such as tsunami triggered by the Güimar debris avalanche (Kelfoun and Druitt, 2005), flank failure of Fogos volcano (Kelfoun, 2008), landslide at reunion island (Kelfoun et al., 2010) and the latest flank failure of Anak Krakatau volcano (Mulia et al., 2020). Both the landslides and seawater are simulated using the general shallow water equations of mass conservation and momentum balance. The mass conservation equation to simulate the landslide is formulated in **Eq. 2.3** and the momentum balance are **Eq. 2.4** and **Eq. 2.5**

$$\frac{\partial h_m}{\partial t} + \frac{\partial}{\partial x}(h_m u_x) + \frac{\partial}{\partial y}(h_m u_y) = 0 \quad (2.3)$$

$$\begin{aligned} \frac{\partial}{\partial t}(h_m u_x) + \frac{\partial}{\partial x}(h_m u_x^2) + \frac{\partial}{\partial y}(h_m u_x u_y) = gh_m \sin \alpha_x - \frac{1}{2} k_{act/pass} \frac{\partial}{\partial x} \cdot (gh_m^2 \cos \alpha) \\ + \frac{\partial T_x}{\rho_m - \rho_w} \end{aligned} \quad (2.4)$$

$$\begin{aligned} \frac{\partial}{\partial t}(h_m u_y) + \frac{\partial}{\partial y}(h_m u_y^2) + \frac{\partial}{\partial x}(h_m u_y u_x) = gh_m \sin \alpha_y - \frac{1}{2} k_{act/pass} \frac{\partial}{\partial y} \cdot (gh_m^2 \cos \alpha) \\ + \frac{\partial T_y}{\rho_m - \rho_w} \end{aligned} \quad (2.5)$$

Where h_m is landslide thickness (m), ρ_m is landslide density and ρ_w is water density fixed at 1000 kg m^{-3} , $u_y u_x$ is landslide velocity (m/s), $k_{act/pass}$ is earth pressure coefficient and $g \text{ (N/m}^2\text{s}^2\text{)}$ is gravitational acceleration, α is ground slope, T_x is total retarding stress in x direction and T_y is total retarding stress in y direction.

Water is simulated using the mass conservation in **Eq. 2.6** and the momentum balance equations **Eq. 2.7** and **Eq. 2.8**.

$$\frac{\partial h_w}{\partial t} + \frac{\partial}{\partial x}(h_w v_x) + \frac{\partial}{\partial y}(h_w v_y) = 0 \quad (2.6)$$

$$\frac{\partial}{\partial t}(h_w v_x) + \frac{\partial}{\partial x}(h_w v_x^2) + \frac{\partial}{\partial y}(h_w v_x v_y) = gh_w \sin \beta_x - \frac{1}{2} \frac{\partial}{\partial x} \cdot (gh_w^2 \cos \beta) + \frac{R_x}{\rho_w} - 3 \frac{\mu_w}{\rho_w h_w} v_x \quad (2.7)$$

$$\frac{\partial}{\partial t}(h_w v_y) + \frac{\partial}{\partial y}(h_w v_y^2) + \frac{\partial}{\partial x}(h_w v_x v_y) = gh_w \sin \beta_y - \frac{1}{2} \frac{\partial}{\partial y} \cdot (gh_w^2 \cos \alpha) + \frac{R_y}{\rho_w} - 3 \frac{\mu_w}{\rho_w h_w} v_y \quad (2.8)$$

Where h_w is water thickness (m), μ_w is water viscosity and β is the slope of ocean bottom formed by initial topography plus the landslide thickness. The total retarding stress (T_x and T_y) is sum of stress between the landslide and the ground (T_{mg}) and drag between water and landslide (T_{mw}), as expressed in **Eq. 2.9**.

$$T = T_{mg} + T_{mw} \quad (2.9)$$

T_{mg} differs depending on the chosen rheological law. The point of interest in this study is to use the stress from the liquefaction analysis for the landslide-induced tsunami simulation (T_{mg}). More details will be discussed in sections 2.4.2 and 2.4.4.

$$T_{mw} = -\frac{1}{2} \rho \left(\tan \beta_m C_f + \frac{1}{\cos \beta_n} C_s \right) \|\mathbf{u} - \mathbf{v}\| (\mathbf{u} - \mathbf{v}) \quad (2.10)$$

The drag between water and landslide (T_{mw}) is calculated using **Eq. 2.10**. Where β_n is the angle formed by intersection of both surface of the bathymetry with a plane normal to the displacement and β_m is the slope of the landslide surface in the direction of the relative displacement, $\mathbf{u} - \mathbf{v}$ is relative velocity of the landslide surface. The coefficient C_f and C_s fix the drag on the surface of the landslide, respectively, normal and parallel to the displacement. The **Eq. 2.3 – 2.6** and **Eq. 2.6 - 2.8** are calculated at the same time step. This represents the interaction between landslide and water.

2.4.2 Estimation of the retarding stress between landslide mass and ground.

We fixed the value for parameters of solid density of 2500 kg/m³, water density of 1000 kg/m³ and water viscosity of 0.001 Pa.s. According to the study by (Kelfoun et al., 2010), a landslide simulation assuming a constant retarding stress ranging from 20 to 100 kPa generally gives better result. For high retarding stress of the water T_{mg} ranges from 10 to 50 kPa. In this study, from the liquefaction simulation of Jono-Oge landslide we obtained the range of shear stress of 1.5 – 3.5 kPa. This range is 10 times lower than the stress range proposed for general cases.

Using tsunami simulations, here we compared 2 cases with different shear strength values. Case 1 considered a higher initial shear strength, $T_{mg} = 20$ kPa, as recommended by Kelfoun et al., 2010. Case 2 used $T_{mg} = 1.5$ kPa, which is the lowest initial shear strength gained from

liquefaction simulation in Jono-Oge. The drag coefficients on the surface normal and parallel to the displacement were $C_f = 2$ and $C_s = 0.01$ following suggestion from Tinti et al., 2006 who proposed the drag coefficient for underwater landslide.

2.4.3 Setting of Landslide Geometry as Tsunami Source

To simulate the landslide-induced tsunami, we first estimate the potential source area. It is difficult to accurately estimate the actual submarine landslide geometry. There are many different interpretations of the tsunami generation mechanism and where the submarine landslide is located at the Palu Bay. Takagi et al., 2019 assumed an initial surface depression based on the survey of land volume lost using Delft 3d flow program. Gusman et al., 2019 modelled three coastal landslides as solid blocks. Liu et al., 2020 modelled seven coastal landslides based on their bathymetric survey. In their studies they did not consider the dynamic simulation of the landslide. The landslides characteristic did not used as a factor that affected the tsunami height.

(Pakoksung et al., 2019) identified six landslides modelled as dense fluid. Their model used the two-layer fluid simulation and did not consider the material characteristic of landslide. Nakata et al., 2020 identified six hypothetical landslides as granular material. This model considered the difference between water and solid density. There were two different set of input types in this model. First regarding the landslide geometry and second is the rheological parameters. Nakata et al., 2020 approach was similar with the model we used in this research. Therefore, our model scenarios used three landslides with the same volume (0.07 km^3) identified near the end of the Palu bay (L1, L2 and L3) show in **Figure 2.16** . We did not use the other landslide locations as they are too far from our study area.

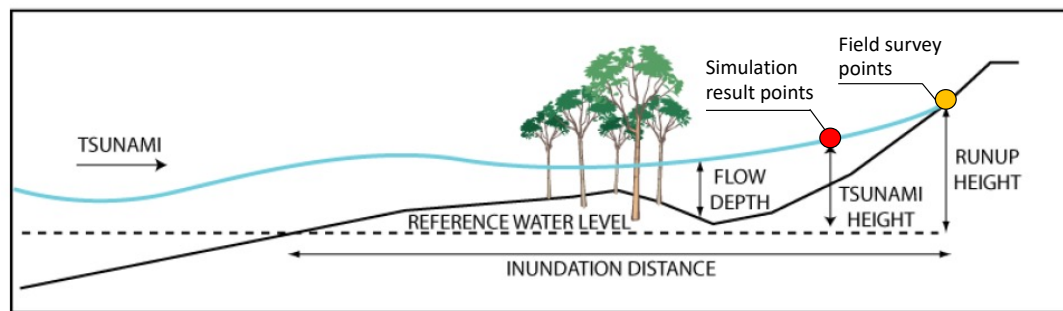


Figure 2.15. The schematic figure shows the difference between of the tsunami height calculated from the simulation and the run-up height gained from the field survey. (Takagi et al., 2019)

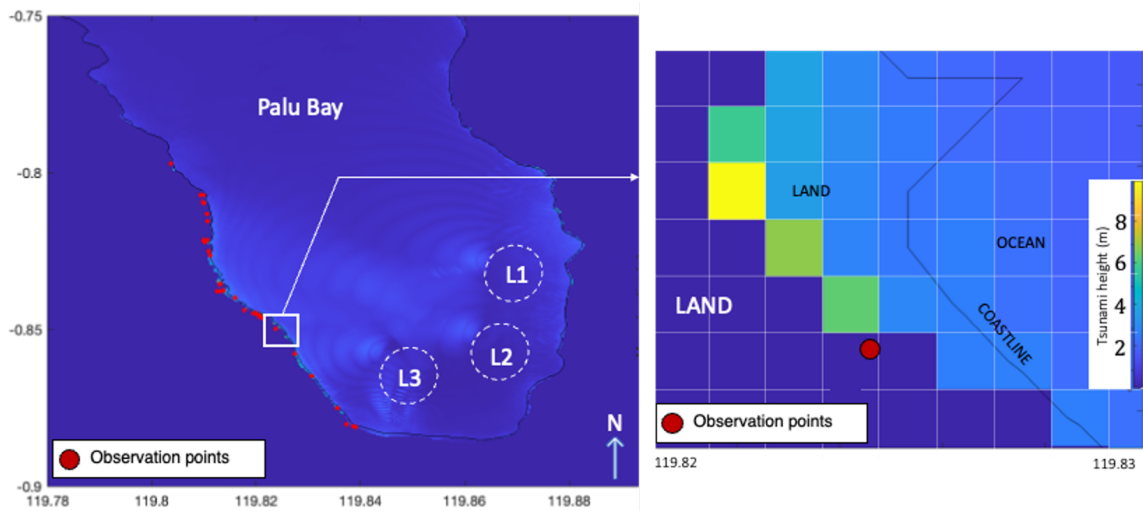


Figure 2.16. Locations of the identified landslides and run-up observation points from post tsunami survey. The inset figure (red box) shows the tsunami height in that area. The blue dot, represent the tsunami height from the survey, in this figure the tsunami height is 5m. The nearest grid of computed tsunami height to the blue dot, shows that the tsunami height is 6m.

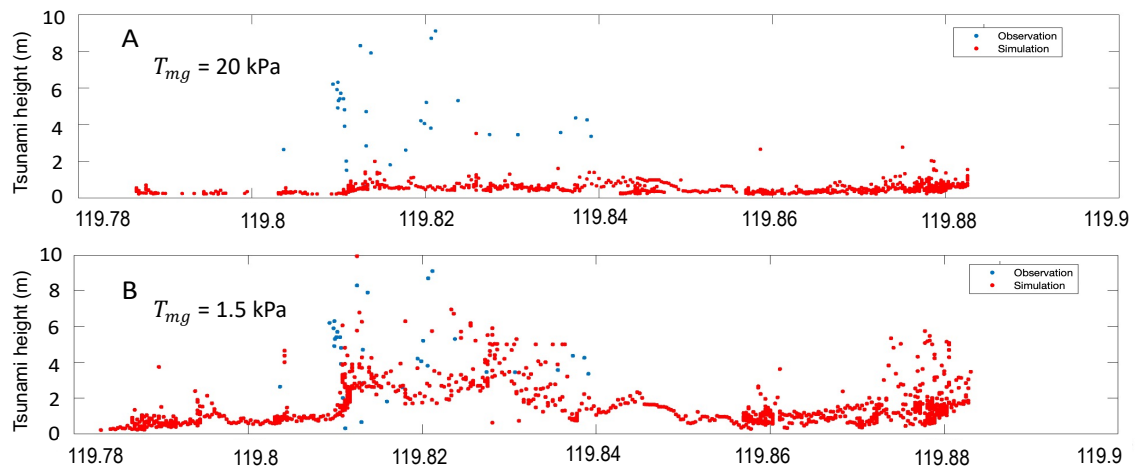


Figure 2.17. Simulation result using different shear strength, (A) 20kPa and (B) 1.5 kPa. The points are in the order of west to east and following along the coastline.

2.4.4 Tsunami Simulation Result

We compared the simulated tsunami heights with the post tsunami survey result (Mikami et al., 2019; Omira et al., 2019; Syamsidik et al., 2019; Taro Arikawa et al., 2018). The definition of tsunami height can be seen in **Figure 2.15**. The observation was based on run-up heights at one pick up point. Note that due to the limited model resolution, the tsunami simulation on land was not very accurate. As shown in **Figure 2.16** some run-up observation points are located on the dry grids (grid color is white). Therefore, the comparisons were made based on the nearest wet grid to the observation points (grid color is not white). This difference caused

subtle underestimations to the observation. A more significant effect to the accuracy of the simulated tsunami is attributed to the landslide characterization represented by the retarding stress value. In addition, considering the complex coastline geometry both tsunami height and run-up fluctuated very much. Thus, when we focused to plot a figure on the longitude (east - west), the small difference at the value of longitude eventually gave a large difference.

Figure 2.16 shows maximum simulated tsunami heights, locations of the landslides and run-up observation points from post-tsunami survey. We assumed that the submarine landslides (L1 - L3) move simultaneously and then the water is affected by the momentum transfer from the sliding mass. This process generated a maximum tsunami height of more than 9 m. The landslides move north-westward, corresponding to the slope of the submarine. From the tide station record and aerial video recording, the wave propagation pattern is getting more complex because of hydrodynamic interactions within the narrow bay.

Figure 2.17 shows comparisons between observed and simulated maximum tsunami heights from the two different stress values discussed previously. The landslide-induced tsunami simulation using the shear strength of 20 kPa have a higher cohesion reducing the mass slide velocity; thus, in turn leads to lower tsunami heights. Therefore, higher observed tsunami heights of more than 4 m along Loli to West Palu (coordinate 119.8-119.84 East) were underestimated by this model (**Figure 2.17A**). On the other hand, using the preferred shear strength of 1.5 kPa the simulated tsunami heights show much better agreement with the observations (**Figure 2.17B**). The RSME calculation (**Eq. 2.11**) used to find out the accuracy between two different stress values.

$$RSME = \sqrt{\frac{\sum_{i=1}^N (Xc_i - Xa_i)^2}{N}} \quad (2.11)$$

Where N is sample size, Xc is the computed tsunami height from simulation and Xa is the tsunami height from survey. The result is, RSME using 20 kPa is 6.05 and using 1.5 kPa is 3.6. Lower value of RSME means that the computed height closer to the observation value. Thus, the parameter using the value from inland liquefaction give better result. Therefore, based on these comparisons, the shear strength of 1.5 kPa is more suitable to characterize the submarine landslide of the 2018 Palu event than the generally adopted value of 20 kPa. The common problem in the submarine landslide-induced tsunami simulation is related to the uncertainty of the tsunami genesis or landslide parameterization. This is mostly due to the difficulties of the submarine observation. This study has presented the effect of geotechnical parameter, specifically shear stress in the steady state for the landslide-induced tsunami simulation using the two-layer method. The 2018 Palu event has given us opportunities to compare the landslide-induced tsunami simulation results using the recommended stress value for general cases and the specific stress value gained from the analysis of the on land nearby landslide event. The result then can be validated by using the tsunami heights from the field survey data.

Some highlight points were found, such as:

- 1) Image analysis is convenient because it is one of the tools available without having to visit the site location. The accuracy of this method is quite good, which was made possible because of the special conditions by which the video recorded a house that was

not moving during the landslide. This method relies on a high-quality video resolution, satellite images, and topography data. Furthermore, post-survey data in the study area are valuable for improving the accuracy of the image analysis results. Under certain circumstances, for example, the covid-19 pandemic, it is quite difficult to conduct a local survey. Therefore, an image analysis can be considered a possible option for landslide research.

- 2) Liquefaction in Jono-oge, Palu successfully simulated using the cocktail model from the FLIP ROSE program. The range of shear stress in this area was quite small (1.5 – 3.5 kPa) which is 5 times smaller than the shear stress recommended for general cases.
- 3) The Jono-oge simulation result showed that large shear strain in the bottom layer agrees with the constant retarding stress analysis. It was appropriate to use this value as an input parameter for the landslide-induced tsunami simulation by the Voleflow program.
- 4) With the same volume and geometry, the shear stress value of landslide mass gave quite a significant effect to the tsunami height. The shear stress value from the analysis of liquefaction in Jono-Oge, Palu, of 1.5 kPa can produce four times higher tsunami heights than the stress value suggested for general cases of 20kPa. Therefore, an appropriate landslide characterization is crucial to accurately simulate the corresponding tsunami.

Further research by using higher bathymetry and topography resolution should be conducted to improve the accuracy of this model result. However, the goal on this chapter to show that landslide alone is sufficient to generate tsunami height up to 8 meters.

REFERENCES

- Arikawa, T., Muhari, A., Okumura, Y., Dohi, Y., Afriyanto, B., Sujatmiko, K. A., Imamura, F., 2018. Coastal Subsidence Induced Several Tsunamis During the 2018 Sulawesi Earthquake. *Journal of Disaster Research* sc20181204–sc20181204. <https://doi.org/10.20965/jdr.2018.sc20181204>
- Bradley, K., Mallick, R., Andikagumi, H., Hubbard, J., Meilianda, E., Switzer, A., Du, N., Brocard, G., Alfian, D., Benazir, B., Feng, G., Yun, S.-H., Majewski, J., Wei, S., Hill, E.M., 2019. Earthquake-triggered 2018 Palu Valley landslides enabled by wet rice cultivation. *Nat. Geosci.* 12, 935–939. <https://doi.org/10.1038/s41561-019-0444-1>
- Digital Globe Maxar, 2020. URL <https://www.maxar.com/open-data/indonesia-earthquake-tsunami> (accessed 2.3.20).
- FLIP ROSE [version 7.3], 2020, retrieved from https://www.flip.or.jp/en/e_flip7series.html
- Gusman, A.R., Supendi, P., Nugraha, A.D., Power, W., Latief, H., Sunendar, H., Widiyantoro, S., Daryono, Wiyono, S.H., Hakim, A., Muhari, A., Wang, X., Burbidge, D., Palgunadi, K., Hamling, I., Daryono, M.R., 2019. Source Model for the Tsunami Inside Palu Bay Following the 2018 Palu Earthquake, Indonesia. *Geophys. Res. Lett.* 46, 8721–8730. <https://doi.org/10.1029/2019GL082717>
- Hamzah, L., Puspito, N.T., Imamura, F., 2000. Tsunami Catalog and Zones in Indonesia. *Journal of Natural Disaster Science* 22, 25–43. <https://doi.org/10.2328/jnds.22.25>
- Heidarzadeh, M., Krastel, S., Yalciner, A.C., 2014. The State-of-the-Art Numerical Tools for Modeling Landslide Tsunamis: A Short Review, in: Krastel, S., Behrmann, J.-H., Völker, D., Stipp, M., Berndt, C., Urgeles, R., Chaytor, J., Huhn, K., Strasser, M., Harbitz, C.B. (Eds.), *Submarine Mass Movements and Their Consequences, Advances in Natural and Technological Hazards Research*. Springer International Publishing, Cham, pp. 483–495. https://doi.org/10.1007/978-3-319-00972-8_43

- Iai, S., 2020. Paths Forward for Evaluating Seismic Performance of Geotechnical Structures, in: Kutter, B. L., Manzari, M.T., Zeghal, M. (Eds.), *Model Tests and Numerical Simulations of Liquefaction and Lateral Spreading*. Springer International Publishing, Cham, pp. 639–641.
- Iai, S., Tobita, T., Ozutsumi, O., Ueda, K., 2011. Dilatancy of granular materials in a strain space multiple mechanism model. *Int. J. Numer. Anal. Meth. Geomech.* 35, 360–392. <https://doi.org/10.1002/nag.899>
- Ichii, K., Uemura, K., Orai, N., Hyodo, J., 2020. Numerical Simulation Trial by Cocktail Glass Model in F LIP ROSE for LEAP-UCD-2017, in: Kutter, B.L., Manzari, M.T., Zeghal, M. (Eds.), *Model Tests and Numerical Simulations of Liquefaction and Lateral Spreading*. Springer International Publishing, Cham, pp. 611–627.
- Ichii, K., Yamashita, S., Murakami, Y., Moriwaki, T., Tsubaki, R., 2015. An estimation of the impact force of debris flow in 2014 Hiroshima case. *Journal of Ground Engineering* 33, 139–144.
- Jiang, Q., Chan, D., Xiong, J., Cui, Y., Dong, J., Li, S., 2016. Back analysis of a debris landslide based on a real-time video recording: sliding process and post-slide investigation. *Bull Eng Geol Environ* 75, 647–658. <https://doi.org/10.1007/s10064-015-0831-9>
- JICA, 2019. Survey for disaster information collection in Indonesia. boring survey for basic response for Central Sulawesi Earthquake Phase 1.
- Kelfoun, K., 2008. Rheological Behaviour of Volcanic Granular Flows, in: *International Congress on Environmental Modelling and Software*. Presented at the 4th International Congress on Environmental Modelling and Software, Brigham Young University, Barcelona, Catalonia, p. 9.
- Kelfoun, K., Druitt, T.H., 2005. Numerical modeling of the emplacement of Socompa rock avalanche, Chile. *J. Geophys. Res.* 110, B12202. <https://doi.org/10.1029/2005JB003758>
- Kelfoun, K., Giachetti, T., Labazuy, P., 2010. Landslide-generated tsunamis at Réunion Island. *J. Geophys. Res.* 115, F04012. <https://doi.org/10.1029/2009JF001381>
- Kisah Nyata Korban Selamat Likuifaksi Palu Eps 72 Part 1, <https://www.youtube.com/watch?v=h8u8cGqNTyE&feature=youtu.be&t=464> (accessed on January 27, 2020)
- Kiyota, T., Furuichi, H., Hidayat, R.F., Tada, N., Nawir, H., 2020. Overview of long-distance flow-slide caused by the 2018 Sulawesi earthquake, Indonesia. *Soils and Foundations* 60, 722–735. <https://doi.org/10.1016/j.sandf.2020.03.015>
- Likuifaksi jono oge (palu,sigi,donggala). Si perekam video terbawa likuifaksi., <https://www.youtube.com/watch?v=tXT8MSKehuM> (accessed on 27 January 2020).
- Liu, P.L.-F., Higuera, P., Husrin, S., Prasetya, G.S., Prihantono, J., Diastomo, H., Pryambodo, D.G., Susmoro, H., 2020. Coastal landslides in Palu Bay during 2018 Sulawesi earthquake and tsunami. *Landslides* 17, 2085–2098. <https://doi.org/10.1007/s10346-020-01417-3>
- Mikami, T., Shibayama, T., Esteban, M., Takabatake, T., Nakamura, R., Nishida, Y., Achiari, H., Rusli, Marzuki, A.G., Marzuki, M.F.H., Stolle, J., Krautwald, C., Robertson, I., Aránguiz, R., Ohira, K., 2019. Field Survey of the 2018 Sulawesi Tsunami: Inundation and Run-up Heights and Damage to Coastal Communities. *Pure Appl. Geophys.* 176, 3291–3304. <https://doi.org/10.1007/s00024-019-02258-5>
- Montgomery, J., Wartman, J., Reed, A.N., Gallant, A.P., Hutabarat, D., Mason, H.B., 2021. Field reconnaissance data from GEER investigation of the 2018 MW 7.5 Palu-Donggala earthquake. *Data in Brief* 34, 106742. <https://doi.org/10.1016/j.dib.2021.106742>
- Mulia, I.E., Watada, S., Ho, T., Satake, K., Wang, Y., Aditya, A., 2020. Simulation of the 2018 Tsunami Due to the Flank Failure of Anak Krakatau Volcano and Implication for Future Observing Systems. *Geophys. Res. Lett.* 47. <https://doi.org/10.1029/2020GL087334>
- Nakata, K., Katsumata, A., Muhari, A., 2020. Submarine landslide source models consistent with multiple tsunami records of the 2018 Palu tsunami, Sulawesi, Indonesia. *Earth Planets Space* 72, 44. <https://doi.org/10.1186/s40623-020-01169-3>
- Omira, R., Dogan, G.G., Hidayat, R., Husrin, S., Prasetya, G., Annunziato, A., Proietti, C., Probst, P., Paparo, M.A., Wronna, M., Zaytsev, A., Pronin, P., Giniyatullin, A., Putra, P.S., Hartanto, D., Ginanjar,

- G., Kongko, W., Pelinovsky, E., Yalciner, A.C., 2019. The September 28th, 2018, Tsunami In Palu-Sulawesi, Indonesia: A Post-Event Field Survey. *Pure Appl. Geophys.* 176, 1379–1395. <https://doi.org/10.1007/s00024-019-02145-z>
- Pakoksung, K., Suppasri, A., Imamura, F., Athanasius, C., Omang, A., Muhari, A., 2019. Simulation of the Submarine Landslide Tsunami on 28 September 2018 in Palu Bay, Sulawesi Island, Indonesia, Using a Two-Layer Model. *Pure Appl. Geophys.* 176, 3323–3350. <https://doi.org/10.1007/s00024-019-02235-y>
- QGIS Development Team, 2020. QGIS Geographic Information System. Open Source Geospatial Foundation Project.
- Robertson, I., Esteban, M., Stolle, J., Takabatake, T., Mulchandani, H., Kijewski-Correa, T., Prevatt, D., Roueche, D., Mosalam, K., 2019. StEER - Palu Earthquake And Tsunami, Sulawesi, Indonesia: Field Assessment Team Early Access Reconnaissance Report (Earr). <https://doi.org/10.17603/DS2JD7T>
- Souisa, M., Hendrajaya, L., Handayani, G., 2018. Study on Estimates of Travel Distance, Velocity and Potential Volume of Amahusu Sliding Plane using Energy Conservation Approach in Conjunction with Geoelectric Survey. *J.Math.Fund.Scie* 50.
- Syamsidik, Benazir, Umar, M., Margaglio, G., Fitrayansyah, A., 2019. Post-tsunami survey of the 28 September 2018 tsunami near Palu Bay in Central Sulawesi, Indonesia: Impacts and challenges to coastal communities. *International Journal of Disaster Risk Reduction* 38, 101229. <https://doi.org/10.1016/j.ijdr.2019.101229>
- Takagi, H., Pratama, M.B., Kurobe, S., Esteban, M., Aránguiz, R., Ke, B., 2019. Analysis of generation and arrival time of landslide tsunami to Palu City due to the 2018 Sulawesi earthquake. *Landslides* 16, 983–991. <https://doi.org/10.1007/s10346-019-01166-y>
- Tinti, S., Pagnoni, G., Zaniboni, F., 2006. The landslides and tsunamis of the 30th of December 2002 in Stromboli analysed through numerical simulations. *Bull Volcanol* 68, 462–479. <https://doi.org/10.1007/s00445-005-0022-9>
- Watkinson, I.M., Hall, R., 2019. Impact of communal irrigation on the 2018 Palu earthquake-triggered landslides. *Nat. Geosci.* 12, 940–945. <https://doi.org/10.1038/s41561-019-0448-x>
- Yamamoto, W., Tobita, T., 2020. Mechanism of occurrence of gentle slope landslide in the 2018 Sulawesi, Indonesia Earthquake. *Proceeding of Japan Society of Natural Disaster*.
- Yazdi, M., Bouwmans, T., 2018. New trends on moving object detection in video images captured by a moving camera: A survey. *Computer Science Review* 28, 157–177. <https://doi.org/10.1016/j.cosrev.2018.03.001>
- Zhao, C., Lu, Z., 2018. Remote Sensing of Landslides—A Review. *Remote Sensing* 10, 279. <https://doi.org/10.3390/rs10020279>
- Zienkiewicz, O.C., Bettis, P., 1982. Soils and other saturated media under transient, dynamic conditions: general formulation and the validity of various simplifying assumptions, in: *Soil Mechanics – Transient and Cyclic Loads*. John Wiley & Sons, Ltd, pp. 1–16.

CHAPTER 3 DEFINITION AND CONCEPT OF INTUITIVE TSUNAMI EVACUATION

Studies on human behavior during emergencies can be divided into two categories. First is behavioral psychology, which predominantly consists of qualitative psychological research. The second category focuses on group behavioral modeling and empirical studies. This study falls under this category. To ascertain the impact of various evacuation parameters, observation methods were employed in the study. The movement of populations in both real emergencies and specific simulation scenarios were observed. The difficulties in developing a comprehensive study about human behaviors under emergencies are because of the lack of real data and the complex characteristics of human behavior.

The chapter is divided into two parts. The first part defines intuitive tsunami evacuation. It also elaborates on factors that influence evacuation decisions in people experiencing emergencies because of calamities. The second part defines the concept behind the model for evacuation initiation model. First is the concept of reality-of-evacuation-start (RES) and RES source, and second is the concept of awareness-level-of-danger (ALD) and ALD threshold,

3.1 Definition and example of intuitive tsunami evacuation

3.1.1 Tsunami evacuation and evacuation phase

Evacuation is the immediate and urgent movement away from a threat or hazard. During an emergency evacuation, people in dangerous places should move to a safe place before the danger strikes. A tsunami is categorized as a rapid-onset hazard because of its unpredictable nature and the speed of its manifestation, and this disaster requires rapid evacuation. The evacuation decision time is critical and intricate by nature since the process determines the magnitude of the impact in terms of lives lost or affected. Therefore, there are three important issues to be considered for Tsunami evacuation: (1) whether to evacuate, (2) where to evacuate, and (3) how to evacuate.

The evacuation period for a tsunami can be phased from the occurrence of the earthquake to the onset of the tsunami. Originally, the tsunami evacuation phase consisted of a response phase and an evacuation movement phase. However, (Makinoshima et al., 2020) modified these phases to include more stages (**Figure 3.1**). Currently, the tsunami evacuation framework includes the notification stages of early, mid, and late periods that represent the time from the tsunami generation to its inundation. Based on that figure (**Figure 3.1**) Notifications, in this study, are defined as the information provided to people for initiating evacuation. Notifications are continuously provided during disasters, therefore there is a continuous risk cognition stage along the evacuation process. The framework of time required for evacuation is shown in **Figure 3.2**, when the disaster happened there will be alarm, cues or warning. People need time to perceive and interpret the cues. Some can process the cues as information of danger, which will make them to act. Others, who perceive this situation is not dangerously enough choose to stay or delay the movement.

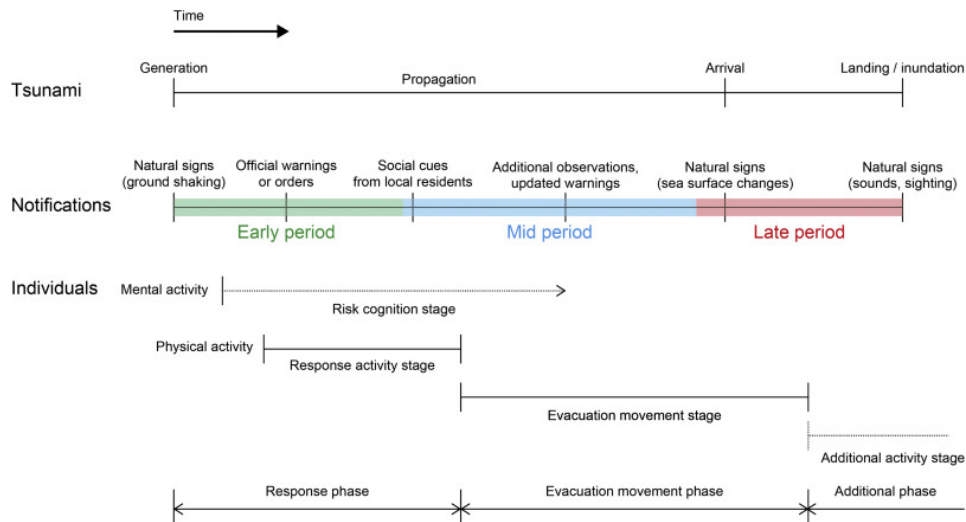


Figure 3.1. Phase during tsunami evacuation process (Makinoshima et al., 2020)

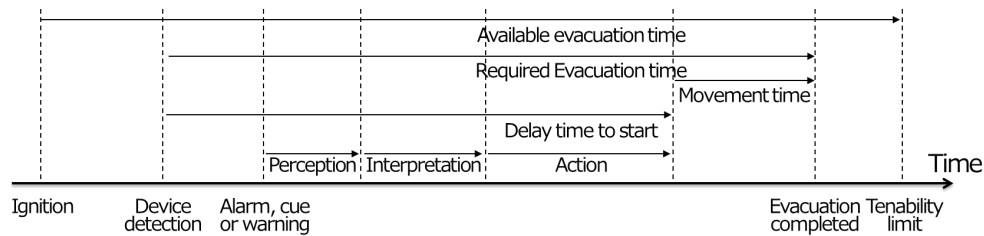


Figure 3.2. Time required for evacuation (Yung, 2008)

In this study, we examine the changes in behavior, from response stage to evacuation movement stage, in people experiencing a tsunami emergency. The phase of interest in this study is the behavior change from response stage into evacuation movement stage. During the response phase, individuals gather all the cues from environmental, social and warning information related to the hazard. The individuals then interpreted the cues and eventually lead to the decision to evacuate or stay-in-place. This behavior defined as the initiation of tsunami evacuation or can also be called as start of evacuation.

3.1.2 Logical and Intuitive evacuation behavior

The process of public (non-expert) evacuation initiation has often been discussed within the framework of action that is based on logical decision-making (reference). For example, when experts (such as the government) inform about dangerous conditions to a non-expert (such as a resident) then the non-expert, after receiving the information, will take action to start evacuating. This approach is a rational human behavior and the accumulation of such research results led to the construction of an advanced tsunami warning system (Bernard and Titov, 2015). It can be said that evacuation measures based on these findings have exerted certain effects.

In recent years, there have been tsunami evacuation cases that cannot be explained by a logical decision-making framework. For example, during the tsunami in Samoa (2009), the death ratio compared to the tsunami magnitude was low even though there had been no established tsunami warning system. (Okumura et al., 2011) conducted a detailed interview

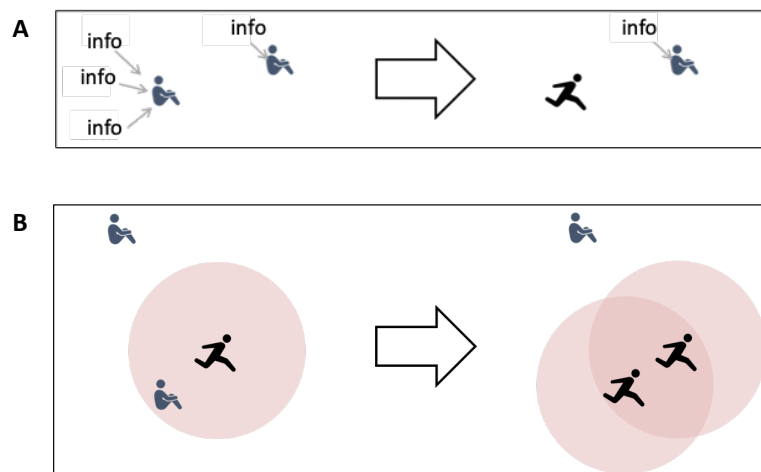


Figure 3.3. A) Initiation of evacuation based on logical judgment. B) Initiation of evacuation based on intuitive judgment (Dohi et al., 2016)

survey of survivors in American Samoa to clarify the cause why the causalities in Tsunami Samoa were lower than expected. From the logical judgment viewpoint, the behavior of starting evacuation, in this case, cannot be explained. The cause, however, can be explained through a concept known as a joint construction of reality. Here, not only expert experts but each inhabitant is also regarded as an important source of information. Together, they raise a sense of urgency in the community and initiate evacuation behavior. In the case of Samoa, various actions of the residents themselves, such as the mayor's call for evacuation and the act of ringing the bell by the residents, heightened the sense of crisis in the community, which led to the start of the evacuation and greatly reduced human damage. The whole process was different from the conventional approach, and the start of evacuation was understood at both the individual and community levels.

Similarly, during the Sumatra earthquake (2004), a tsunami of more than 10 m struck for about 8 minutes after the earthquake occurred on the Simeuleu Island in Aceh, northwestern Indonesia, located 50 km south of the epicenter of the M 9.3 earthquake. At that time, no tsunami warning was announced, and the term tsunami was also unfamiliar to the Indonesian people. Nevertheless, almost all people from Simeuleu Island evacuated to the surrounding mountains immediately. On an island with a population of about 80,000, only seven people had been killed by the tsunami, although about 4,000 houses had washed away. The tsunami knowledge (known as Smong in the local language) had been transferred, after the deadly tsunami of 1907, from generation to generation through cultural practices such as songs and poems (Gaillard et al., 2008). The idea of reality of evacuation start (RES) in this study is based on the above-mentioned reality.

Figure 3.3 shows a schematic diagram comparing the way of thinking based on logical and intuitive judgment with regard to the start of evacuation. **Figure 3.3A** is a way of thinking based on logical judgment. Residents, when they obtain information from public institutions, make logical judgments based on their own knowledge and experience to start evacuating. Subsequently, **Figure 3.3B** shows that residents intuitively start evacuation behavior because of the atmosphere of "must escape" (evacuation start reality) created by various people

including local residents and natural phenomena. This study focuses on the initiation of evacuation based on intuitive judgment.

3.2 Evacuation Triggers

When a disaster occurs, all people do not react uniformly, at the same time. Some people immediately notice the emergency situation and move to a safer place. Others either do not notice the danger or do not feel the urgency to move. For example, in the interview, people give testimony such as:

“I felt the weak ground shaking and stayed at my house. Around 5 minutes after the ground motion stopped, I saw message of a “tsunami threat” in the television given by the government agency. I heard my neighbor calling me to evacuate so I went to the shelter...” (UNDRR and UNESCO-IOC, 2019). The interviewee had felt the ground shaking and this should have been an obvious signal to activate the evacuation plan. Why then did this person still stay inside the house? Was the shaking not strong enough? Did this person wait for a warning notification from authorities through the radio or television? How did the instruction from the neighbor make this person evacuate? This person, it can be said, needed a trigger to make a choice about moving to a safer place. To conclude, evacuation initiation needs a trigger, some are obvious some are subtler. This person needed a trigger, that for them, move to the safer place is the right choice at that moment. However, at present, there is little information on which trigger can have the biggest impact on the decision to initiate an evacuation.

Questionnaires are popular fundamental tools for acquiring information on public knowledge and the perception of natural hazards (Bird, 2009). In general, post-disaster surveys mostly use questionnaires to seek information about evacuation behavior. The kind of questions asked include, “What made you decide to evacuate?” (Harnantyarini et al., 2020; Muhari et al., 2007; Rafliana et al., 2016; Takabatake et al., 2019). However, the evacuation process is not comprehensively depicted by this method. An estimation of the impact and exposure of environment, social, or warning cues for evacuees is not revealed in the responses to such questionnaires. Therefore, the only information that could be concluded from these questionnaire-based studies was the kind of trigger that influenced people.

3.3 Evacuation Modeling

Over time, evacuation modelling has developed from simple engineering equations that do not consider behavioral tendencies, to more sophisticated models that have the potential for representing factors that influence evacuee behavior and decision-making process (Lovreglio et al., 2019). In general, current tsunami evacuation plans are developed based on (1) simplified evacuation routes and evacuees’ movements/behavior and (2) detailed evacuation modeling representing evacuation routes and evacuees’ movements in a realistic manner (Muhammad et al., 2021). The simplified approach to human behavior usually assumes evacuees act uniformly and no interaction during the evacuation process. In term of simplified evacuation route, it defined as a straight line connecting the evacuee to the evacuation point without considering available transportation networks and obstacles. Simple model usually used GIS-based model, their goal is to determine the shortest evacuation routes (Taubenböck et al., 2009). Nowadays,

agent-based model, using netlogo, widely used for developing more realistic tsunami evacuation scenarios. An appropriate evacuation plan is important to support effective evacuation due to the complexity of tsunami evacuation in emergency (Mas et al., 2015).

This research, focused on from the recognition to the movement phase during tsunami evacuation and use the initiation of evacuation model develop by (Dohi et al., 2016). This tsunami evacuation simulation considers the interactions between the internal and external factors that initiate evacuation among people. This model describes both individual and group characteristics indicating that there are interactions between individuals. The flowchart of this tsunami evacuation modeling is shown in **Figure 3.4**. The important components of this model are the reality-of-evacuation-sources (RES) and the awareness-level-of-danger (ALD).

3.4 Reality-of-evacuation-start and factors affecting it

Social reality is the base idea of evacuation start reality. The concept of social reality has been defined by various researchers. (Berger et al., 1966) said that social reality is a society that constructed by externalization, objectification, and internalization. (Gergen, 1982) points out that all objects or events are jointly constructed through the relationships of people. And the whole of objects or events recognized by people is a reality. Kondo on (Dohi, 2016) proposes a co-construction model of reality around media events, which models the relationship between the world, reality, and information as a hierarchical structure. For example, during tsunami evacuation, the entity (stakeholder) of all residents evacuating, local government officials involved in evacuation guidance, media personnel engaged in disaster reporting, and experts conducting disaster research, build reality while interacting with each other. The construction of reality is not only a human or social phenomenon but also a natural phenomenon (Dohi, 2016). In this study, as shown in **Figure 3.3** people are triggered by the

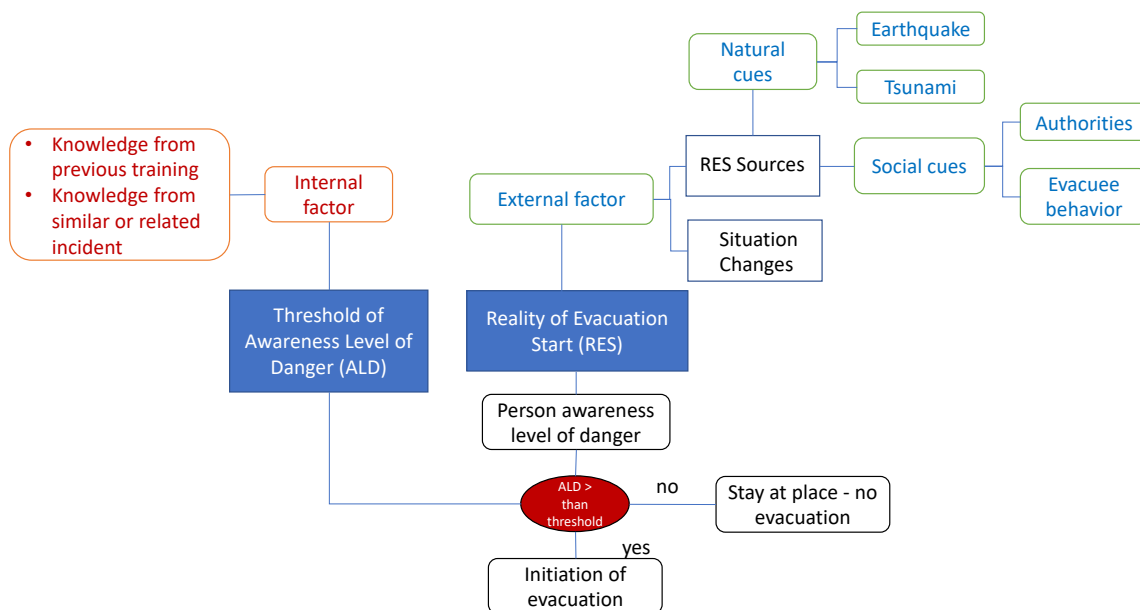


Figure 3.4. The intuitive decision-making for evacuation initiation.

atmosphere of "must escape" (RES), fostered in the entire region. The increasing sense of crisis generated by various cues intuitively pushes people to start evacuating as shown in **Figure 3.4**.

According to the intuitive decision-making process, the first stage of the evacuation process is the risk cognition stage (**Figure 3.1**). In this stage, individuals will scan and process the information. Overall, two factors affect human behavior, internal and external factors (Lovreglio et al., 2019). Internal factors will influence individuals to search their memory for previously stored patterns, with the hope that insights drawn from pre-stored knowledge will prove effective in solving the current problem. Pre-stored knowledge could emerge from key learning points picked from past training exercises or previous experiences on similar incidents.

External factors will influence individuals to rely on information generated from observing the various cues associated with a particular incident such as natural cues from the ground motion during an earthquake, sea level change, or loud sounds from the sea during the tsunami; and social cues from the other evacuee behavior and notifications by authorities. The external factor is situation awareness where individuals continuously filter information gained from various cues. In this sense, information will keep accumulating throughout the disaster period and elevate the sense of urgency among individuals, which will eventually generate the atmosphere of "must escape." In a group of people, the surrounding people, who exceed the individual thresholds to start moving, become a source of information.

3.5 Definition of reality-of-evacuation-start source

An evacuation decision is triggered by one or several factors (reference). Those factors can be separated by a source such as natural cause, warning, and behavior cause; by exposure, impact, and time.

3.5.1 Impact of RES source

The impact is a marked effect that makes people recognize their level of danger. While exposure is the spatial distribution of those factors, some sources can reach a wide area and still have a relatively similar impact level while other sources can only reach small areas (**Figure 3.5**). Exposure is time-dependent, from the start of the disaster until the evacuation. For example, ground movement during earthquakes makes a big impact on people, but the exposure, though widely felt, has an exposure period of only a few minutes (1-5 minutes). Subsequently, exposure to other people's behavior creates an impact only within the radius of people's of limited human visibility, but this factor will trigger people to start evacuating. As impact and exposure are dependent on time and space, it is, therefore, possible that people are exposed to many factors at the same time and this can cause their level of danger to increase.

The example of RES source exposure shown in **Figure 3.5**, in the beginning at 60 seconds the RES source is ground motion caused by earthquake and all people in this area can feel this shaking. After that at 180 seconds, the ground motion stopped and radio broadcasting message from authorities to disseminate information of earthquake warning. On this period, one person (A) starts to evacuate and moving toward the higher ground. While running, person A also shouting, calling people to evacuate. Now, person A became as new RES source, his action now gives information about the dangerous situation. In this example, person C observe the behavior of Person A and hearing his call to evacuate. At $t=180$ s, Person C exposed by 3 RES

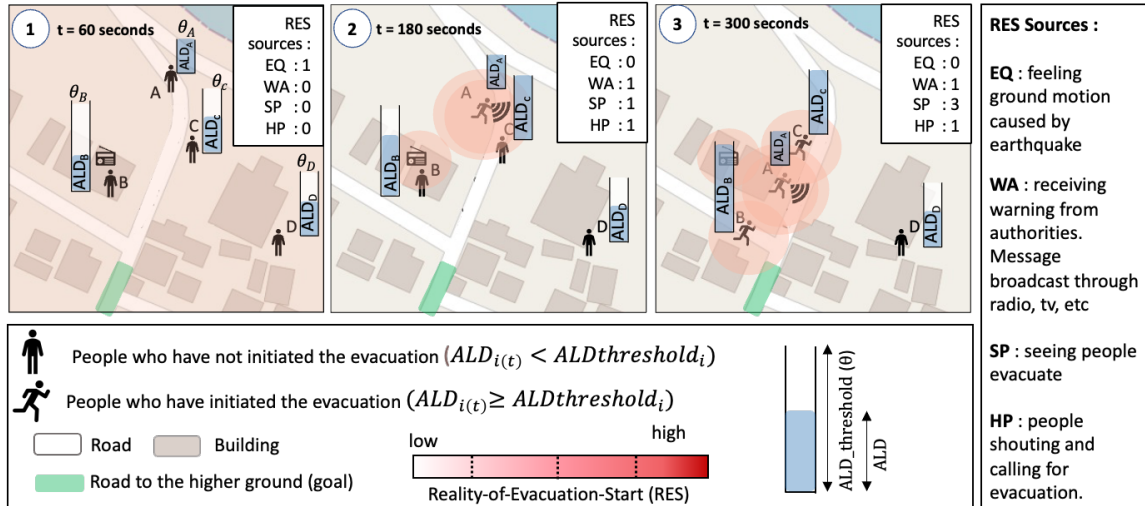


Figure 3.5. Evacuation initiation process as result from the effect of reality-of-evacuation (RES) sources to the awareness level of danger (ALD) in people.

sources, the previous experience of feeling ground motion, seeing people evacuating and hearing people calling for evacuation. Person D stay quite far away from other people and in his location no TV, radio, or siren. Until $t=300$ seconds, Person D only exposed by 1 RES source, feeling ground motion.

3.5.2 Exposure of RES source

In this study, we focused on the range of influence of the sources that foster evacuation start reality, and classified them into four types as shown in **Table 3.1**. (1) The whole area type reflects the effects felt by the entire target area, such as the shaking of the ground felt during an earthquake. (2) The whole area type includes the non-influenced area, and the size and position of the inundated area changed because of the expansion or the approach of the inundated area because of the tsunami. (3) The circular shape affects the concentric circles

Table 3.1. Classification of RES sources by the area exposure

	② whole area	② partial area	③ round shape	④ partial round shape
Area type				
Effective area	Whole area.	Whole area with partial non-effective area	Circular area.	Circular area with partial non-effective area
Cause	Earthquake	Tsunami inundation	Evacuee calling for evacuation	Evacuee move to evacuate
RES source	Feeling ground motion	Seeing tsunami coming	Hearing other evacuees	Seeing other evacuees

*The range of influence changes over time in the direction indicated by the arrow.

centered on the source, such as the call of evacuees and auditory information such as disaster prevention notifications administered through radio. (4) The circular shape, including the non-influenced area, affects the concentric circles centered on the source like visual information such as evacuation part of the affected area. Note that (2), (3), and (4) can be handled statically if the source is not changed over time. Next, the method of setting the range of influence in (3) and (4) is described using both the auditory and visual information.

3.5.3 Estimation of RES source weight

Source weight is a unique numerical value given to each RES source that expresses the magnitude influencing people to initiate the evacuation. This magnitude relatively represents the exposure and impact of the source. A previous study by Dohi, 2016, used data from social surveys to calculate the weight. The procedure to gain the weight is as below:

- 1) first on the survey data identify the percentage of residents (i_s) affected by source (m_s) and the percentage of residents affected by the evacuation (p_s),
- 2) calculate the influence or weight of the RES source ($W_{i_s(t)}$) by using **Eq. 3.1**.

$$W_{i_s(t)} = p_s / m_s \quad (3.1)$$

- 3) During the disaster, earthquake happen in the beginning so, weight of feeling ground motion should calculate first. The p_{quake} and m_{quake} used the data from social survey.
- 4) The initial of the weight of feeling ground motion (W_{quake}) should be adjusted by trial-and-error simulation until the simulation result of people who evacuated immediately after the earthquake similar with the value from social survey.
- 5) The weight for other RES sources (W_{i_s}) is arrange by the ratio to (W_{quake}).

The (W_{quake}) is critical because it will be used to calculate other source weight. This is also the weight that come first, means this people who evacuate immediately after the earthquake did not expose by another RES source. This group of people purely start evacuating just by the influence of feeling ground motion.

3.6 Definition of awareness level of danger (ALD) and ALD threshold

It states that there is a psychological amount of evacuation intention in the decision-making of residents' evacuation, which changes with the occurrence of an event. When disaster happened there are individual differences related to evacuation initiation time. Individual will start to evacuate when the threshold is exceeded. This threshold is varying between individual, it depends on the internal factor. For example, people who participate on the training drill have more knowledge about tsunami than people who never participate. As the result, threshold of people having tsunami knowledge is lower and more easily to exceed than people with no tsunami knowledge, because threshold determined by internal factor. Threshold is embedded to people (created from a long-term process) and the threshold is remains constant during the disaster.

Specifically, the start of evacuation is as follows:

- (1) Reality of Evacuation Start *RES* is form by sources (**Eq. 3.2**).

$$RES_{(x,y,t)} = \sum_{i_s=1}^{n_s} (R_{i_s(x,y,t)} X_{i_s(t)} W_{i_s(t)}) \quad (3.2)$$

Where $R_{i_s(x,y,t)}$ is the function related to the spatial relationship between person i and the RES source i_s at time step t , $X_{i_s(t)}$ is the function indicating whether the person (ip) is functioning as a source at time t , and $W_{i_s(t)}$ is the influence level of the RES source based on its impact and exposure. In this example (**Figure 3.5**), all residents perceived ground motion at $t = 60$ s because of the earthquake, and some residents received a warning from radio at $t = 180$ s while other residents saw and/or heard other people evacuating.

(2) Residents are surrounding by evacuation start reality *RES*. Residents feel the sense of urgency, this situation elevated their Awareness-Level-of-Danger (*ALD*) (**Eq. 3.3**)

$$ALD_{i_p(t)} = \min \left\{ \theta_{i_p}, \int_{c_{i_p}} RES_{(x,y,t)} ds \right\} \quad (3.3)$$

where $ALD_{i_p(t)}$ is the sense of urgency of a person (i_p) at time t , and θ_{i_p} is the threshold value of the person (i_p).

(3) Third, the timing of each resident to start evacuating differ because of the variation of ALD threshold (θ) in individuals. When the sense of crisis *ALD* exceeds the upper limit/threshold, then the evacuation action is started (**Eq. 3.4**)

$$X_{i_p(t)} = \begin{cases} 0, & ALD_{i_p(t)} < \theta_{i_p} \\ 1, & ALD_{i_p(t)} \geq \theta_{i_p} \end{cases} \quad (3.4)$$

In this model, the person (i_p) starts tsunami evacuation after $ALD_{i_p(t)}$ reaches the upper limit (θ_{i_p}) and to function as the RES source. Person with a low ALD threshold evacuate faster than person with a high ALD threshold. For example, in **Figure 3.5** Person B evacuates after being exposed to two sources: feeling the ground motion, and receiving warning on the radio. Person C evacuates after being exposed to three sources: feeling the ground motion, seeing Person A evacuating, and hearing Person A calling for evacuation. Person D does not evacuate until the end at $t = 300$ s because feeling ground motion is the only source exposed to person D. Based on this example, we can conclude that Person A has the lowest ALD threshold, this person starts to evacuate after feeling the ground motion while person B, C and D stay at their position.

REFERENCES

- Berger, P.L., Thomas, L., Thomas, L., 1966. The social construction of reality: a treatise in the sociology of knowledge. Garden City, N.Y. : Doubleday.
- Bernard, E., Titov, V., 2015. Evolution of tsunami warning systems and products. Phil. Trans. R. Soc. A. 373, 20140371. <https://doi.org/10.1098/rsta.2014.0371>.

- Bird, D.K., 2009. The use of questionnaires for acquiring information on public perception of natural hazards and risk mitigation – a review of current knowledge and practice. *Nat. Hazards Earth Syst. Sci.* 9, 1307–1325. <https://doi.org/10.5194/nhess-9-1307-2009>
- Dohi, Y., 2016. Development of tsunami evacuation simulator focusing on social reality. Kyoto University.
- Dohi, Y., Okumura, Y., Koyama, M., Kiyono, J., 2016. Evacuee Generation Model of the 2011 Tohoku Tsunami in Ishinomaki. *J. Earthquake and Tsunami* 10, 1640010. <https://doi.org/10.1142/S1793431116400108>
- Gaillard, J.-C., Clavé, E., Vibert, O., Azhari, Dedi, Denain, J.-C., Efendi, Y., Grancher, D., Liamzon, C.C., Sari, D.R., Setiawan, R., 2008. Ethnic groups' response to the 26 December 2004 earthquake and tsunami in Aceh, Indonesia. *Nat Hazards* 47, 17–38. <https://doi.org/10.1007/s11069-007-9193-3>
- Gergen, K.J., 1982. *Toward Transformation in Social Knowledge*. Springer New York, New York, NY. <https://doi.org/10.1007/978-1-4612-5706-6>
- Harnantary, A.S., Takabatake, T., Esteban, M., Valenzuela, P., Nishida, Y., Shibayama, T., Achiari, H., Rusli, Marzuki, A.G., Marzuki, M.F.H., Aránguiz, R., Kyaw, T.O., 2020. Tsunami awareness and evacuation behaviour during the 2018 Sulawesi Earthquake tsunami. *International Journal of Disaster Risk Reduction* 43, 101389. <https://doi.org/10.1016/j.ijdr.2019.101389>
- Lovreglio, R., Kuligowski, E., Gwynne, S., Strahan, K., 2019. A modelling framework for householder decision-making for wildfire emergencies. *International Journal of Disaster Risk Reduction* 41, 101274. <https://doi.org/10.1016/j.ijdr.2019.101274>
- Makinoshima, F., Imamura, F., Oishi, Y., 2020. Tsunami Evacuation Processes Based on Human Behaviour in Past Earthquakes and Tsunamis: A Literature Review. *Progress in Disaster Science* 7, 100113. <https://doi.org/10.1016/j.pdisas.2020.100113>
- Mas, E., Koshimura, S., Imamura, F., Suppasri, A., Muhari, A., Adriano, B., 2015. Recent Advances in Agent-Based Tsunami Evacuation Simulations: Case Studies in Indonesia, Thailand, Japan and Peru. *Pure Appl. Geophys.* 172, 3409–3424. <https://doi.org/10.1007/s00024-015-1105-y>
- Muhammad, A., De Risi, R., De Luca, F., Mori, N., Yasuda, T., Goda, K., 2021. Are current tsunami evacuation approaches safe enough? *Stoch Environ Res Risk Assess.* <https://doi.org/10.1007/s00477-021-02000-5>
- Muhari, A., Diposaptono, S., Imamura, F., 2007. Toward an Integrated Tsunami Disaster Mitigation: Lessons Learned from Previous Tsunami Events in Indonesia. *Journal of Natural Disaster Science* 29, 13–19. <https://doi.org/10.2328/jnds.29.13>
- Okumura, Y., Harada, K., Kawata, Y., 2011. Evacuation Behavior In The 29 September 2009 Samoa Islands Region Earthquake Tsunami. *J. Earthquake and Tsunami* 05, 217–229. <https://doi.org/10.1142/S179343111100108X>
- Rafliana, I., Yulianto, E., Yunita, R., Arif, A., Weniza, Muhari, A., Shusilawati, N., Hanifa, R., 2016. *Kajian Efektivitas Sistem Peringatan Dini Tsunami Indonesia Pada Peristiwa Gempabumi Outer-Rise Samudera Hindia*, 2 Maret 2016.
- Takabatake, T., Shibayama, T., Esteban, M., Achiari, H., Nurisman, N., Gelfi, M., Tarigan, T.A., Kencana, E.R., Fauzi, M.A.R., Panalaran, S., Harnantary, A.S., Kyaw, T.O., 2019. Field survey and evacuation behaviour during the 2018 Sunda Strait tsunami. *Coastal Engineering Journal* 61, 423–443. <https://doi.org/10.1080/21664250.2019.1647963>
- Taubenböck, H., Goseberg, N., Setiadi, N., Lämmel, G., Moder, F., Oczipka, M., Klüpfel, H., Wahl, R., Schlurmann, T., Strunz, G., Birkmann, J., Nagel, K., Siegert, F., Lehmann, F., Dech, S., Gress, A., Klein, R., 2009. “Last-Mile”; preparation for a potential disaster – Interdisciplinary approach towards tsunami early warning and an evacuation information system for the coastal city of Padang, Indonesia. *Nat. Hazards Earth Syst. Sci.* 9, 1509–1528. <https://doi.org/10.5194/nhess-9-1509-2009>

CHAPTER 4 GENERAL CHARACTERISTICS OF EVACUATION INITIATION IN INDONESIA

4.1 Tsunami Evacuation Triggers in Indonesia

The various factors influencing the fatality rates of tsunamis categorized into four classes by (Kubisch et al., 2020). The first category entails characteristics of the tsunami, which can be obtained from the Indonesia Meteorological, Climatological, and Geophysical Agency (<https://inatews.bmkg.go.id/>). The second category includes characteristics of the terrain, as provided by the Indonesia Geospatial Information Agency (<https://tanahair.indonesia.go.id/>), and the third category includes characteristics of tsunami mitigation measures provided by the Indonesian National Board for Disaster Management through hazard and risk maps. Although tsunami-safe zones are marked on these maps, the evacuation routes are not yet complete (<https://inarisk.bnpb.go.id/>). The fourth category involves information on personal characteristics, such as awareness about tsunamis, knowledge of the evacuation routes and zones, as well as individual mental/physical abilities, which are not available as government databases.

A few evacuation studies have been conducted in Indonesia. Early studies have used GIS-based models to determine the shortest evacuation routes (Taubenböck et al., 2009). Later it is progressed by using agent-based model that account evacuee movements (Muhammad et al., 2017) (Mas et al., 2015), and transportation networks and obstacles (Lämmel et al., 2010). More advanced one, include the future tsunami scenario (Muhammad et al., 2021). These studies usually include category 1, 2, and 3 in their model, while personal characteristic often based on estimation without integrating the behavior of local people. Some models assume that all people evacuate at the same time and others consider several groups of people evacuate at different point of time. Whereas research survey revealed that people did not evacuate at the same time. Instead, they respond to a variety of triggers that can initiate them to evacuate (Goto et al., 2012; Harnantary et al., 2020, 2020; Hoppe and Padang Working group, 2007; Mikami et al., 2014; Muhari et al., 2007; Rafliana et al., 2016; Syamsidik et al., 2019; Syamsidik and Istiyanto, 2013; Takabatake et al., 2019).

Evacuation characteristics tend to be site-specific, with several common human responses, such as sensing threats and processing information for decision-making and protective actions. However, identification of general behaviors and finding the priority order of evacuation triggers are necessary. This order will be the standard ranking of tsunami evacuation triggers for Indonesians. A subsequent case study will use this standard to evaluate the personal evacuation characteristics. This has an effect in determining the trigger influence weight, or in our model we called as RES sources weight, on the evacuation generation model.

4.2 Standard model and ranking of Evacuation Triggers in Indonesia

In this study, the standard model is a schematic graph that display the evacuation triggers from high to low influence. Standard model was created using published results of post-disaster field surveys by international survey teams and governmental agencies (**Table 4.1**). We focused on responses to the questions on the factors and events that prompted the people to evacuate. Some researchers called this as evacuation trigger, this research identified that as RES source. Since various methods are used by different researchers for the surveys (interviews,

Table 4.1. Survey result on tsunami evacuation triggers in Indonesia from 2006 – 2018

Event & Method*	Question and survey result [%]	Event & Method*	Question and survey result [%]
Pangandaran, 2006 <i>Interview¹⁾</i>	Warning was the sound of people screaming and running in a panic Observe unusual receding of water before tsunami	Siberut Island, 2016 <i>SA⁶⁾</i>	Feeling the earthquake [30] I received early warning [40]
Padang, 2007 <i>SA²⁾</i>	Feeling the earthquake [33] Received information about tsunami [67]		I heard a tsunami siren [13] Following other people [9]
Mentawai, 2010 <i>MA³⁾</i>	Feeling ground motions [14] Observing neighbors evacuating [14] Information from neighbor or family [43]	Pagai Island, 2016 <i>SA⁶⁾</i>	Feeling the earthquake [31] I received early warning [31] Following other people [4]
Mentawai, 2010 <i>SA⁴⁾</i>	Effects of first tsunami wave [29] Immediately after earthquake [51] Observing other evacuees [9] Other people screaming [25] Observing seawater receding [6] Observing seawater increasing [6]	Palu, 2018 <i>MA⁷⁾</i>	Feeling ground motions [50] Receiving message from authorities [0] Observing other evacuees [83] Hearing someone calling for evacuation [4] Hearing loud sounds from the sea [7] Observing unusual sea surface [12]
Aceh, 2012 <i>MA⁵⁾</i>	I felt strong and long shaking [61] I heard a tsunami siren [16] I heard a large tsunami alert being issued [13] I saw neighbors or many people evacuating [54] My family insisted that we should evacuate [12]	Krakatau, 2018 <i>MA⁸⁾</i>	Feeling ground motions [2] Receiving message from authorities [0] Observing other evacuees [33.7] Hearing someone calling for evacuation [9.9] Hearing loud sounds from the sea [44.6] Observing unusual sea surface [25.7] Observing seawater approaching land [61.4]
Padang, 2016 <i>SA⁶⁾</i>	Feeling the earthquake [16] I received early warning [26] I heard a tsunami siren [9] Following other people [20]		

*SA: Questionnaire only single answer, MA: Questionnaire allow multiple answer

¹⁾(Muhari et al., 2012), ²⁾(Hoppe and Padang Working group, 2007), ³⁾(Mikami et al., 2014), ⁴⁾(Syamsidik and Istiyanto, 2013), ⁵⁾(Goto et al., 2012), ⁶⁾(Rafliana et al., 2016), ⁷⁾(Harnantaryi et al., 2020), ⁸⁾(Takabatake et al., 2019)

single/multiple answer questionnaires), rankings cannot be decided simply based on the average value. Therefore, we developed a methodology to determine the evacuation trigger rankings using questionnaire result (**Figure 4.1**). In this method, rankings are determined by the number of times the trigger becomes the most influential.

In Indonesia, for four out of every nine events (Padang 2007 and 2016, Siberut, and Pagai), the majority choose receiving messages from the authorities as the trigger to initiate evacuation. For two out of nine events, most people choose seeing other evacuees and feeling ground motions as the triggers. Because the triggers have a similar numbers of occurrences we determined influence using **Eq. 4.1**.

$$Rt_i = \frac{\sum VE_{i1}}{n} \quad (4.1)$$

where Rt_i is the average value of the trigger type, n is the number of events, and VE_{i1} is the percentage when the trigger chooses by most people. Thus, the trigger value of seeing evacuee is the average of survey in Mentawai 2010 (57%) and Palu 2018 (83%) then the results is 70%. This value then compares with the trigger value of feeling ground motions, that is the average of survey in Mentawai 2010 (51%) and Aceh 2012 (61%) then the result is 56%. Therefore, seeing evacuees settle as second rank and feeling ground motions as third rank.

Seeing unusual sea surface or tsunami was ranked fourth because one out of nine events, in Krakatau 2018 (61,4%) most people choose this as the trigger to initiate evacuation. Out of nine events, hearing loud sound from the sea and hearing evacuees calling for evacuation, never choose by majority of people as the trigger to initiate evacuation. Therefore, **Eq. 4.2** was used to determine which trigger is more influential,

$$Rt_i = \frac{\sum VE_i}{n} \quad (4.2)$$

where VE_i is the percentage of people choose this trigger and n is the number of events. The trigger value of hearing loud sound from the sea is the average of survey in Palu 2018 (7%) and Krakatau 2018 (45%) then the results is 26%. This value then compares with the trigger

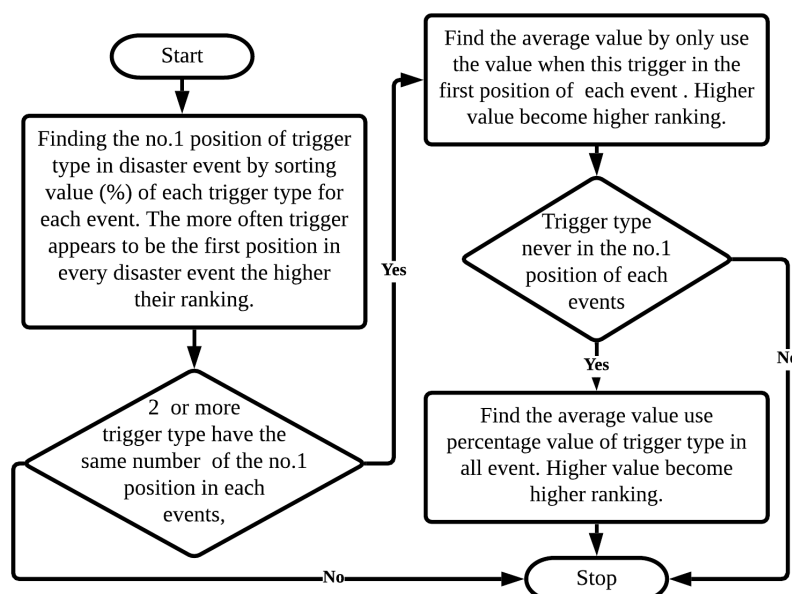


Figure 4.1. Flowchart of method to determine evacuation trigger ranking.

value of hearing evacuees calling for evacuation, that is the average of survey in Mentawai 2010 (25%), Palu 2018 (4%) and Krakatau 2018 (7%) then the result is 13%.

The survey results are plotted in **Figure 4.2**, wherein the large dot represents the RES sources that caused the maximum number of people to evacuate. The standard model (**Figure 4.3**) shows the ranks of the factors that triggered people to start evacuating, in addition to the impact and exposure of those factors. The x-axis shows the timing of when the trigger works during disasters and the y-axis shows its influence forcing people to initiate evacuation.

Human behaviors during the evacuation process are initially random and inconsistent. However, patterns are identified by the evacuation triggers. In the schematic graph (**Figure 4.3**), there are six influential evacuation triggers for Indonesians. The bullets show the times when the trigger is working (y-axis) and the rankings of their influence on evacuation (x-axis). The arrows demonstrates that some evacuation trigger act as a source for another trigger, indicating this is a chain process. For example, receive message from the authorities is the most

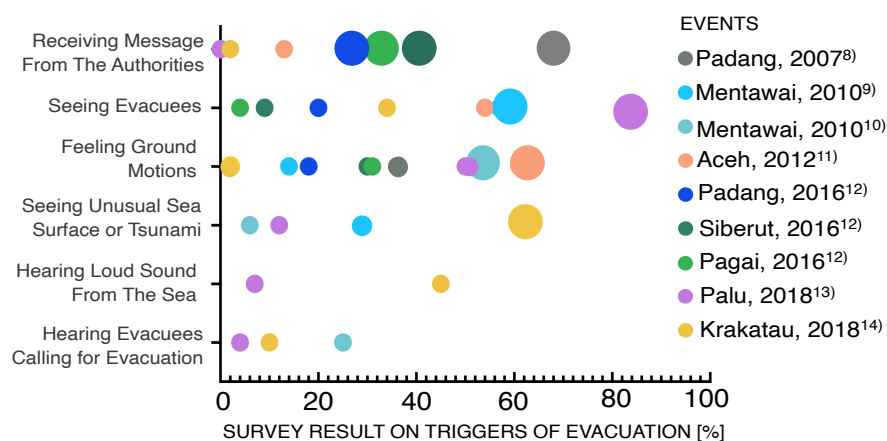


Figure 4.2. Evacuation trigger ranking based on the data collected from previous field surveys. The larger circles indicate this source chosen by majority of people as the reasons why they initiate evacuation.

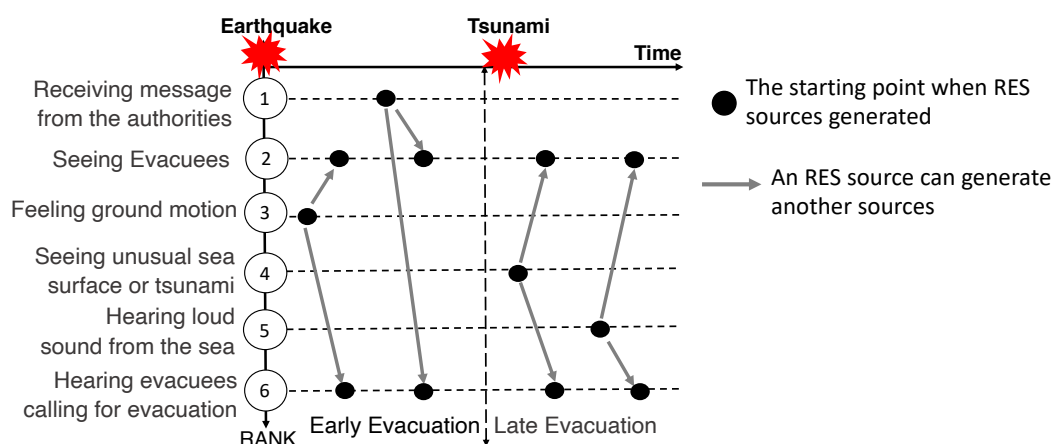


Figure 4.3. Schematic graph of standard model of RES sources rankings based on its influence to initiate evacuation and the point at which such sources work during the beginning of an earthquake to tsunami in Indonesia.

influential trigger after an earthquake. When people receiving messages from the authorities, some start evacuating. Then these evacuees will work as triggers. People who haven't start evacuating will see or/and hear other evacuee. Based on the occurrence time, evacuees can be categorized into two types as early and late evacuees. For example, seeing evacuees can trigger people until tsunami inundation. People who initiate evacuation upon seeing others before arrival of the tsunami are categorized as early evacuees, and those who evacuate upon tsunami arrival are late evacuees. The latter is termed as a late evacuation because the available evacuation time keeps reducing.

4.3 Video Analysis of Evacuation Initiation

One of the impacts of technological developments is the increasing number of smartphone users, and the ease of sharing content on the internet. After the 2018 Palu tsunami there were a lot of video upload into the internet and can easily accessed through social media. Post-event survey gave information of evacuation behavior to some extent; however, this data could not show the details of evacuation process. Video analyses provide information that is not captured by the field survey, such as responses from people after expose by evacuation triggers and duration of evacuation trigger working on people until they initiate to evacuate.

In this study, two video were used to analyze the evacuation behavior. First video was recorded by closed circuit television (CCTV) and the second by smartphone. Since the CCTV is a static video, it gives a precise set of continuous records of people movement. On the contrary, the video recorded by people using smartphone were moving dynamically and can only capture a glimpse of people movement. The abundance of evacuation information depends on the video quantity and quality. CCTV provide better quality footage however the numbers of available video are very limited. On the other hand, there are many footages captured by smartphone, but most have a low quality. However, smartphone video is crucial for reality-of-evacuation- (RES) source analysis since the footage can record the sound during the evacuation process.

Many aspects can be investigated in both of these videos. In our study, we will focus our analysis on:

1. What kind of RES sources exposed to the people
2. How long the duration of these RES source exposed to the people
3. When people decided to start evacuation.

We noticed that there were a different kind of behavior of people stay indoor with the people outdoor after they exposed by the information sources. The noticed behavioural patterns in evacuations are observed and organised in order of activation.

4.3.1 The Static Video Analysis

The video used for this analysis were from CCTV footage in Kampung Nelayan Hotel (KN Hotel) that located on the southeast coast of Palu Bay. There are 6 cameras installed but only 4 of camera capture the evacuee behavior. The footage duration is 2 minutes 30 seconds, but in our analysis only 120 second used. This 120 second was start from the beginning of earthquake occurred and finished after tsunami inundated the CCTV location. Along the time, all people captured in the footage was observed. It was found that 4 CCTV at least captured

the behaviors of 53 people, however due to camera location some people was not clearly seen in the footage. According to the footage shown in **Figure 4.4**, 30 persons stayed near the building (captured on camera 2), while 22 persons were on the road near the shoreline (captured by cameras 3 and 4). From **Figure 4.5** and **Figure 4.6** we can divide these people into three groups based on their responses after exposed by RES sources. Group 1 (persons 1–8 and 31–53) evacuated immediately after feeling the ground motions; group 2 (persons 9–11, 14, 15) evacuated before the sight of the tsunami. People in the group 1 and 2 are the early evacuees. Group 3 (persons 12, 13, 16-30) evacuated after noticing the tsunami arrival and categorized as late evacuees. At least 22 out of the 30 people (85 %) in groups 2 and 3 could see 23 other people (group 1 captured by camera 4), evacuating for at least 40 seconds with a distance of 68 m in front of them. However, this situation did not force them to initiate evacuation. Interestingly, we observed that when other evacuees approached these groups, one person initiated evacuation by running into th nearest building. This behavior created a chain reaction where the entire group initiated evacuation by running into the nearest building. In **Figure 4.6**, differences are observed in the influences between the standard model of evacuation trigger ranking and footage analysis. From the footage, it was noted that feeling ground motions influenced most people to initiate evacuation (57%). Our hypothesis is that the people in the group 1 (persons 31-53) initiate evacuation by not only feeling ground motions but also by seeing other evacuees. However due to the absence of footage of their behaviors for 0-50 s, there is insufficient evidence to explain this gap.

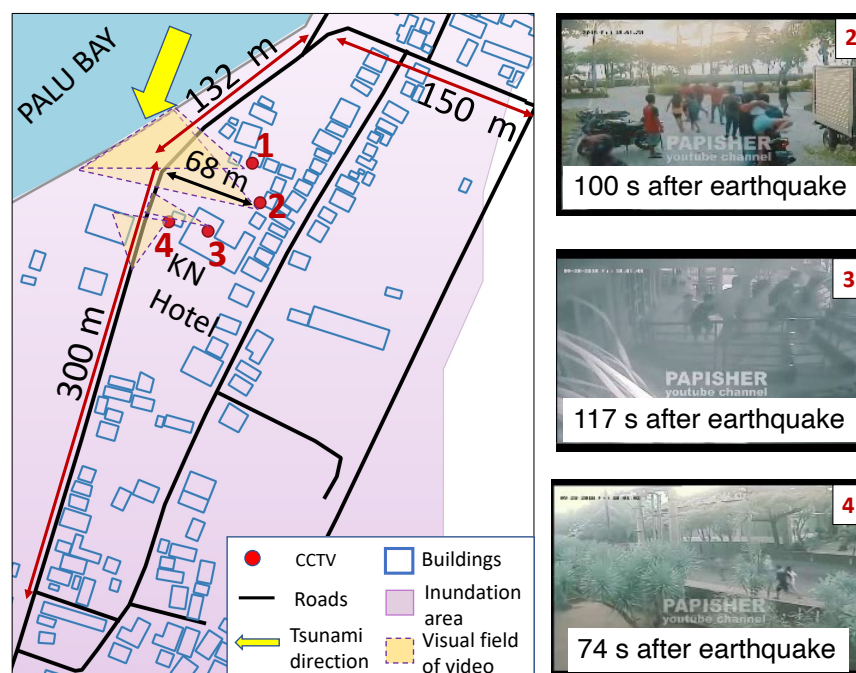


Figure 4.4. Environmental setting of the 2018 Palu tsunami (open street map, 2020) recorded in the KN Hotel (-0.86404 E, 119.879 S) CCTV. Video from (Carvajal et al., 2019)

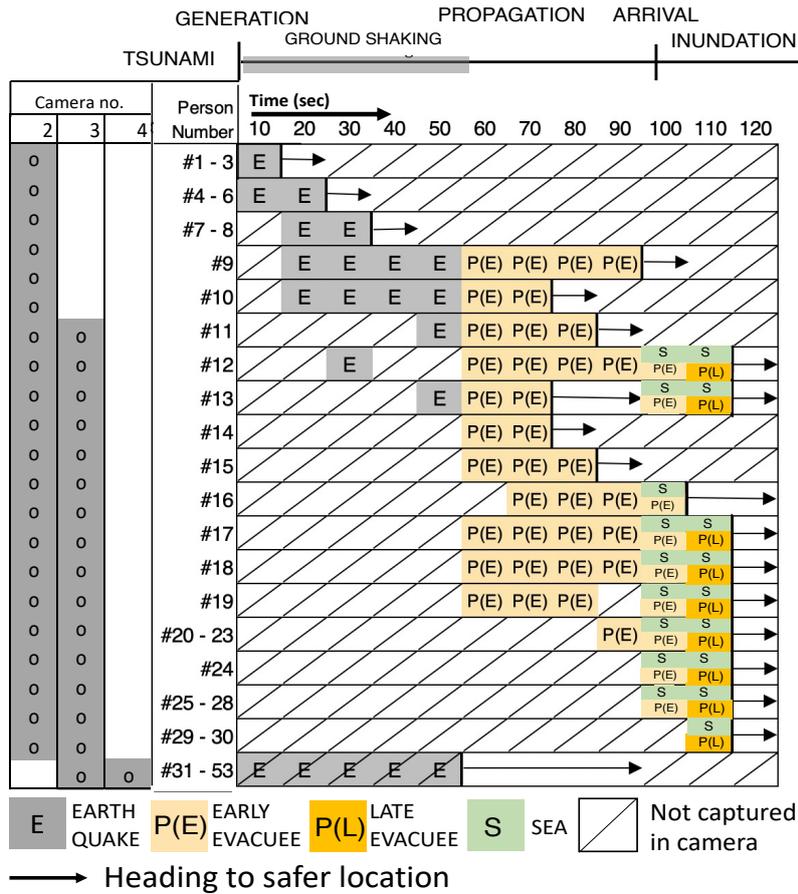


Figure 4.5. Analysis of the responses of 53 people exposed to the RES source observed from CCTV recording

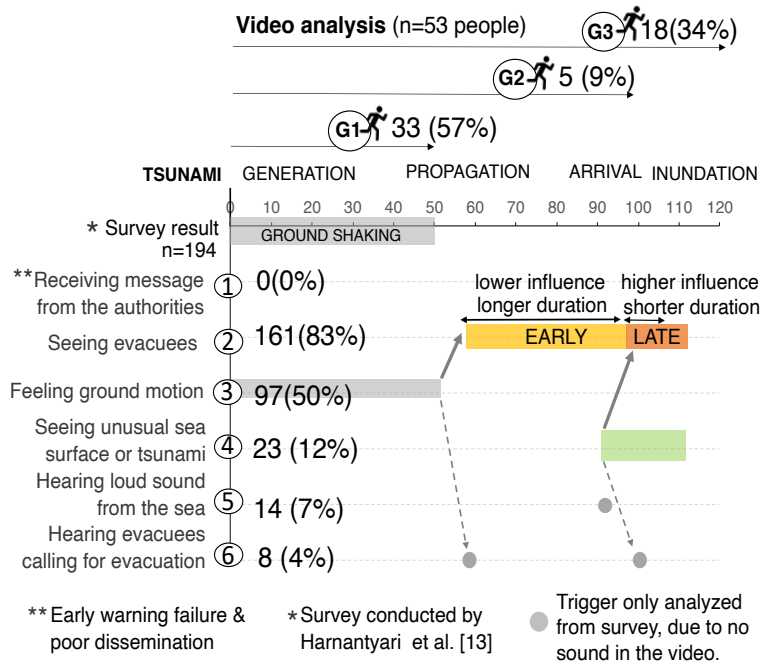


Figure 4.6. Comparison between people response to evacuation triggers from questionnaire survey to the dynamic of evacuation start process from footage analysis.

4.3.2 The Dynamic Video Analysis

The dynamic video analysis was using footages recorded in the commercial area, the three-store shopping center (Palu Grand Mall) that located on the west coast of Palu Bay. There were 4 footages recorded by different phone camera available on this area. These 4 videos at least captured 278 people, consist of 29 people on the road, 30 people on the 1st floor, 31 people on the 2nd floor, 154 people on the 3rd floor, and 34 people on the rooftop. All footages record the situation after earthquake occurred until tsunami arrival to the beach.

Table 4.2. Ratio of evacuee who initiate to move when the second tsunami arrive at land.

Location	Number of people	ratio
Road	25/29	86%
1 st floor	29/30	96%
3 rd floor	111/142	78%

Since the footage begin after the earthquake it is not possible to determine whether the people on the upper floors started evacuating after the earthquake or whether they were already on the upper floors from the beginning. Parameters obtained from the phone footage are similar to the aforementioned parameters; however, as a phone camera also includes sound, the following data could also be obtained: (1) the number of people who were shouting, calling people to evacuate and (2) number of people who evacuated after hearing other people calling for evacuation. Therefore 3 RES source were observed: (1) seeing other evacuee (SP), (2) hearing other evacuee calling for evacuation (HP), and (3) seeing tsunami approaching land (TS). The observation of response of 278 people to those 3 RES sources is shown **Figure 4.7**. The behavior of each people was analyzed for every 10 seconds. The vertical axis shows the evacuees ID of each 278 people. The horizontal axis shows the time when video start shooting. As mentioned above, the footage was shooting dynamically therefore for some people the time when the source exposed to them, and their action is not fully confirmed. The red line means the time was confirmed since it was shown in the video. Some action time was not confirmed but information can be deducted from their action that was captured on the video. The part without any notation (white blank) means at this time people was not shown in the video, and information cannot be deducted from the action that was capture in the video. The black dot represents the action start point. The vertical blue dotted line shown the time when tsunami hit the land.

The number of evacuees that their action can be confirmed to some extent in the video was 200 from 278. Based on the RES source, it was found that 181 people seeing tsunami approaching land, 186 people seeing other evacuee, and 171 hearing others evacuee calling for evacuation. It shows the type of RES source and their duration time give various impact to initiate people evacuate.

The 1st floor in this table also includes the stair that connecting ground floor to 1st floor. The evacuee location also affected their evacuation initiation. The percentage of people who started moving when the 2nd wave arrived is shown in **Table 4.2**. Evacuees at the rooftop are omitted because they were not clearly visible in the video. The 1st floor in **Table 2** includes the stairwell that connected the ground floor to the 1st floor. Almost all evacuees (96%) from the

There was a difference in the time needed to initiate evacuation between individuals and groups. Individuals refer to one or two evacuees, and groups refer to three or more evacuees. There were 25 individuals and 253 groups. A total of 90% of people acted in groups; of these, 12 out of 29 people acted individually (41%), and 17 people acted in groups (59%) on the road. The average evacuation start time was 109 s and 67 s for individuals and groups, respectively.

The presence of other people was shown to have impact on an individual's decision to evacuate. Individuals appear to be more influenced by people who are close rather than farther away. There was a difference of 42 s in the average evacuation start time between individuals and groups. Notably, the individuals that were part of a group had a quicker response time. This result is consistent with findings regarding the observation of other evacuees, the influences of this RES source varies depending on the distance between the evacuees and people who not yet evacuating. The influence of RES sources generated by the behavior of people are inconsistent and gradually increase as the distance between the sources and people decreases.

REFERENCE

- Goto, Y., Muzailin, A., Fadli, N., 2012. Response of the People in Banda Aceh just after the 2012 April 11 Off-Sumatra Earthquake (M8.6).
- Harnantaryi, A.S., Takabatake, T., Esteban, M., Valenzuela, P., Nishida, Y., Shibayama, T., Achiari, H., Rusli, Marzuki, A.G., Marzuki, M.F.H., Aránguiz, R., Kyaw, T.O., 2020. Tsunami awareness and evacuation behaviour during the 2018 Sulawesi Earthquake tsunami. *International Journal of Disaster Risk Reduction* 43, 101389. <https://doi.org/10.1016/j.ijdr.2019.101389>
- Hoppe, M.W., Padang working group, 2007. Early Warning experiences in Padang after first Bengkulu earthquake, 12 September 2007. German–Indonesian Cooperation for Tsunami Early Warning System.
- Kubisch, S., Guth, J., Keller, S., Bull, M.T., Keller, L., Braun, A.Ch., 2020. The contribution of tsunami evacuation analysis to evacuation planning in Chile: Applying a multi-perspective research design. *International Journal of Disaster Risk Reduction* 45, 101462. <https://doi.org/10.1016/j.ijdr.2019.101462>
- Lämmel, G., Rieser, M., Nagel, K., Taubenböck, H., Strunz, G., Goseberg, N., Schlurmann, T., Klüpfel, H., Setiadi, N., Birkmann, J., 2010. Emergency Preparedness in the Case of a Tsunami—Evacuation Analysis and Traffic Optimization for the Indonesian City of Padang, in: Klingsch, W.W.F., Rogsch, C., Schadschneider, A., Schreckenberg, M., *Pedestrian and Evacuation Dynamics 2008*. Springer Berlin Heidelberg, Berlin, Heidelberg, pp. 171–182. https://doi.org/10.1007/978-3-642-04504-2_13
- Mas, E., Koshimura, S., Imamura, F., Suppasri, A., Muhari, A., Adriano, B., 2015. Recent Advances in Agent-Based Tsunami Evacuation Simulations: Case Studies in Indonesia, Thailand, Japan and Peru. *Pure Appl. Geophys.* 172, 3409–3424. <https://doi.org/10.1007/s00024-015-1105-y>
- Mikami, T., Shibayama, T., Esteban, M., Ohira, K., Sasaki, J., Suzuki, T., Achiari, H., Widodo, T., 2014. Tsunami vulnerability evaluation in the Mentawai islands based on the field survey of the 2010 tsunami. *Nat Hazards* 71, 851–870. <https://doi.org/10.1007/s11069-013-0936-z>
- Muhammad, A., De Risi, R., De Luca, F., Mori, N., Yasuda, T., Goda, K., 2021. Are current tsunami evacuation approaches safe enough? *Stoch Environ Res Risk Assess.* <https://doi.org/10.1007/s00477-021-02000-5>
- Muhammad, A., Goda, K., Alexander, N.A., Kongko, W., Muhari, A., 2017. Tsunami evacuation plans for future megathrust earthquakes in Padang, Indonesia, considering stochastic earthquake scenarios. *Nat. Hazards Earth Syst. Sci.* 17, 2245–2270. <https://doi.org/10.5194/nhess-17-2245-2017>
- Muhari, A., Diposaptono, S., Imamura, F., 2007. Toward an Integrated Tsunami Disaster Mitigation: Lessons Learned from Previous Tsunami Events in Indonesia. *Journal of Natural Disaster Science* 29, 13–19. <https://doi.org/10.2328/jnds.29.13>

- Rafliana, I., Yulianto, E., Yunita, R., Arif, A., Weniza, Muhari, A., Shusilawati, N., Hanifa, R., 2016. *Kajian Efektivitas Sistem Peringatan Dini Tsunami Indonesia Pada Peristiwa Gempabumi Outer-Rise Samudera Hindia*, 2 Maret 2016.
- Syamsidik, Benazir, Umar, M., Margaglio, G., Fitrayansyah, A., 2019. Post-tsunami survey of the 28 September 2018 tsunami near Palu Bay in Central Sulawesi, Indonesia: Impacts and challenges to coastal communities. *International Journal of Disaster Risk Reduction* 38, 101229. <https://doi.org/10.1016/j.ijdr.2019.101229>
- Syamsidik, Istiyanto, D.C., 2013. Tsunami Mitigation Measures for Tsunami Prone Small Islands: Lessons Learned From The 2010 Tsunami Around The Mentawai Islands Of Indonesia. *J. Earthquake and Tsunami* 07, 1350002. <https://doi.org/10.1142/S1793431113500024>
- Takabatake, T., Shibayama, T., Esteban, M., Achiari, H., Nurisman, N., Gelfi, M., Tarigan, T.A., Kencana, E.R., Fauzi, M.A.R., Panalaran, S., Harnantaryari, A.S., Kyaw, T.O., 2019. Field survey and evacuation behaviour during the 2018 Sunda Strait tsunami. *Coastal Engineering Journal* 61, 423–443. <https://doi.org/10.1080/21664250.2019.1647963>
- Taubenböck, H., Goseberg, N., Setiadi, N., Lämmel, G., Moder, F., Oczipka, M., Klüpfel, H., Wahl, R., Schlurmann, T., Strunz, G., Birkmann, J., Nagel, K., Siegert, F., Lehmann, F., Dech, S., Gress, A., Klein, R., 2009. “Last-Mile”; preparation for a potential disaster – Interdisciplinary approach towards tsunami early warning and an evacuation information system for the coastal city of Padang, Indonesia. *Nat. Hazards Earth Syst. Sci.* 9, 1509–1528. <https://doi.org/10.5194/nhess-9-1509-2009>

CHAPTER 5 ANALYSIS OF THE REALITY-OF- EVACUATION-START SOURCES

The previous chapter introduce the general characteristic of evacuation initiation in Indonesian based on the past tsunami disaster. The more detail analysis using the video captured the situation of the 2018 Palu tsunami give information about impact of RES sources to Indonesia people. However, the video did not give information of RES source exposure and due to short video duration; quality problem; and irregular shoot there were some uncertainties on the observation result. Therefore, in this chapter, tsunami evacuation simulation was used as a method that enables to model the reality-of-evacuation-start. Using the data gained from survey and video analysis it possible to do quantitative and spatiotemporal analysis of factors affecting intuitive tsunami evacuation initiation.

5.1 Model Setting

The area for tsunami evacuation simulation was the residential area located in the west side of Palu Bay as shown in **Figure 5.1**. The reason for this location was chosen that the area is a residential area near the location where CCTV installed. In Fig. 5.1A. the north area (red box) is a town house complex that guarded by wall and only have one main entering gate. The south area (yellow box) is public houses. The sea on the east side of this area and the west side has higher topography. Tsunami hit both area A and B during the 2018 Palu tsunami.

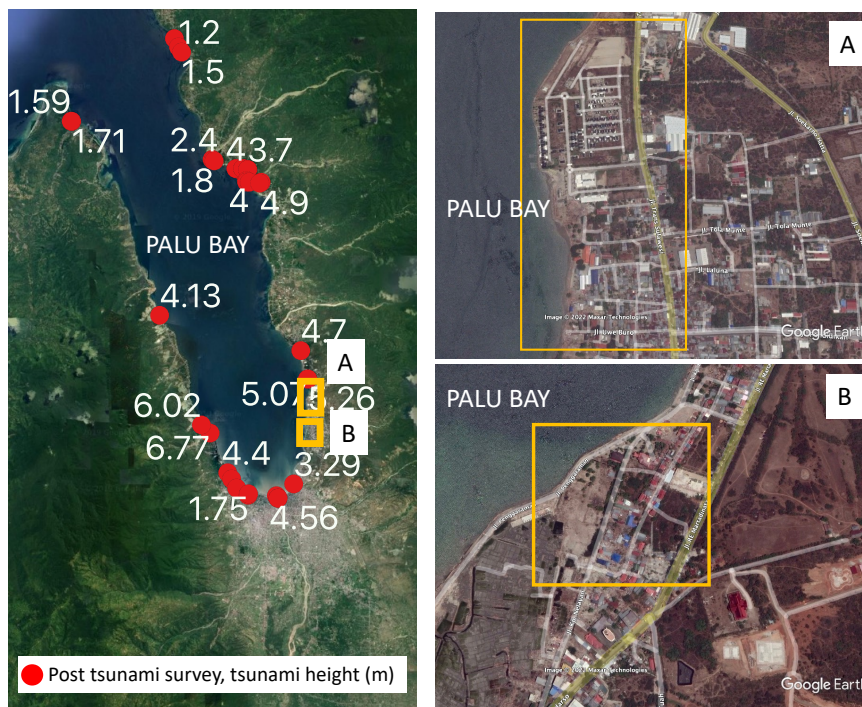


Figure 5.1. Palu map, A) The residential area as a target area for tsunami evacuation simulation and B) location of CCTV, installed at Hotel Nelayan. (map from google earth, accessed in 2020)

The setting of parameters and conditions to the tsunami evacuation simulation shown in **Table 5.1**. The duration of ground shaking by the earthquake determined from the CCTV record, it was 50 seconds. People can move during ground shaking, this condition also based on the CCTV records, the footage shows that people can run even when ground had not stopped shaking. This simulation focuses on 500 people. In this study all people were outside the building and randomly distributed around the area.

In this simulation, people can obtain danger information from this RES source; ground shaking, shouting evacuees, evacuating people, and tsunami. Message from the authorities, such as information from TV, radio or internet and warning from tsunami siren also included in the model. However, since none of authorities received by the people then the weight is 0.

Previous study by (Dohi et al., 2016) determine the weight using the questionnaire survey after the 2011 Great East Japan Tsunami conducted by Cabinet Office (Government of Japan) as shown in **Table 5.2**. The questionnaire included information number of evacuee exposed by RES source and how many of them start to evacuate after that. However, in the 2018 Palu tsunami, only information about what RES source triggered people to start evacuating. The only exposure known was all people can feel the ground shaking, it means the exposure was 100%.

Table 5.1. Parameters and setting condition to the tsunami evacuation initiation model.

Target area (m ²)	1384 x 396
Number of people	500
Duration of ground shaking (s)	50
Start time of tsunami inundation after the earthquake occurred (s)	120
Total time for analysis (s)	600

Table 5.2. Questionnaire survey asking what is the reason that makes them start to evacuate.

RES sources	Exposure (%)		Impact (%)	
	in Iwate, Miyagi, Fukushima*	Palu*	Ishinomaki*	Palu**
Ground motion	100	100	45.6	50
Tsunami	Varied for each case	50	-	12
Warning from TV, radio or internet*	61.1	-	48	-
Municipal RCS	51.8	-	53.6	-
People calling for evacuation	80.2	88	27	4
Seeing people evacuate	86.9	96	16.8	83

* From questionnaire survey conducted by cabinet data office government of Japan, 2014

** From questionnaire survey conducted by Harnantyari et al., 2020

Table 5.3. Weight of RES source for input parameter in the evacuation simulation.

Sources	Range	Weight
Ground motion	all area	0.39×10^{-3}
Tsunami	1/3 area	0.19×10^{-3}
Warning from TV, radio or internet	-	0
Municipal RCS	-	0
Hearing evacuee	32 m	0.036×10^{-3}
Seeing evacuee	110 m	0.69×10^{-3}

There was no information about the exposure in the social survey of 2018 Palu tsunami. From USGS data it was known that the ground motion was felt in the entire region (**Figure 2.1**) so all Palu residence should feel the shaking. Based on that information, the exposure of feeling ground motion is 100%. Exposure value of other RES sources was estimate from the exposure data in Iwate, Miyagi and Fukushima during 2011 Great East Japan tsunami (**Table 5.2**). The coastal area in Palu is flat and not many tall buildings surrounding, so the exposure value was estimated to be 10% higher. The exposure of tsunami estimated from the post-survey, the inundation in the target area of this study was up to 350 meters, we assumed 50% of people in the area could see the tsunami coming to the beach.

Based on this information we used **Eq. 5.1** to calculate the weight of ground shaking. The other RES sources then determined by the ratio to the ground shaking.

$$W_{eq}^{id} = W_{eq}^{jp} \times \frac{P_{eq}^{id}}{P_{eq}^{jp}} \times \frac{T_{eq}^{jp}}{T_{eq}^{id}} \quad (5.1)$$

where W_{eq}^{id} is the weight for feeling ground motion in Indonesia, W_{eq}^{jp} is the weight for feeling ground motion in Ishinomaki, Japan, P_{eq}^{id} is number of resident in Palu that start to evacuate after feeling ground motion, P_{eq}^{jp} is number of resident in Ishinomaki that start to evacuate after feeling ground motion, T_{eq}^{jp} ground motion duration in Ishinomaki, T_{eq}^{id} ground motion duration in Palu. The weights of the evacuation trigger parameters are equal to their exposure ratios to the information sources. For instance, the ground motions has significant impact with a wide exposure of 1–5 min; however, the exposure stops once the earthquake ends. On the other hand, seeing evacuees can only have impact within the limited radius of human visibility; however, this triggers work until the evacuees finish their evacuation. The parameter used for the simulation shown in **Table 5.3**.

In the simulation the first 50s, all residents could only obtain information from ground shaking. After that people could obtain information from another RES sources. From $t=50$ s until $t=110$ s, the RES sources worked are seeing and hearing another evacuee. Tsunami came at $t=110$ s, at this time 3 kind of RES sources worked. More exposure from RES source increasing the residents ALD. Then, those who's their ALD exceed threshold, start moving to evacuate and became as new RES sources. The simulation result can be seen on **Figure 5.2**.

The evacuation simulation demonstrated that the number of evacuation routes affects the time required for the evacuees to reach the goal areas. The right-side area has lesser and farther

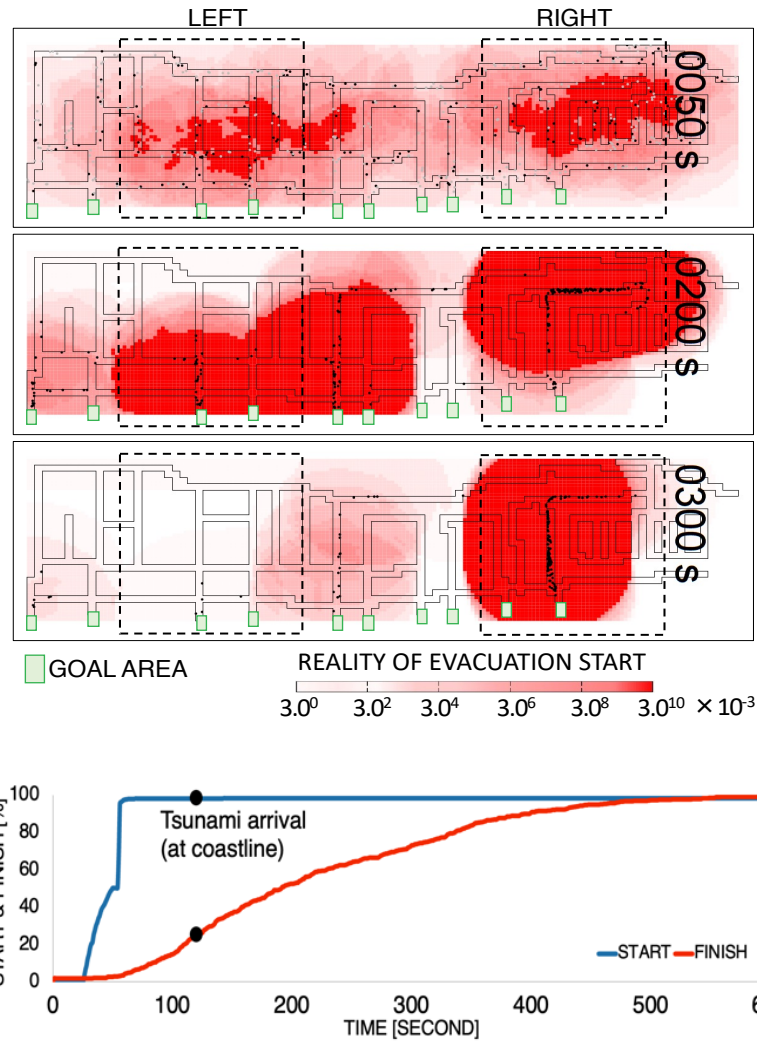


Figure 5.2. Numerical simulation of the evacuation during the 2018 Palu tsunami using a set of parameters obtained from the analysis of a previous Indonesian disaster case.

goal, which has the advantage of longer exposure to triggers. However, this situation can cause bottlenecks and required longer time to reach the goal compared with the left side area. In terms of comparison with Palu questionnaire result (**Table 5.2**), this gives a good agreement that 50% people evacuate after feeling ground motions. However, for the response time, the results show that people commence evacuations immediately after the ground motions stop (98%). We cannot validate this from the field survey, so parameter adjustment is needed to improve the evacuation generation simulation. Therefore, the information from video is needed to adjust the input parameter for the model and to validate the simulation result.

5.2 Environmental Source - Earthquake

During the 2018 Palu tsunami, there were two RES sources categorized as environmental sources. First was ground shaking caused by earthquake and second was unusual sea level caused by tsunami. The adjustment of ground shaking is critical since it act as the initial RES sources and affecting another RES source that worked after ground shaking stop.

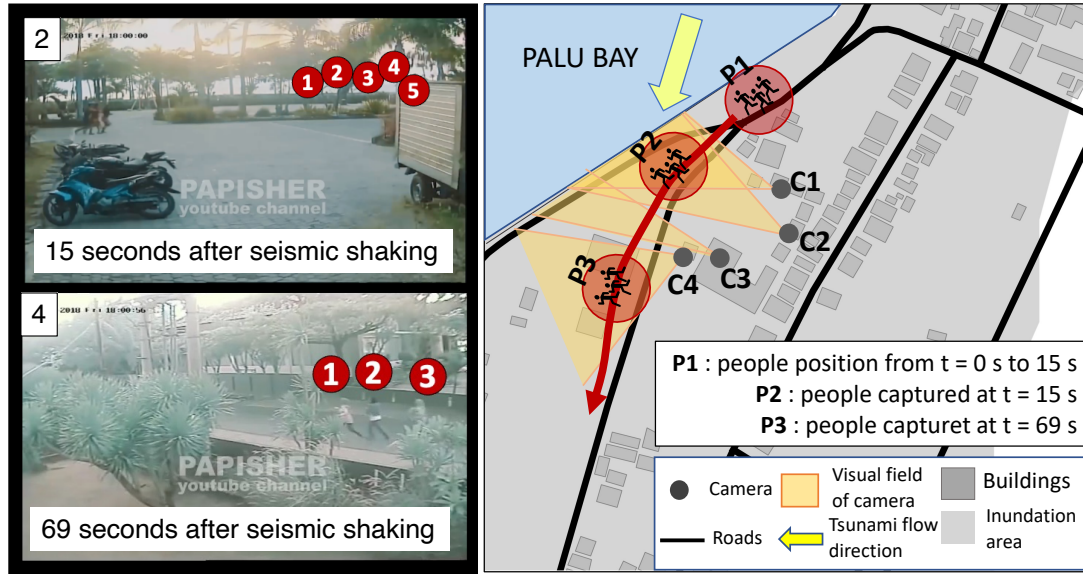


Figure 5.3. Footage shows a group of early evacuees. First, they were captured in camera 2 (P2) and in camera 4 (P3); the map shows the direction of their movement. (video from Carvajal et al., 2019)

Owing to the location of the cameras, some activities of the evacuees are not clearly visible on the footage. A tsunami evacuation start simulation, developed by Dohi et al, 2016, is used to determine the probable number of evacuees in this uncovered area. Footage captured by phone cameras are also included in the study to analyze the behavior of evacuees, after hearing the cry of people calling for evacuation. The quantitative parameters obtained from the surveillance camera footage are the following: (1) the time sequence that showed which triggers induced the people to evacuate, (2) number of evacuees who started evacuation before the tsunami arrival, and (3) number of evacuees when the tsunami hit the beach.

Figure 5.3 shows a surveillance camera capturing the movement of people for a long duration; however, some action cannot be clearly seen. The footage analysis, as shown in **Figure 4.5** and **Figure 4.6**, assumed 58% of people start evacuating after feeling ground motion. This group was already running 15 s after the start of the earthquake (P2); they continue running approximately 50 s later (P3). At P3, their behaviors were clearly captured by camera 4, at P2 not clearly captured by camera 2, and at P1, they were not captured on any camera. This problem can lead to under or over estimation of evacuee numbers. To validate the footage analysis the tsunami evacuation model was used to find more reasonable number of evacuees. The detail of scenario shown in **Table 5.4**. This scenario based on various reality-of-evacuation-start (RES) source ratio, between feeling ground motion (EQ), seeing other evacuees before tsunami hits (SPe) and seeing other evacuees when tsunami hits (SP1) affected number of people on the group of early evacuees (G1 and G2) and late evacuees (G3). In the scenario only ground shaking as RES sources was used to generate evacuee. From the footage analysis there were 2 things known. First, there were 8 people clearly seen on the video who start evacuating during ground shaking period (0-50s). Second, at least 32% of people start evacuating after tsunami arrival. Therefore, based on this information the maximum number

of people who immediately evacuate after feeling ground motion were 58% and the minimum number were 19%.

The result from simulation result using scenarios from can be seen on **Figure 5.4**, showing the relation between number of evacuees and the time when they decided to start evacuating. **Figure 5.4**, showed that if assuming only feeling ground motion (EQ) working as an RES source for people at P1, also described under scenario 1 in **Table 5.4**, then all people in unison start evacuation only 50 seconds after the earthquake. This condition does not portray the situation captured in the footage. Scenario 4 represents a more realistic result where at least

Table 5.4. Scenarios based on ratio of evacuee start evacuating only after feeling ground motion (EQ), total number of people (n) is 53 people.

Scenario	Group 1 (people)	Group 2 (people)	Group 3 (people)	Weight ($W_{i_s(t)}$) of RES sources		
				EQ	SP(e)	SP(l)
S1	31 (58%)	5 (9%)	17 (32%)	1	0.26	2.18
S2	25 (47%)	11(21%)	17 (32%)	0.8	0.31	2.18
S3	20 (38%)	16 (30%)	17 (32%)	0.7	0.36	2.18
S4	15 (28%)	21 (40%)	17 (32%)	0.5	0.41	2.18
S5	10 (19%)	26 (49%)	17 (32%)	0.3	0.46	2.18

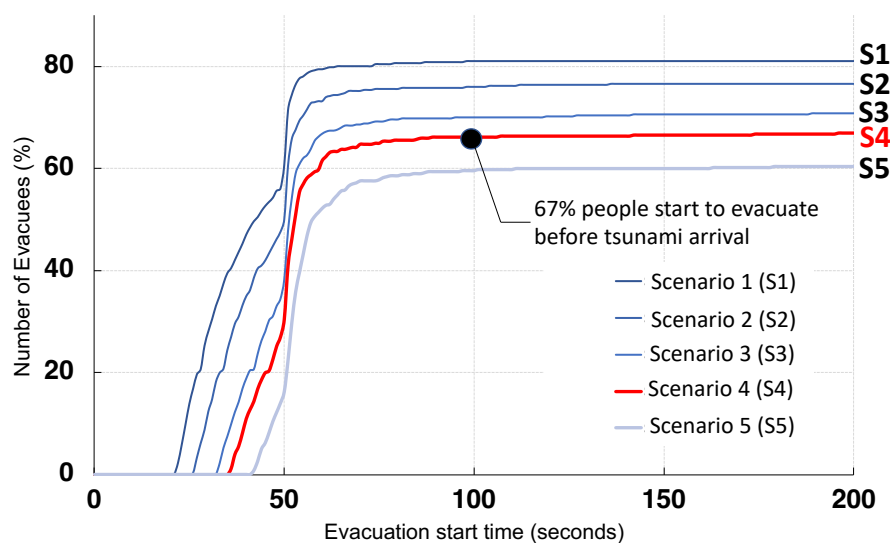


Figure 5.4. Simulation result based on ratio of evacuee start evacuating after feeling ground shaking.

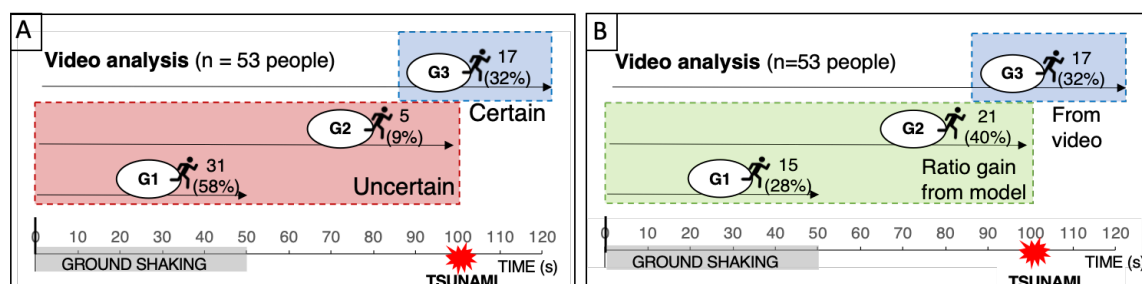


Figure 5.5. Distribution ratio of early evacuees (G1 and G2) based on, A) assuming only EQ work as RES source and B) EQ and SPe work as RES sources.

67 % of the early evacuees begin the evacuation before the arrival of the tsunami; the other 33% late evacuees start evacuation when the tsunami hits. The result is very close to the numbers of late evacuees clearly seen in the footage (32%). **Figure 5.5** shows a comparison with previous result (**Figure 5.2**), that assuming only EQ working as RES source for people at P1 and 100% put into G1. In this study, the result from numerical simulation provides better ratio and in accordance with the previous research about tsunami evacuation trigger ranking in Indonesia that seeing other people evacuation on the higher ranking than feeling ground motion. So, the adjustment of seeing another evacuee also need to be done.

5.3 Social source

During evacuation, people affected by other people behaviors. People ALD will increasing when they notice other people start evacuating or hearing other people calling for evacuation. The milling behavior also happened because of this source. People in general tend to follow the majority of people behavior. Based on the trigger ranking (**Figure 4.2** and **Figure 4.3**) the RES source worked on Indonesia people are seeing people start evacuating and hearing other people calling for evacuation. **Figure 5.2** shows instant evacuation happened; therefore, not only ground shaking but also adjustment parameter of other RES source needs to be done.

5.3.1 Seeing other's evacuee

Footage analysis both from static and dynamic video shows that there is different impact between seeing early evacuee (before tsunami arrive to their area) and seeing late evacuee (able to notice tsunami will arrive to their area). The footage also shows that distance to the evacuee also affecting people behavior. The distance of 110 m used in the numerical simulations was too broad for use as an effective range in Palu. The effective range of seeing evacuees based on visibility range should be adjusted. **Figure 5.6** show the situation in the CCTV that seeing evacuee with the distance 68 m did not make people start evacuating. While people start evacuating when they see the behavior of people near them with the distance only 11 m. The scenario used for this simulation is weight of seeing evacuee divided by two, depend on the disaster timeline. The weight for early evacuee had lower influence than the late evacuee. It starts after ground shaking (50s) and finished after tsunami arrive (120s). The weight for late evacuee had higher influence than the late evacuee and it start after tsunami arrive (120s) and ended until simulation finished. The detail of this setting parameter shown in **Table 5.5**. The result on **Figure 5.7** shows that before tsunami arrival, influence from seeing evacuee was not as high as previous result **Figure 5.2**. After tsunami arrival influence was higher than before as seen in the figure (120s). It also shows that not all people initiate to evacuate after feeling ground shaking and seeing other people. After tsunami arrival then 86% of people start evacuating. This result show better resemblance with the information observes in the video.

Table 5.5. Weight of RES source for input parameter in the evacuation simulation.

Sources	Range	Weight
Ground motion	All area	0.5
Seeing early evacuee	110 m	0.41
Seeing late evacuee	110 m	2.18
Tsunami	1/3 area	0.35

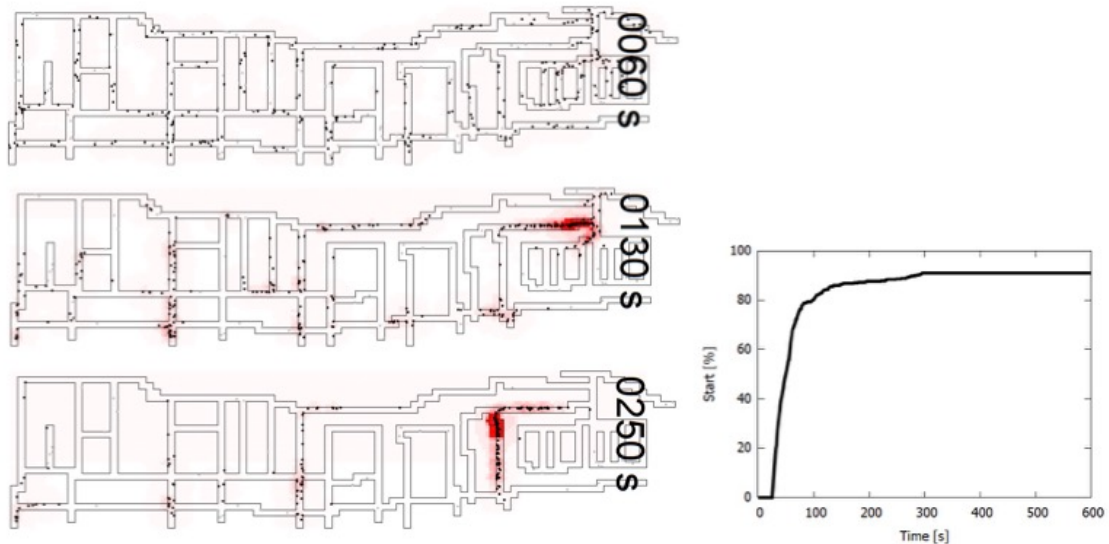


Figure 5.7. Simulation result using the scenario of different influence between seeing early evacuee and seeing late evacuee.

event. Analysis of footage and numerical simulation provided two important observations. First, evacuation trigger influences vary by the distance between evacuees and people who are yet to evacuate. Second, the influences of evacuation triggers from the behavior of other people vary by the time of occurrence. Late evacuees have greater influence and need shorter duration on initiating evacuation than early evacuees



Figure 5.6. Distance between people capture by camera 2 (Figure 4.4) to the evacuee running in front of them (68m) and the radii of group of people waiting in this area (11m).

Table 5.5. Weight of RES source for input parameter in the evacuation simulation.

Sources	Range	Weight
Ground motion	All area	0.5
Seeing early evacuee	110 m	0.41
Seeing late evacuee	110 m	2.18
Hearing early evacuee	32 m	0.05
Hearing late evacuee	32 m	0.13
Tsunami	1/3 area	0.35

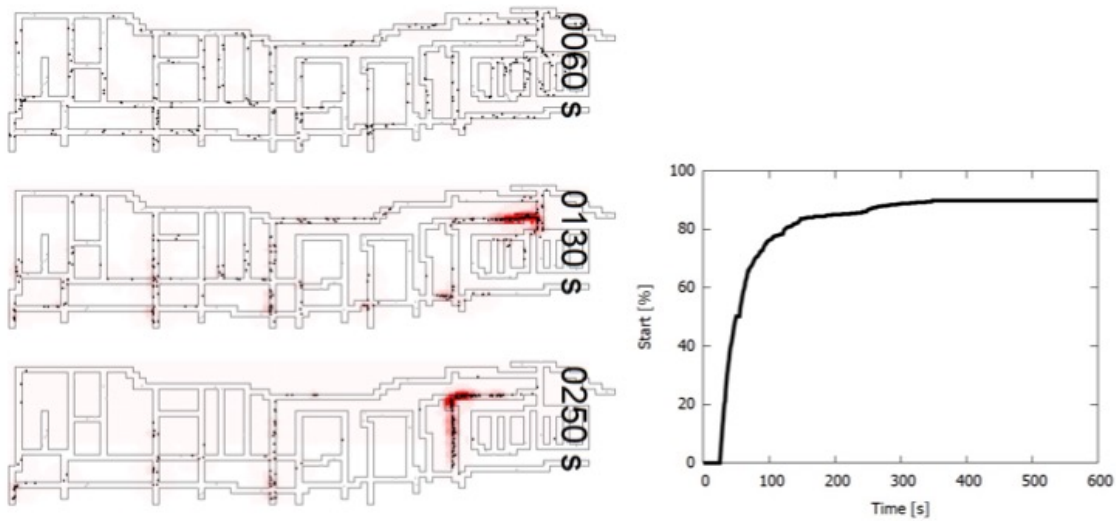


Figure 5.8. Simulation result using the scenario of different influence between seeing and hearing early evacuee and seeing and hearing late evacuee.

5.3.2 Hearing other’s evacuee calling for evacuation

From video captured by phone camera, during the disaster we can hear some people make noise, such as praying, crying, or shouting. However just few people gave a clear instruction. In the footage when evacuee shouting “tsunami, go inside the building” or “tsunami, go upstairs” then the people who hear this calling will follow the instruction. The static video analysis also shows that influence given by RES source during early evacuation was lower than in the late evacuation. Using this two information the adjustment of hearing other evacuee calling for evacuation was carried out. The detail of input parameter as shown in **Table 5.5**. There was not much difference on the simulation result between **Figure 5.7** and **Figure 5.8**. This is probably because the weight used as an input were too small, comparing with other RES source. The analysis on commercial area (**Figure 4.7**) shows that 30% of people start evacuating after hearing people shouting. However, this situation happened when the distance between evacuee was short. When people in the building shouting to the people on the road, their action did not triggered people on the road to start evacuating.

5.3.3 Comparison of RES sources and Evacuation Triggers between Indonesia and Japan

In Indonesia, hearing people calling for evacuation as a RES source is the last ranked (6th) trigger for evacuation (Figure 4.2). After the 2018 Palu tsunami (Table 5.2), multiple-answers questionnaires showed that 4% of the evacuees heard people calling for evacuation. In this study, we aimed to confirm whether hearing people calling for evacuation truly had a meager influence on elevating the ALD of people. The analysis of four footages recorded in the commercial area (Figure 4.7) Regarding hearing other people calling for evacuation, at least five people were caught on camera shouting. These five people became the RES sources, and at least 60 people reacted to them. This implies that 30% of the people evacuated because of hearing other people calling for evacuation—this is a very high percentage compared to the questionnaire results in Palu.

To understand the difference one camera was chosen for a detailed analysis of evacuee behavior. The environment where the footage was captured is shown in Figure 5.9. The footage was shot from the 2nd floor before the 1st tsunami hit. During the disaster, many people make noises, such as praying, crying, or shouting. From the detail analysis as shown in Figure 5.10, it is known that 60% of people exposed by the noises from people. However, only one person gave clear instructions.

In the footage (Figure 5.10), when the evacuee shouted “tsunami, go inside the building” or “tsunami, go upstairs,” the people who heard this reacted favorably to the instruction. Unfortunately, the exposure area is limited, and the farther away the sound source, the more challenging it would be for people to hear the instructions. Furthermore, the instructions blended with the noisy environment, making it harder to hear. As a result, people on the road and stairwell were unaffected, while people nearby were influenced by the instructions.

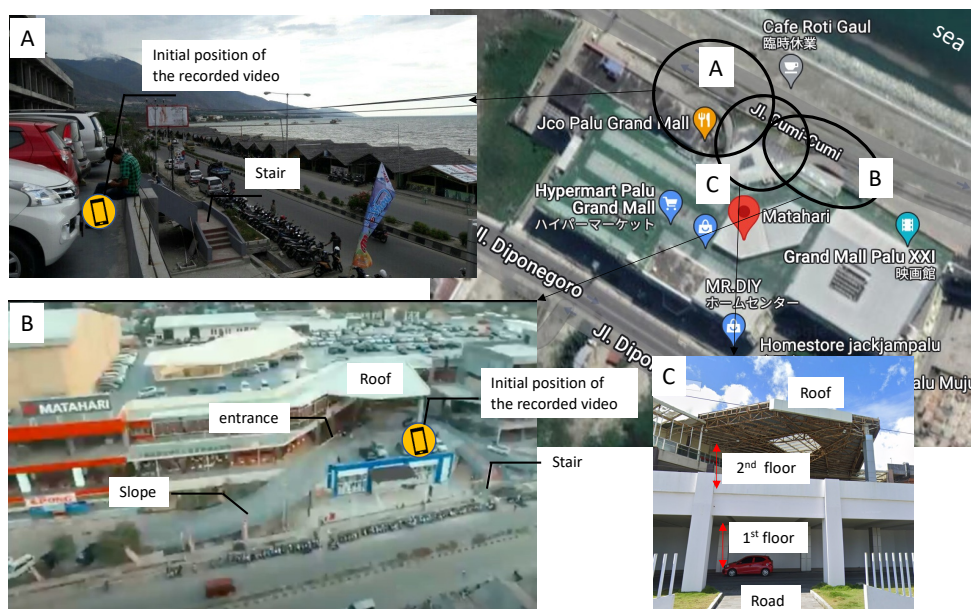


Figure 5.9. Building setting of the commercial area. **A** point of view from the left side of the 2nd floor, **B** aerial view of the building, and **C** floor setting of the building. (picture from, (“Google Maps,” 2022)(“foursquare palu grand mall,”2022) , (CNN Indonesia,2022))

The RES source of hearing other people calling for evacuation is presumed to have a greater impact than that revealed by the post-tsunami interview survey (Table 5.2) : 4% and 9% in the 2018 Palu and Krakatau tsunamis, respectively. Interestingly, the questionnaire survey in Ishinomaki, Japan showed that shouting evacuees influenced 27% of people to start tsunami evacuation (Table 5.3).

In Indonesia, seeing other people had a significantly higher influence on people to initiate evacuation, 83% in Palu. In Japan, hearing had a greater impact than seeing. The low percentage of hearing was probably because of 1) small exposure area where only few people could be fully exposed by the RES sources, and 2) people shouting unclear instruction. Instead of urging others to evacuate, most people were crying or screaming because they were afraid of the tsunami. The interview (UNDRR and UNESCO-IOC, 2019) shows the testimony from 43 years old female, she said “I couldn’t shout, could not. Just silent. I ran. I ran to the street, people shouted: The seawater is rising! Everybody runs! We were all running.”. So, there are two conditions, first people shouting unclear instruction or did not shout at all. This challenge may be resolved by preparing them to act calmly when a disaster occurs. Residents should participate in tsunami drills and be trained to shout clear instructions when in a dangerous situation. With proper training, more evacuees could hopefully act as RES sources and urge other people to start evacuating.

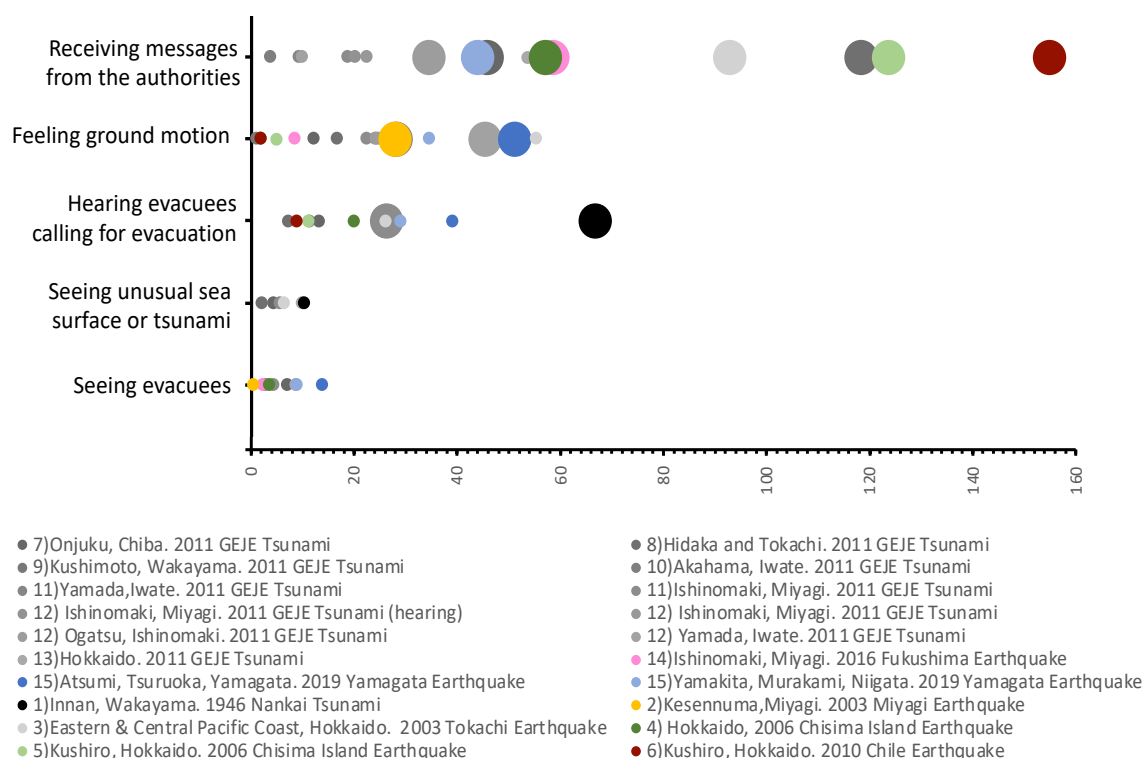


Figure 5.11. Evacuation trigger based on the data collected from previous field surveys in Japan (Table 5.6). The larger circles indicate this source chosen by majority of people as the reasons why they initiate evacuation.

The previous discussion used a comparison between the case study in the 2018 Palu tsunami and the 2011 Great East Japan Tsunami in Ishinomaki. In the previous discussion (**Chapter 4.2**), using the method developed in this study, the standard of tsunami evacuation trigger in Indonesia was found. This same method was then applied to find Japan's tsunami evacuation trigger ranking. The plot was created using 20 studies covering nine tsunami and earthquake events in Japan (**Table 5.6**). The oldest tsunami event is the 1946 Nankai tsunami,

Table 5.6. Survey result on tsunami evacuation triggers in Japan from 1946 – 2019

No	Event**	Survey location	Method*	Conducted by
1	1946 Nankai Tsunami	Innan City, Wakayama Prefecture	SA	Kawata et al., 2005
2	2003 Miyagi Earthquake	Kesenuma City, Miyagi Prefecture	SA	Katada et al., 2005
3	2003 Tokachi Earthquake	Eastern & Central Pacific Coast in Hokkaido	MA	Matsuo et al, 2004
4	2006 Chisima Island Earthquake	4 municipalities along the Okhotsk Sea coast and the Pacific coast in Hokkaido	SA	Honma and Katada, 2008
5	2006 Chisima Island Earthquake	Kushiro City, Hokkaido	MA	Kato et al., 2009
6	2010 Chile Earthquake	Kushiro City, Hokkaido	MA	Kato and Suwa, 2011
7	2011 GEJE Tsunami	Onjuku, Chiba Prefecture	SA	Isagawa et al., 2012
8	2011 GEJE Tsunami	Hidaka and Tokachi, Hokkaido	MA	Mizuki and Hirakawa, 2011
9	2011 GEJE Tsunami	Kushimoto City, Wakayama	SA	Ogasawara et al., 2013
10	2011 GEJE Tsunami	Akahama City, Iwate Prefecture	SA	Kambara et al., 2014
11	2011 GEJE Tsunami	Yamada City, Iwate Prefecture	SA	Ichiko, 2015
		Ishinomaki City, Miyagi Prefecture	SA	
		Ishinomaki City, Miyagi Prefecture	SA	
12	2011 GEJE Tsunami	Ishinomaki City, Miyagi Prefecture	HS	Goto et al., 2015
		Ishinomaki City, Miyagi Prefecture	SA	
		Ogatsu Town, Ishinomaki City Yamada City, Iwate Prefecture	SA SA	
13	2011 GEJE Tsunami	6 Municipalities, Coastal of Hokkaido	SA	Tanaka et al., 2013
14	2016 Fukushima Earthquake	Ishinomaki City, Miyagi Prefecture	SA	Sato et al., 2017
15	2019 Yamagata Earthquake	Atsumi District, Tsuruoka City, Yamagata Prefecture	MA	Sato and Imamura, 2020
		Yamakita District, Murakami City, Niigata Prefecture	MA	

*SA: Questionnaire only single answer, MA: Questionnaire allow multiple answer, HS: Hearing survey

**GEJE: Great East Japan Earthquake

and the most recent one is the 2019 Yamagata earthquake. Some surveys use the multiple-answers method so that the trigger percentage can be higher than 100%.

The standard ranking is the first approach to compare the evacuation trigger in Indonesia with Japan. There are several important issues to note.

1. The numbers of surveys covering the 2011 Great East Japan Earthquake and Tsunami are more than half of the total surveys (11 out of 20 surveys).
2. The old tsunami event, the 1946 Nankai Tsunami, is included in this rank. At this time, a tsunami early warning system was not established yet.
3. Hearing the loud sound from the sea did not include this rank because the surveys in Japan did not ask about this trigger.

From the plot (**Figure 5.11**), it is known that the number one ranking is receiving messages from the authorities (11 out of 20 surveys). The second rank is feeling ground motion (5 out of 15 events), and the third rank is hearing evacuees calling for evacuation (3 out of 15 events). Seeing tsunami coming and seeing evacuees have never been the most prevalent trigger to make people choose to start evacuating. This trigger is on the fifth and sixth rank, respectively.

Receiving a message from authorities became the number one rank to make people start evacuating, both in Japan and Indonesia. In Japan, the tsunami warning system was first developed in 1941 (Bernard and Titov, 2015). It has been 80 years of the establishment and the introduction of evacuation based on warning. Indonesia's tsunami warning system is much younger, only 14 years since its first establishment in 2008. Considering the importance of this trigger, the success of disseminating the correct messages to the public is a crucial matter. The fact that in Indonesia, the TEWS always fails to disseminate warnings in past tsunami events shows that evacuation-based warnings should not be the only option. Intuitive tsunami evacuation should be encouraged in the communities.

There is not much difference in the rank of evacuation-trigger by natural cues, feeling ground motion, and seeing unusual sea surface or tsunami between Japan and Indonesia. Interestingly, the big gap comes from the rank of evacuation trigger by social cues. Hearing people calling for evacuation is the third rank in Japan and the lowest rank in Indonesia. Seeing evacuees is the second rank in Indonesia but the lowest in Japan. The CCTV video analyzed in Chapter 4.3 shows that Indonesian people tend to quit the building after feeling ground motion and staying outside the building. The interview (UNDRR and UNESCO-IOC, 2019) shows the testimony of a Male, 41 years old. He said, "The earthquake was so strong. I could not stand it. People lied if they said they could stay upright during the earthquake. At the time I was getting ready to pray (Maghrib) at the mosque, I took off my clothes; when it happened, I ran outside naked". This reveals that some people go out of the building after feeling ground motion. When people go out of the building, they can see people running, so intuitively they follow what other people are doing. In Japan, after the earthquake, people stayed inside the building and sought disaster information through media. Therefore, they could not see what other people were doing outside the building.

Further research on the difference in tsunami evacuation initiation is important because this indicates that the disaster risk reduction strategy should not be generic among countries. Another testimony from 40 years old female who worked as a food vendor strengthens that statement; she said "In the training, we waited for the earthquake to stop first, but it didn't stop, and then the waves came. It was as high as the house over there. Oh! This is the tsunami. We

ran and shouted 'tsunami!'. We did not know what tsunami looked like before. We just realized that it was indeed tsunami. I have never experienced it. We just saw it on the TV, right?" (UNDRR and UNESCO-IOC, 2019). Therefore, educational material for tsunami training and drills must consider the local characteristics.

REFERENCES

- Bernard, E., Titov, V., 2015. Evolution of tsunami warning systems and products. *Phil. Trans. R. Soc. A*. 373, 20140371. <https://doi.org/10.1098/rsta.2014.0371>
- CNN Indonesia, Kondisi Terkini “Palu Grand Mall” Pascagempa & Tsunami <https://www.youtube.com/watch?v=4xZXgCmi77c&t=2s> (accessed 2022-05-17)
- Carvajal, M., Araya-Cornejo, C., Sepúlveda, I., Melnick, D., Haase, J.S., 2019. Nearly Instantaneous Tsunami Following the Mw 7.5 2018 Palu Earthquake. *Geophys. Res. Lett.* 46, 5117–5126. <https://doi.org/10.1029/2019GL082578>
- Dohi, Y., Okumura, Y., Koyama, M., Kiyono, J., 2016. Evacuee Generation Model of the 2011 Tohoku Tsunami in Ishinomaki. *J. Earthquake and Tsunami* 10, 1640010. <https://doi.org/10.1142/S1793431116400108>
- Foursquare Palu Grand Mall 2022. <https://ja.foursquare.com/v/palu-grand-mall/50442722067dab59d76e88d4/photos> (accessed 2022-05-17)
- Google Maps, <https://www.google.com/maps/place/Palu+Grand+Mall/> (accessed 2022-05-17)
- Honma, M., Katada, T., 2008. Study on the Relationship between Disaster Advance Information and Resident Evacuation in Tsunami Disaster Prevention, *Journal of Disaster Information Studies*, Vol.6, pp.61-72, https://doi.org/10.24709/jasdis.6.0_61. (In Japanese)
- Ichiko, T., 2015. A Discussion for “self-active Tunami Evacuation” in the Great East Japan Earthquake -Comparative analysis between Yamada Town and Ishinomaki City, *Journal of Japan Association for Earthquake Engineering*, Vol.15, No.5, pp.5_31-5_40, https://doi.org/10.5610/jaee.15.5_31. (In Japanese)
- Isagawa, T., Murao, O., Ohno, R., 2012. Coastal Residents' Behavior in The Event of Tsunami Questionnaire surveys before and after the Tohoku region pacific coast earthquake at Onjuku, Chiba prefecture, *Journal of Architecture and Planning*, Vol.77, No.681, pp.2525-2532, <https://doi.org/10.3130/aija.77.2525>. (In Japanese)
- Kambara, K., Kubota, A., Kurose, T., Hagiwara, T., Fukushi, K., Tanaka, A., 2014. Study on the Evacuation Behaviors of Elderly Residents in Rural Communities During the Great East Japan Earthquake In Relation To The Built Environment, *Journal of Architecture and Planning*, Vol.79, No.701, pp.1593-1602, <https://doi.org/10.3130/aija.79.1593>. (In Japanese)
- Katada, T., Kodama, M., Kuwasawa, N., Koshimura, S., 2005. Issues Of Resident's Consciousness and Evacuation from The Tsunami in Kesennuma City, Miyagi Pref. After The 2003 Miyagi Earthquake, *Journal of Disaster Research*, Vol.2005, No.789, pp.789_93-789_104, https://doi.org/10.2208/jscej.2005.789_93. (In Japanese)
- Kato, F., Suwa, Y., Hayashi, H., 2009. Decision Making on Evacuation from Tsunami of the Earthquake Off Chishima Islands in 2006, *Proceedings of Hydraulic Engineering, JSCE*, vol.53, pp.865-870. (In Japanese)
- Kato, F., Suwa, Y., 2011. Survey on Evacuation in Kushiro City from the Chilean-EarthquakeTsunami in 2010, *Journal of Japan Society of Civil Engineers, Ser. B2 (Coastal Engineering)*, Vol.67, No.2, pp. I_1271-I_1275, https://doi.org/10.2208/kaigan.67.I_1271. (In Japanese)
- Kawata, Y., Kono, T., Shiroshita, H., Goto, R., 2005. Improvement of Coping Capacity of Local Community against Disaster Considering Evacuation Trigger during the 1946 Nankai Tsunami, Japan, *Proceedings of Coastal Engineering, JSCE*, Vol. 52, pp.1261-1265. (In Japanese)

- Mizuki, C., Hirakawa, K., 2011. Awareness of Tsunami and Evacuation Activities of the Residents in Hida ka and Tokachi Coast on the 3.11 Great East Japan Earthquake-Tsunami Occurrence, *Geographical Studies*, Vol.86, No.1, pp.97-107, <https://doi.org/10.7886/hgs.86.97>. (In Japanese)
- Ogasawara, T., Nakahata, M., Matsubayashi, Y., Sakai, S., 2013. Survey On Evacuation Against 2011 Tohoku Earthquake Tsunami In Kushimoto Town In Wakayama Prefecture, *Journal of Japan Society of Civil Engineers*, Ser. B3 (Ocean Engineering), Vol.69, No.2, pp. I_37-I_42, https://doi.org/10.2208/jscejoe.69.I_37. (In Japanese)
- Sato, S., Imamura, F., Aizawa, K., Yokoyama, K., Sato, K., Iwasaki, M., Minakawa, M., Togawa, N., 2017. Evacuation Behavior Caused by the 2016 Fukushima Earthquake and Tsunami in Ishinomaki City, Miyagi Prefecture, *Journal of Japan Society of Civil Engineers*, Ser. B2 (Coastal Engineering), Vol.73, No.2, pp. I_1603-I_1608, https://doi.org/10.2208/kaigan.73.I_1603. (In Japanese)
- Sato, S., Imamura, F., 2020. Evacuation Behavior Caused by A Short Arrival-Time Tsunami: Case of the 2019 Yamagata Earthquake and Tsunami, *Journal of Japan Society of Civil Engineers*, Ser. B2 (Coastal Engineering), Vol.76, No.2, pp. I_1309-I_1314, https://doi.org/10.2208/kaigan.76.2_I_1309. (In Japanese)
- Tanaka, G., Watanabe, Y., Nakatsugawa, M., 2013. Evacuation Behaviors of Coastal Residents in Hokkaido for the 2011 Tohoku Earthquake Tsunami, *Journal of Japan Society of Civil Engineers*, Ser. B2 (Coastal Engineering), Vol.69, No.1, pp.48-63, <https://doi.org/10.2208/kaigan.69.48>. (In Japanese)
- UNDRR, UNESCO-IOC, 2019. *Limitations and Challenges of Early Warning Systems: A Case Study of the 2018 Palu-Donggala Tsunami*, IOC Technical Series. United Nations Office for Disaster Risk Reduction (UNDRR), Regional Office for Asia and the Pacific, and the Intergovernmental Oceanographic Commission of United Nations Educational, Scientific and Cultural Organization.

CHAPTER 6 CONCLUSION

This research focused on understanding the natural phenomena of the landslide-induced tsunami and the social phenomena of tsunami evacuation. We used a new approach to find the parameters for the numerical simulation of the landslide-induced tsunami wave. For analyzing the social phenomena, we observed the atmosphere of "must escape" cues created from natural, social and authority messages, and their influence on the residents, to initiate evacuations. The 2018 Palu tsunami was used as a case study because it could address gaps in understanding of evacuation behavior during a non-typical tsunami. We developed a method to estimate the impact and exposure of each cue quantitatively, then used this parameter to simulate the evacuation initiation process. The results provided the information to analyze:

- 1) The similarities and differences between the evacuation during the typical seismic tsunami and the non-typical seismic tsunami.
- 2) Comparison between the evacuation behavior in Indonesia and Japan.
- 3) Find problems and recommendations for evacuation strategies for future non-typical seismic and non-seismic tsunami disasters.

Chapter 2 proposed a new approach to address the difficulty of determining the parameters of submarine landslides. Numerical simulation of landslide-induced tsunami often oversimplified the landslide mechanism, for example, assuming landslide as a block of solid sliding into the water (reference), making a rough assumption on the landslide parameters, and assuming landslide as a rigid mass. This approach usually leads to underestimating the tsunami height and inundation area. In the 2018 Palu event, the earthquake was followed by immediate cascading disasters of coastal subsidence, landslides both on land and submarine, and tsunami. This situation allowed us to analyze the landslide phenomena on land to characterize the submarine landslide causing the tsunami. Due to unavoidable circumstances, in this case, the Covid-19 pandemic, it is pretty challenging to conduct a local survey. We, therefore, used the accessible online information. Video of landslides in Jono-Oge landslide in areas in Palu, and soil sampling analysis from the other landslide area in Palu, Balaroa (12 km to the north of Jono-Oge), and Sibalaya (20 km to the south of Jono-Oge). We analyzed the data and found information on landslide velocity, displacement, and pore water pressure through optical analysis, mathematical calculations, and numerical simulation. Then finally, we were able to find the shear stress value that can be used as an input parameter in the tsunami generation model (Volcflow). The shear stress from the liquefaction analysis in Jono-Oge, Palu, 1.5 kPa, can produce four times higher tsunami heights than the stress value suggested for general cases (20kPa). This result showed that:

- An appropriate landslide characterization is crucial to simulate tsunami accurately.
- In the future, it is possible that only a landslide, without a strong earthquake, is enough to generate a destructive tsunami. It means ground motion will not be available as a critical RES source.

Chapter 3 explains the definitions and concepts about tsunami evacuation used in this research. The tsunami evacuation phase is the passage of time from the earthquake occurrence to the tsunami arrival. The phase of interest in this study was the behavior change from the response stage into the evacuation initiation stage. The intuitive tsunami evacuation is the framework behind people's decision to start the evacuation. Two crucial aspects affecting their decision were the RES and awareness-level-of-danger (ALD). RES was caused by environmental, social, and warning information cues. We called these cues RES sources. ALD is the sense of urgency to save lives immediately. ALD threshold can be different among people, and it depends on their understanding of disaster because of training, experience, or emergency drills. This chapter described the method of:

- Past-survey interview to find the type of RES sources that functioned as a trigger for Indonesian people to start evacuating.
- Video analysis to estimate the impact and exposure of the RES sources quantitatively and qualitatively.
- Numerical simulation of tsunami evacuation, that expresses behavior at the start of evacuation and evacuee movement after the initiation.

Chapter 4 describes the post-disaster survey findings and focuses on the people's responses to the reason that prompted them to evacuate. The results show common behaviors among Indonesian people. It revealed six RES sources:

- 1) receiving a message from the authorities,
- 2) seeing evacuees,
- 3) feeling ground motion,
- 4) seeing unusual sea surface or tsunami,
- 5) hearing loud sounds from the sea, and
- 6) hearing evacuees calling for evacuation.

Video analyses provided information that was not captured by the field survey. The observation of 53 individuals from six static cameras installed in the hotel located on the east coast of Palu Bay shows that:

- The ground shaking happened for 50 seconds. In this period, no building collapsed, and people could move.
- The tsunami came to the beach around 110 seconds after the earthquake, or only 60 seconds after ground shaking stopped.
- There were 17 (32%) late evacuees, who started to evacuate only after seeing the tsunami hitting their location. Their action was clearly seen in the video.
- There were 38 (68%) early evacuees, who started to evacuate before the tsunami came into their location. Due to the camera location, the behavior of 22 individuals during the first 68 seconds after the earthquake was not seen clearly in the video.
- Feeling the ground move was the first RES exposure source. People did not evacuate immediately after feeling the ground motion.
- Seeing people evacuating was the second RES exposure source. Seeing evacuees before the tsunami was less impactful compared to seeing them after people had seen the tsunami wave.
- The action of evacuees near the people who had not started evacuating was more impactful.

The observation of 200 individuals captured on the four phone cameras in the commercial area (Palu Grand Mall), located on the west coast of Palu Bay shows that:

- At least five people were caught on camera shouting. They became the auditory RES source for other people calling for evacuation. Around 60 people reacted to this auditory notification, implying that 30% of the exposed people had been influenced by this RES source.
- The evacuee location also affected the evacuation initiation. Almost all evacuees (96%) on the road and the 1st-floor moved from their current position when the first tsunami came.
- There was a difference in the time needed to initiate evacuation between individuals and groups. The average evacuation start time was 109 s for individuals and 67 s for groups.
- When evacuees shouted clear instructions such as “tsunami, go inside the building” or “tsunami, go upstairs,” the people who heard this reacted favorably to the instruction. Unfortunately, the exposure area was limited, and the farther away the sound source, the more challenging it became for people to hear the instructions

Chapter 5 shows the implementation of tsunami evacuation simulation in the residential area located on the east coast of Palu Bay. This model analyzes RES in a spatiotemporal manner. In using this model, it is necessary to set a weight that represents the degree of influence of the RES sources and the ALD threshold for each resident. The weight of the RES source was estimated by using the information on exposure and impact obtained from the post-disaster survey and video analysis. The ALD threshold of each resident was not uniform. Random numbers were used to express the threshold variation. The RES sources used in this model were feeling the ground move, seeing other people evacuating, hearing other people calling for evacuation, and seeing a tsunami coming. Due to the failure of tsunami warning during the 2018 Palu tsunami, the RES source of message from authorities was not included in this model. To reconstruct the evacuation process corresponds to what is depicted in the CCTV video, approximately 28% of residents should started tsunami evacuation immediately after feeling ground motion.

- To reconstruct the evacuation process corresponding to what was depicted in the CCTV video, approximately 28% of residents should have started tsunami evacuation immediately after feeling the ground move.
- The influenced weight of RES sources generated by social cues, both seeing and/or hearing other people, was not constant. Instead, the impact should gradually increase as the distance between the source and people decreases.
- The weight of seeing an evacuee and/or hearing other people calling for evacuation should not be constant all the time. When the tsunami arrived, the impact of other peoples’ behavior should be higher than before.
- Based on the scenario, it was found that to achieve this, 75% of residents would have to decide on early evacuation, before the tsunami came, and at least 47% of the residents would evacuate immediately after feeling the ground move because of the earthquake. This group of people would not wait for other cues, such as receiving messages to evacuate from the authorities, observing other people’s behavior, or waiting until they saw or heard the tsunami’s arrival.

A study on evacuation initiation in the 2011 Great East Japan tsunami in Ishinomaki was conducted in 2016. The author (Dohi, 2016) mentioned that for future studies it is necessary to

establish a verification or validity confirmation method that provides quality assurance for the calculation of the start of evacuation. It is no exaggeration to say that the establishment of verification and validation methods that ensure accuracy and reliability will greatly contribute to the academic development of the start of evacuation. Analysis of RES source for the case study in Ishinomaki used a post-disaster questionnaire survey conducted by the Japanese cabinet office. Questionnaires are a popular fundamental tool for acquiring information on public knowledge and their perceptions on natural hazards (Bird, 2009). However, the evacuation process cannot be comprehensively depicted by this method. An estimation of the impact and exposure of environmental, social, or warning cues for evacuees is challenging. This study combined information from questionnaire surveys, video observations, and a numerical simulation for a more comprehensive and quantifiable result. Furthermore, information regarding individual behavior and interactions among evacuees in the group was obtained.

The multiple-answers questionnaires of the 2018 Palu tsunami, showed that 4% of the evacuees heard people calling for evacuation. From the video analysis and numerical simulation, 30% of people exposed by the RES source of hearing other people calling for evacuation. This RES source being more effective in small radii. The same condition also applies to seeing other people. We can conclude that RES sources generated by social cues, both seeing and/or hearing other people, are not constant but gradually increase as the distance between the source and people decreases. The impact of RES sources in Indonesia is notably distinct from those in Ishinomaki, Japan. In Palu, Indonesia, seeing other people had a greater impact on getting people to start evacuating than hearing people calling for evacuation.

While a case study comparison has the advantage to show the differences in detail, general comparison is needed to provide a broader picture. In general, the only available data was the post-disaster questionnaire, and therefore, only the rank of evacuation triggers could be compared, without knowing the exposure and impact. The results showed that receiving messages from authorities was the highest evacuation trigger in Indonesia and Japan. The ground motion ranked second in Japan and third in Indonesia. Interestingly, there was a wide gap between the rankings of "seeing other evacuees." It ranked second in Indonesia but was at the lowest rank for Japanese people. In the video and the questionnaire, Indonesian people quit the building after they felt the ground moving and stayed outside. In Japan, after the earthquake, people stayed inside the building and sought disaster information through media. Therefore, they could not see what other people were doing outside the building.

Most tsunamis are generated by earthquakes and before a tsunami lands, people can feel the ground move. Feeling the ground move became a critical evacuation trigger because it is the first RES source to elevate people's urgency to evacuation. Many countries, such as Indonesia, New Zealand, and Chile are campaigning for self-evacuation. The governments advise people to immediately evacuate if they perceive a strong or long-duration shaking of the ground. In Japan, people are encouraged to practice "tsunami tendenko," a quick tsunami evacuation without waiting for others. This can effectively trigger evacuation if people know that earthquakes generate a tsunami. However, everyone cannot be expected to practice immediate self-evacuation. Moreover, not all tsunamis are preceded by an earthquake. Therefore, further research should examine RES sources to determine appropriate evacuation strategies for non-seismic tsunamis. Further research on the difference in tsunami evacuation initiation is

important because this indicates that the generic disaster risk reduction strategy among countries should be reviewed before implement to the public. Educational material for tsunami training and drills must also consider the local characteristics.

In such evacuation studies, a hazard analysis considering the uncertainty of future tsunami events is often neglected. Our finding from the analysis of landslide-induced tsunami shows that a submarine landslide is enough to generate a destructive tsunami. The government of Indonesia published the Indonesia earthquake catalog in 2017, and because of a unique event in 2018 Palu, the book was updated in 2021. The scientific community published numerous research focused on the probability of tsunami earthquake hazards. The development of tsunami warning technology also addressed for earthquake tsunamis. This tendency is understandable since more than 75% of tsunamis are generated by earthquakes. Moreover, a study for landslide-induced tsunamis is hard to conduct. One of the biggest obstacles is the submarine survey. This study considers the possibility of investigating inland soil as input for the landslide-induced tsunami simulation. The assessment of future landslide-induced tsunamis should not be ignored. The evacuation plan should also consider the risk of landslide-induced tsunami disasters.

To mitigate future similar disasters in the region, the high-frequency ocean surface radars are another potential tsunami observing system. Existing studies demonstrate that owing to the high spatial sampling, tsunami current velocities observed by radars are well-suited for tsunami data assimilation and produce accurate forecasts (Mulia et al., 2020). This direct tsunami observation method is required for non-seismic or uncommon tsunami source mechanisms. Indonesia's Meteorology, Climatology and Geophysics Agency (BMKG) are operating high-frequency ocean surface radars in Bali, Labuhan, and Sunda Strait to monitor sea surface currents in real-time. This warning system could be very impactful for Indonesian people, especially if we consider that receiving a message from authorities ranked as the number one RES source.

REFERENCES

- Bird, D.K., 2009. The use of questionnaires for acquiring information on public perception of natural hazards and risk mitigation – a review of current knowledge and practice. *Nat. Hazards Earth Syst. Sci.* 9, 1307–1325. <https://doi.org/10.5194/nhess-9-1307-2009>.
- Dohi, Y., 2016. Development of tsunami evacuation simulator focusing on social reality. Kyoto University.
- Mulia, I.E., Watada, S., Ho, T., Satake, K., Wang, Y., Aditiya, A., 2020. Simulation of the 2018 Tsunami Due to the Flank Failure of Anak Krakatau Volcano and Implication for Future Observing Systems. *Geophys. Res. Lett.* 47. <https://doi.org/10.1029/2020GL087334>

Acknowledgements

I would like to express the deepest appreciation and forever grateful to Prof. Yoshihiro Okumura for his valuable guidance and endless supports during my doctoral study.

I am highly thankful to Prof. Koji Ichii for his guidance on my research.

My special thanks to the thesis committee: Prof. Shingo Nagamatsu and Prof. Tetsuo Tobita for their insightful comments and suggestions to improve the quality of my research.

I greatly appreciate the financial support from the Monbukagakusho scholarship provided by the Ministry of Education, Culture, Sports, Science and Technology, Japan.

My sincere thanks to Iyan Eka Mulia for taking time to teach and help my research.

My appreciation to Soichiro Murata, Jo Ohtani, Kana Yamashina, Takai Tamaki, Haruka Ishida and Kenji Yamazaki for their contribution on my research.

My thanks also go to all the professor in the Program of Disaster Management, Satomi Yao, Yoko Kumase and all the staff in the Faculty of Societal Safety Sciences, Kansai University who provided me an opportunity to join and adapt to the Japanese culture and traditions, particularly in the working environments.

I am thankful to all members of Okumura Laboratory for their kindness and good memories.

I am also thankful to all members of Indonesia Students Association in Osaka-Nara for their friendship and support during my study life in Osaka.

To my mother, sister, family, and my best friends in Indonesia and Osaka, I am blessed and forever in debt to have you all in my life.